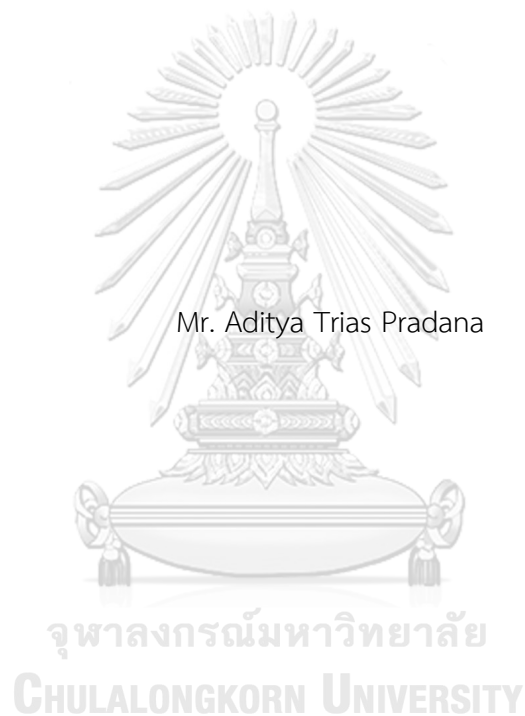SPRAY DRIED ASIATIC ACID-PALM OIL NANOEMULSION WITH IMPROVED
CHARACTERISTICS AND ANTIHYPERTENSIVE EFFECT STUDY IN RAT MODEL OF
HYPERTENSION

Mr. Aditya Trias Pradana

A Dissertation Submitted in Partial Fulfillment of the Requirements
for the Degree of Doctor of Philosophy in Industrial Pharmacy
Department of Pharmaceutics and Industrial Pharmacy
FACULTY OF PHARMACEUTICAL SCIENCES
Chulalongkorn University
Academic Year 2021

นาโนอิมัลชันกรดเอเชียติก-น้ำมันปาล์มแบบพ่นแห้งที่มีคุณลักษณะเพิ่มขึ้นและการศึกษาผลต้าน
ความดันโลหิตสูงในแบบจำลองหนูที่มีความดันโลหิตสูง

นายอดิตยา ไตรแอส ปราดานา

จุฬาลงกรณ์มหาวิทยาลัย
CHULALONGKORN UNIVERSITY

วิทยานิพนธ์นี้เป็นส่วนหนึ่งของการศึกษาตามหลักสูตรปริญญาเภสัชศาสตรดุษฎีบัณฑิต
สาขาวิชาเภสัชกรรมอุตสาหการ ภาควิชาวิทยาการเภสัชกรรมและเภสัชอุตสาหกรรม
คณะเภสัชศาสตร์ จุฬาลงกรณ์มหาวิทยาลัย
ปีการศึกษา 2564

Thesis Title	SPRAY DRIED ASIATIC ACID-PALM OIL NANOEMULSION WITH IMPROVED CHARACTERISTICS AND ANTIHYPERTENSIVE EFFECT STUDY IN RAT MODEL OF HYPERTENSION
By	Mr. Aditya Trias Pradana
Field of Study	Industrial Pharmacy
Thesis Advisor	Professor GARNPIMOL RITTHIDEJ, Ph.D.
Thesis Co Advisor	Vudhiporn Limprasutr, DVM., Ph.D.

Accepted by the FACULTY OF PHARMACEUTICAL SCIENCES, Chulalongkorn University in Partial Fulfillment of the Requirement for the Doctor of Philosophy

.... Dean of the FACULTY OF PHARMACEUTICAL SCIENCES

(Professor PORNANONG ARAMWIT, Ph.D.)

DISSERTATION COMMITTEE

.... Chairman

(Professor Varaporn Junyaprasert, Ph.D.)

.... Thesis Advisor

(Professor GARNPIMOL RITTHIDEJ, Ph.D.)

.... Thesis Co-Advisor

(Vudhiporn Limprasutr, DVM., Ph.D.)

.... Examiner

(Assistant Professor JITTIMA CHATCHAWALSAISIN, Ph.D.)

.... Examiner

(Assistant Professor Dusadee Charnvanich, Ph.D.)

.... Examiner

(VEERAKIET BOONKANOKWONG, Ph.D.)

อดิตยา ไตรแอส ปราดานา : นาโนอิมัลชันกรดเอเชียติก-น้ำมันปาล์มแบบพ่นแห้งที่มี
คุณลักษณะเพิ่มขึ้นและการศึกษาผลต้านความดันโลหิตสูงในแบบจำลองหนูที่มีความดัน
โลหิตสูง. (SPRAY DRIED ASIATIC ACID-PALM OIL NANOEMULSION WITH
IMPROVED CHARACTERISTICS AND ANTIHYPERTENSIVE EFFECT STUDY IN
RAT MODEL OF HYPERTENSION) อ.ที่ปรึกษาหลัก : ศ. ภญ. ดร.กาญจน์พิมล ฤทธิ
เดช, อ.ที่ปรึกษาร่วม : อ. สพ.ญ. ดร.วุฒิพร ลิ้มประสูตร

จุฬาลงกรณ์มหาวิทยาลัย
CHULALONGKORN UNIVERSITY

สาขาวิชา	เภสัชกรรมอุตสาหการ	ลายมือชื่อนิสิต ....
ปีการศึกษา	2564	ลายมือชื่อ อ.ที่ปรึกษาหลัก ....
		ลายมือชื่อ อ.ที่ปรึกษาร่วม ....

6271007733 : MAJOR INDUSTRIAL PHARMACY

KEYWORD: Asiatic acid, Palm oil, Spray dry, Nanoemulsion, Microencapsulation, Antihypertensive, ACE-inhibitor, Lecithin, Tween, Maltodextrin, Rats

Aditya Trias Pradana : SPRAY DRIED ASIATIC ACID-PALM OIL NANOEMULSION WITH IMPROVED CHARACTERISTICS AND ANTIHYPERTENSIVE EFFECT STUDY IN RAT MODEL OF HYPERTENSION. Advisor: Prof. GARNPIMOL RITTHIDEJ, Ph.D. Co-advisor: Vudhiporn Limprasutr, DVM., Ph.D.

Hypertension is a risk factor for premature death worldwide.It is characterized by an increase in blood pressure, so it needs therapy to regulate it and keep the value normal. Asiatic acid (AA) and palm oil (PO) were alternative antihypertensive agents that were promising to be developed. Both were natural compounds obtained from the Centella asiatica and Elaesis guineensis plants. However, low solubility, low absorption, rapid metabolism, low bioavailability and high oxidation were the limitation for both of them as an active compounds. Thus, a combination of nanoemulsion formulation and drying with a spray dryer was necessary to improve the physicochemical characteristics of the products and the effectiveness as an anti-hypertensive agent. From a series of evaluations, it was found that a spray-dried nanoemulsion product had been formed. This spherical microparticle had good physicochemical characteristics and stability, with the ability to quickly disperse into nanodroplets. Furthermore, LTM2 with optimum characteristics, highest solubility and rapid dissolution rate was selected to be continued in the activity study in Sprague-Dawley (SD) rats. The results of the study showed that spray-dried nanoemulsion AA succeeded in lowering blood pressure and acted as an ACE-inhibitor better than asiatic acid powder.

Field of Study: Industrial Pharmacy	Student's Signature ....
Academic Year: 2021	Advisor's Signature ....
	Co-advisor's Signature ....

ACKNOWLEDGEMENTS

the one who makes me believe that "after a rainstorm there will always be a rainbow, and a great storm will make us see the most beautiful rainbow".

Aditya Trias Pradana

TABLE OF CONTENTS

LIST OF TABLES

LIST OF FIGURES

จุฬาลงกรณ์มหาวิทยาลัย
CHULALONGKORN UNIVERSITY

List of Abbreviations

AA   = Asiatic Acid

ACE   = Angiotensin-Converting Enzyme

ACEI   = Angiotensin-Converting Enzyme Inhibitors

APIs   = Active Pharmaceutical Ingredients

ARB   = Angiotensin II Receptor Blocker

AT2   = Angiotensin II

BCS   = Biopharmaceutical Classification System

BP   = Blood Pressure

BUN   = Blood Urea Nitrogen

CCB   = Calcium Channel Blocker

Cl   = Chloride

CV   = Cardiovascular

DOCA   = Deoxycorticosterone Acetate

eNOS   = Enzyme endothelial nitric oxide synthase

HPLC   = High Pressure Liquid Chromatography

HVAC   = Heating, Ventilation and Air-Conditioning

IR   = Infrared

K   = Potassium

L   = Lecithin

LPM   = Lecithin-Poloxamer 188-Maltodextrin

LTM   = Lecithin-Tween 80-Maltodextrin

M = Maltodextrin

MDRS = Morphologically-Directed Raman Spectroscopy

Na = Sodium

NaCl = Natrium Chloride (Sodium Chloride)

NCDs = Noncommunicable Diseases

NO = Nitric Oxide

P = Poloxamer 188

PDI = Polydispersity Index

PO = Palm Oil

RAAS = Renin-Angiotensin-Aldosterone System

S = Span 80

SD = Sprague-Dawley

SEM = Scanning Electron Microscopy

SHR = Spontaneously Hypertensive Rat

SPM = Span-Poloxamer 188-Maltodextrin

T = Tween 80

TEM = Transmission Electron Microscope

TGA = Thermogravimetric Analysis

XRD = X-ray Diffraction

WHO = World Health Organization

CHAPTER 1

INTRODUCTION

1.1. Background and rationale

Hypertension is one of the most non-communicable diseases (NCDs) which is a worldwide problem. This disease is a serious risk factor for heart disease, stroke, cardiovascular and renal diseases (1,2). Based on data from the World Health Organization (WHO), hypertension complications have been calculated to cause 9.4 million deaths worldwide annually (1). it is even known that 14.6 million (one in four) people died globally from ischemic heart disease and stroke in 2013 (3).
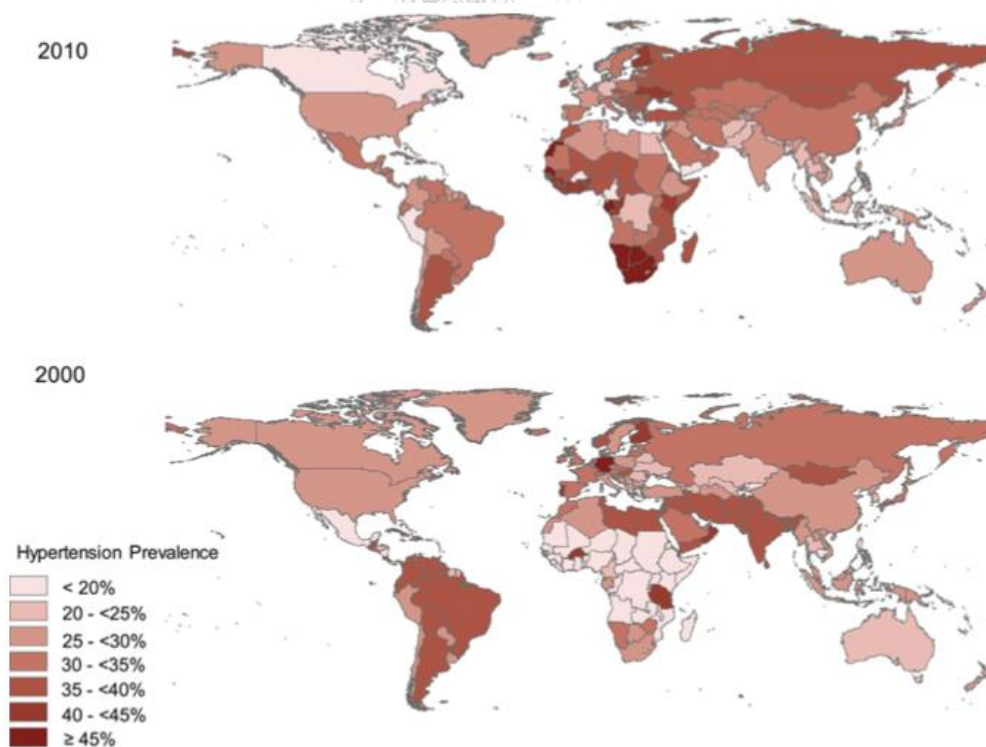
Figure 1 Worldwide prevalence of hypertension in adults ≥ 20 years (3)
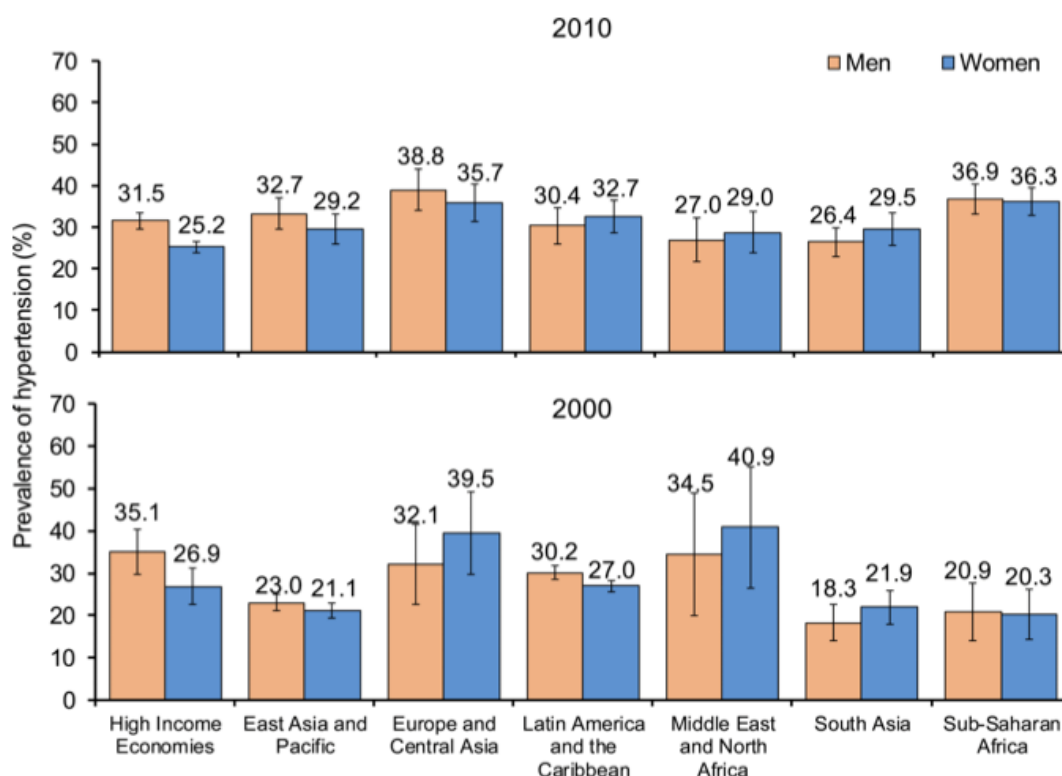
Figure 2 Prevalence of hypertension in adults ≥ 20 years by world region and sex (3)

Figures 1 and 2 show the prevalence and change in cases of hypertension during 2000 - 2010. In 2000, 26.4% of the adult global population (972 million people) suffered from hypertension, and the number increased to 31.1% (1.4 billion people) in 2010 (3). The estimated prevalence of hypertension among male and female patients was 32.1% and 29.5%, respectively (2). In addition, it was also seen that the prevalence of hypertension was higher in low- and middle-income countries (31.5%) than high-income countries (28.5%) worldwide. The prevalence of hypertension also decreased by 2.6% in high-income countries but increased by 7.7% in low- and middle-income countries over the 10 years to 2010. This was related to the lower proportions of awareness, treatment, and control of hypertension. in low- and middle-income countries than in high-income countries (3). Secondary intervention such as types of diet, physical activity, self-awareness, social support, healthcare

services, until collaborative efforts from national and international stakeholders are indeed very important in fighting the problem of hypertension globally (1–3).

In patients, hypertension is described as increased blood pressure in the arteries. Primary therapy needs to be given, because of the cardiovascular risk which can even has an impact on death (4). Several mechanisms in the body can control the blood pressure, especially the renin-angiotensin-aldosterone system (RAAS). When pathophysiologic irregularities occur, an angiotensin-converting enzyme inhibitors (ACEi), angiotensin II receptor blockers (ARBs), calcium channel blockers (CCB), thiazide diuretics and β-adrenoceptor antagonists (β - blockers) are drugs commonly used in regulating the blood pressure (4,5). Apart from primary therapy with several kinds of antihypertension drugs, some natural products for antihypertensives were also highly developed. Among the interesting antihypertensive agents to be developed are asiatic acid (6–11) and palm oil (12–14).

Asiatic acid (AA) is an isolate from *Centella asiatica*, a medicinal herb commonly found in tropical regions such as Asia, Africa, South America and Oceania. This plant is commonly consumed as salads in daily meals or serve as juice for Southeast Asian (11,15). In its medicinal use, AA has limitations regarding the physicochemical and pharmacokinetic properties. Solubility, lipophilicity, absorption, metabolism, elimination rate and bioavailability are the major problem to be developed from AA. Asiatic acid is poorly absorbed and highly metabolized in the liver by CYP450 enzymes. This is exacerbated because of the low solubility of asiatic acid in aqueous media, so that the oral bioavailability is very low to be able to provide effectiveness as an antihypertensive. Several dosage forms can be an alternative in improving delivery of AA, such as nanoparticles, transdermal, multiple emulsions, liposomes, and solid dispersion complexations (10).

Meanwhile, palm oil (PO) is a vegetable oil obtained from the *Elaesis guineensis* plant which contains rich in vitamins A and E, and does not contain lipid-raising fatty acids (myristic acid) as its saturated fatty acid content (13,14). Palm oil has the

potential as an antihypertensive agent because of its ability as a strong antioxidant and is effective in reducing arterial thrombosis, atherosclerosis and platelet aggregation (14,16). However, its ease of oxidation is also a disadvantage of palm oil. This oxidation can reduce its half-life and vitamin content. One way to avoid oxidation is the encapsulation process, which protects the compound inside the system (17,18).

Nanoemulsion is a dosage form that can be produced for nanoencapsulation purposes. The oil phase is emulsified to form small droplets by utilizing emulsifying agents. The nanoemulsion formation process is carried out using the high-energy method with an ultrasonication process. Parameters in the manufacturing process (eg, energy and production time) have been screened and set consistently. Nanoemulsion is prospective to be formulated with asiatic acid because of its advantages, including good physical stability, higher solubility and increase in the bioavailability (19). The emulsifying agent is absolutely necessary in nanoemulsion because it reduces the interfacial tension between the oil and aqueous phase and prevent the possibility of the aggregation (20). In this research, span 80, lecithin, poloxamer 188 and tween 80 were used for the purpose of reducing the interfacial tension between the oil-water phase in optimal ratio.

Meanwhile, to reduce the possibility of oxidation, the drying process with a spray dryer was carried out to the nanoemulsion (21). Spray drying formed an encapsulated system to retain the active system and prevent the effect of the Oswald ripening event which possible to cause agglomeration (22). In this process, critical parameters such as inlet temperature, aspirator rate, pump flow and nozzle clean maintained constantly to produce high yield and reproducible product. Meanwhile maltodextrin and magnesium stearate were used as a carrier and lubricant, respectively to maintain the stability of the product thermodynamically.

This research aimed to see the improvement of asiatic acid characteristics and its activity as an antihypertensive agent. Characterization and evaluation were carried

out by several tests, such as particle size, morphology, heat resistance, crystallinity, product recovery (yield), drug content, flowing properties, solubility, dissolution rate, non-invasive antihypertensive activity and ACE activity inhibition. Formula with the most optimum characteristics was recommended for further evaluation in the activity increasement determination. The focus of activity evaluated in this study was ACE inhibition of asiatic acid before and after modification in spray dried nanoemulsion formulation.

1.2 Objectives

The objectives of this research are:

1. To prepare spray dried asiatic acid-palm oil nanoemulsion with good physical characteristics, high product yield and high content.
2. To develop spray dried asiatic acid-palm oil nanoemulsion with higher aqueous solubility and dissolution rate compared with its pure form in gastric and intestinal fluid media.
3. To evaluate the antihypertensive activity of asiatic acid by forming the spray dried asiatic acid-palm oil nanoemulsion in rat model of hypertension.

1.3 Scope of the research

The scope of this research work will cover:

1. The preparation and optimization of the condition in nanoemulsion formulation and drying with spray dryer.
2. The formulation process of asiatic acid nano/microencapsulate with optimal active compound-emulsifier ratio and process parameters.
3. Characterization, physicochemical evaluation and antihypertensive activity determination of asiatic acid nano/microencapsulate and its comparison with asiatic acid pure form

1.4 Research design

Experimental research

1.5. Benefits of the research

This research was useful for improving physicochemical characteristics, solubility, bioavailability, and activity of asiatic acid-palm oil as antihypertensive agent.
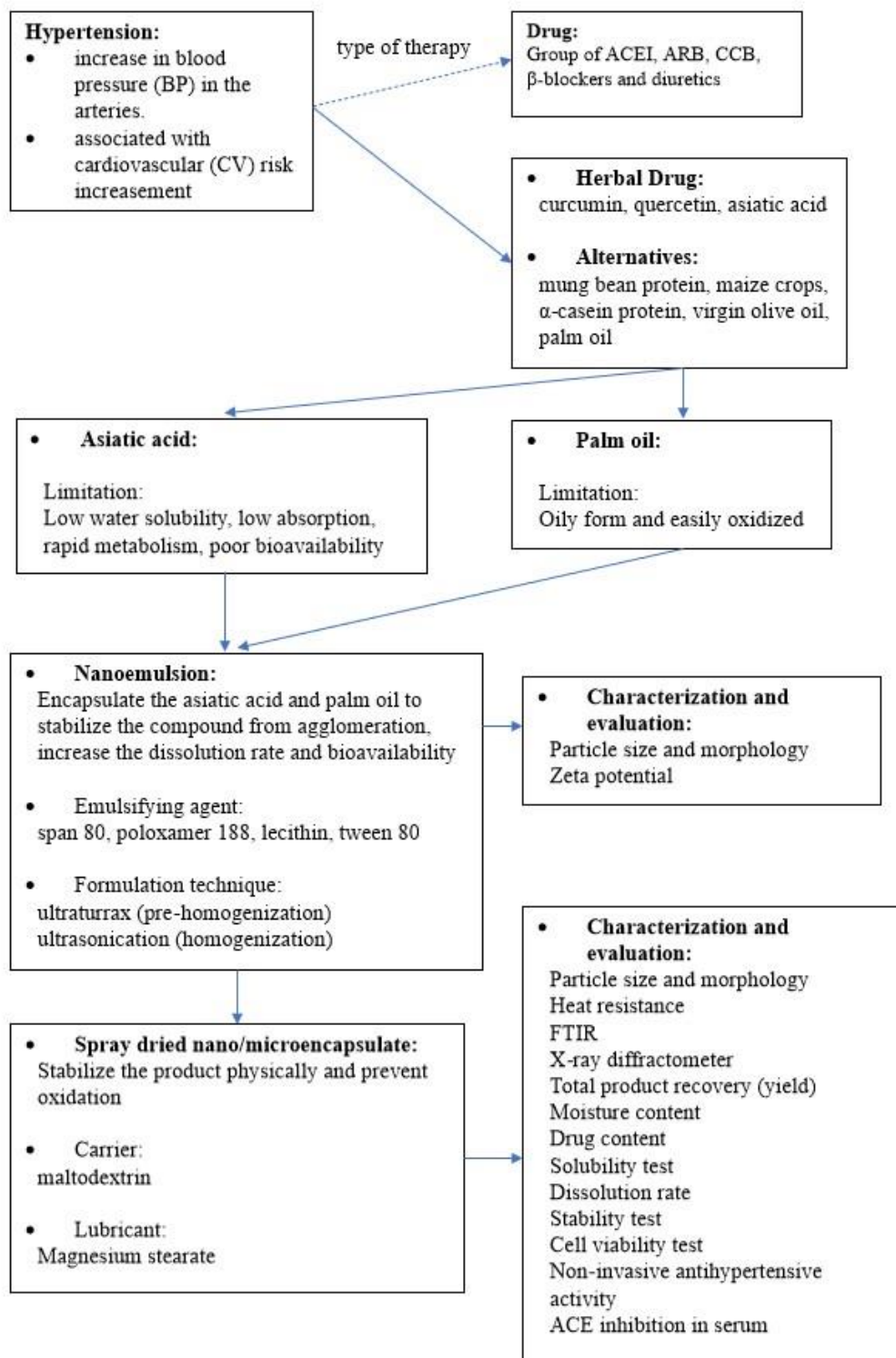
Figure 3 Conceptual framework of the study

CHAPTER 2

LITERATURE REVIEW

2.1. Hypertension

Hypertension is a disease that can be described by an increase of blood pressure (BP) in the arteries. This disease is associated with a cardiovascular (CV) risk increasement which can cause morbidity and mortality (4).

Hypertension resulted from unknown pathophysiologic causes essential or primary hypertension. It was generally caused by the influence of genetic factors that play a role in regulating the balance of blood pressure regulating pathways, such as sodium value. This type of hypertension can only be controlled and cannot be cured. A small percentage of patients has a specific cause of their hypertension, which called as secondary hypertension. This type of hypertension can be caused by comorbid disease, another drug that increases blood pressure or renal dysfunction. If the cause can be identified, hypertension in these patients can be mitigated or potentially be cured (4).

Some factors can control blood pressure include renin-angiotensin-aldosterone system (RAAS) or vasodepressor mechanisms and problems in neuronal mechanisms, peripheral autoregulation, and sodium, calcium, and natriuretic hormones (4).

Table 1 Blood Pressure Classification (4)

Classification	Systolic Blood Pressure (mm Hg)		Diastolic Blood Pressure (mm Hg)
Normal	<120	and	<80
Prehypertension	120-139	or	80-89
Stage 1 hypertension	140-159	or	90-99
Stage 2 hypertension	≥160	or	≥100

Based on the Table 1 it can be seen that hypertension is divided into normal, prehypertensive, stage 1 hypertension and stage 2 hypertension. Hypertensive crises with extreme BP are shown at values of more than 180/120 mm Hg and need to reduce less than 140/90 mm Hg for hypertensive patients. Clinical trials have proven that antihypertensive drug therapy helps reduce the risk of CV and death rates in patients with high blood pressure (4).

2.2. Antihypertensive therapy
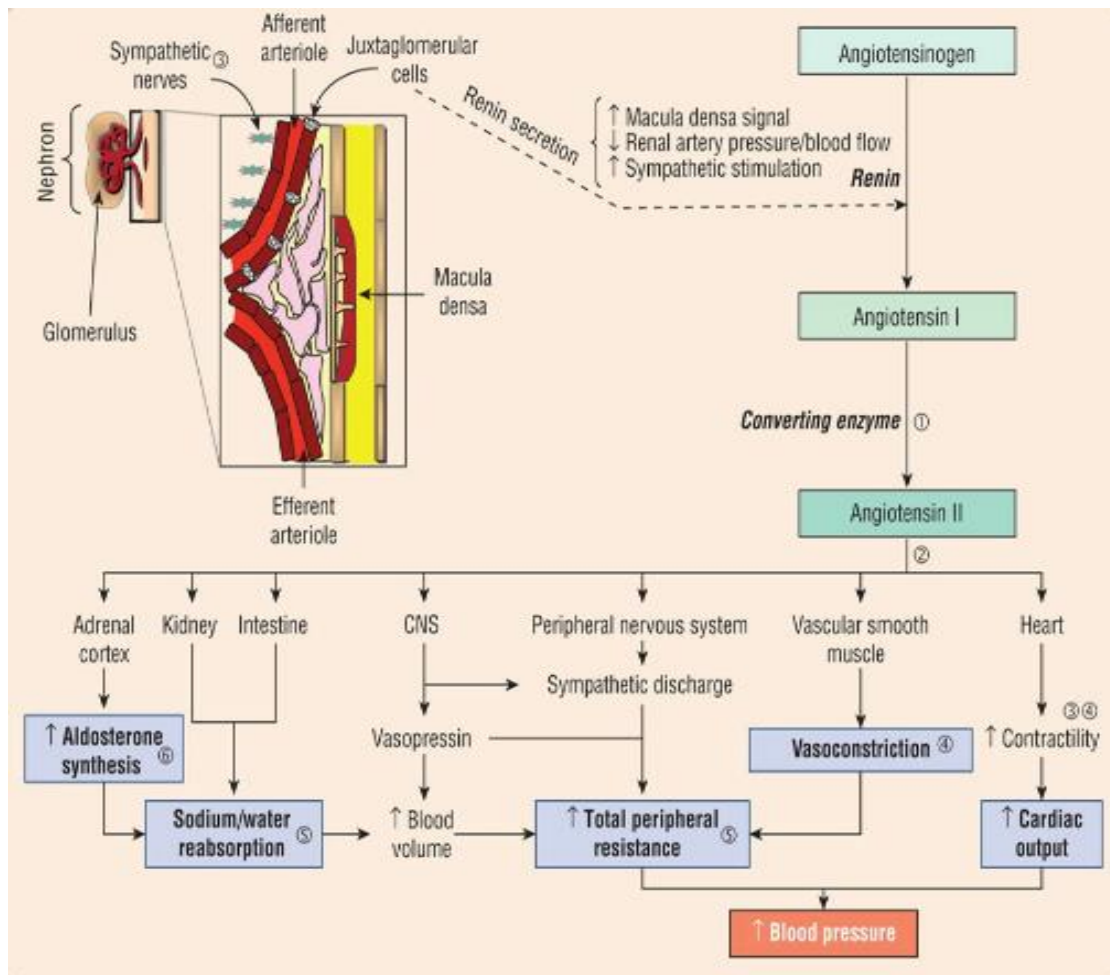
Figure 4 Renin-angiotensin-aldosterone system diagram (4)

Figure 4 shows that RAAS plays an important role in regulating arterial blood pressure. RAAS was triggered by renin, angiotensinogen and angiotensin regulates the sodium, potassium, and blood volume to control the homeostatic of peripheral blood vessel. Interventions in RAAS became very important in the treatment of hypertension and reduce the risk of morbidity and mortality from CV events (4).
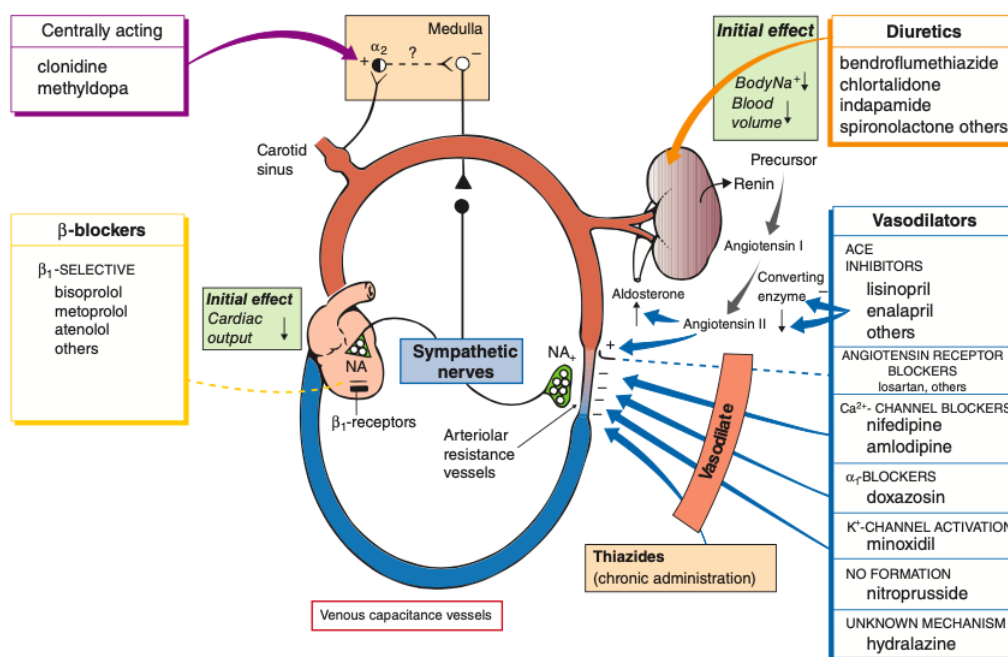
Figure 5 Different mechanism of antihypertensive drugs (5)

An angiotensin-converting enzyme inhibitors (ACEi), angiotensin II receptor blocker (ARB), calcium channel blocker (CCB), and thiazide shown in Figure 5 are the first-line antihypertensive agents for most patients (4). Angiotensin II is a vasoconstrictor and stimulates aldosterone production. Angiotensin converting enzyme (ACE) inhibitors and angiotensin receptor blockers (ARBs) decrease the synthesis of angiotensin II or antagonize its action at the angiotensin II receptor and improve the peripheral condition. Calcium channel blockers block the entry of calcium into vascular smooth muscle and are mostly used in older patients. β-adrenoceptor antagonists (β-blockers) and thiazide diuretics reduce blood pressure by mechanisms that are not fully understood (5). There are vasoactive substances synthesized by endothelial cells at vascular endothelium and smooth muscle also that are important in regulating the blood pressure. The most important and potent vasodilator released in endothelium is nitric oxide (NO), this substance can relax the vascular epithelium and regulate arterial blood pressure (4).

Some alternative substances are also being developed for antihypertensive therapy such as peptide of mung bean protein (23) or maize crops (24), α-casein

protein (25), virgin olive oil (26), and palm oil (12–14). Several isolates from plants such as curcumin (27–29), quercetin (30), and asiatic acid (6–11) are also alternative substances in hypertension treatment that promote to develop.

2.3. Asiatic acid

Asiatic acid (AA) is a major pentacyclic triterpenoid component found in *Centella asiatica* with a molecular structure shown in Figure 6. AA is biosynthesized by cyclization of squalene and present in the leaves, flowers, bark, stem, roots, and rhizomes of the plants (10).

Asiatic acid has been known to be used for wound healing, various skin conditions, inflammatory, diabetic, hyperlipidemic, cardiovascular problem, metabolic syndrome, obesity, osteoporosis, Alzheimer's, Parkinson's diseases and also as antihypertensive, gastroprotective, neuro protective, endothelial cells protector, antioxidant, anti-depressant, anti-cancer and relieving anxiety (6–11,31,32). Several pharmacological activities are resulted from several mechanisms performed by asiatic acids such as modulate many enzymes, receptors, growth factors, transcription factors, apoptotic proteins, and cell signaling cascades (10).
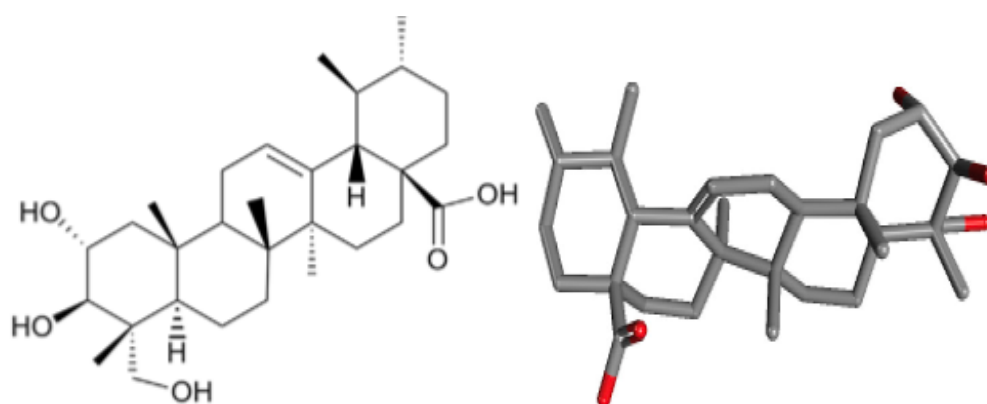
Figure 6 Molecular structure of asiatic acid in 2D and 3D conformer (10,31,33)

In hypertension therapy, AA attenuates the high blood pressure and heart rate with several mechanism such as ACE inhibition, attenuating RAS activation (by angiotensin II and angiotensin converting enzyme activity inhibition in blood), enhancing nitric oxide, lowering reactive oxygen species formation and acting as cytoprotective compound (6–11,32).

2.3.1. Pharmacokinetics of Asiatic Acid

Asiatic acid solubility is very low in water, with the concentration of 0.1583 mg/mL in saturated saline. Poor solubility of asiatic acid results in the low absorption and bioavailability, because it is transported by passive diffusion in jejunum as major site of absorption. The t½ of asiatic acid is 9.493 min, indicating that the asiatic acid is easy to be metabolized by CYP450 enzyme in the pharmacokinetics profile (10,31).

Table 2 Content of Asiatic Acid in Plasma (µg/mL) And Tissues (µg/g) of Mice (modified from (33))

	plasma	brain	heart	liver	kidney	colon	bladder
ASA, 4 week	–[a]	0.4 ± 0.1[a]	2.8 ± 0.6[a]	6.2 ± 0.8[a]	3.4 ± 0.6[a]	3.0 ± 0.6[a]	1.3 ± 0.2[a]
ASA, 8 week	0.46 ± 0.09[b]	1.2 ± 0.3[b]	4.5 ± 0.8[b]	10.4 ± 0.9[b]	6.6 ± 0.8[b]	5.9 ± 0.5[b]	2.9 ± 0.6[b]

Groups of mice were supplemented with a normal diet plus 0.5% of asiatic acid for 4 or 8 weeks. After the end of treatment, mice were killed after an overnight fast. Table 2 shows that the level of asiatic acid in plasma and tissues increased as the feeding period was increased from 4 weeks to 8 weeks (P <0.05). After 8 weeks, the liver had the highest content of asiatic acid, followed by kidney and colon. The hepatic level of asiatic acid was in the range of 6.2–10.4 µg / g tissue (33). The pharmacokinetic data was collected preclinically and clinically and suggested that AA is distributed in almost every tissue by binding with albumin (10).

Asiatic acid can be absorbed quickly into the blood, shown by 30 min of maximum plasma concentration. However, the amount that absorbed is very small with a C_{max} of 394.2 ng mL^{-1}. Compared with the absolute bioavailability profile after intravenous administration, its orally administration bioavailability is 16.25%. The results shows that the poor solubility and rapid metabolism of asiatic acid may be resulting the low C_{max}, t½ and bioavailability (31).

2.4. Palm oil

Palm oil (PO) is a vegetable oil that is popularly used worldwide. Palm oil is obtained from the fruit of the tropical plant *Elaesis guineensis* and contributes approximately 23% of the consumption rate for cooking and frying. Palm oil is rich in vitamins A and E, and has an unsaturated to saturated fatty acid ratio close to 1. PO does not contain lipid-raising fatty acids (myristic acid) as its saturated fatty acid content (13,14). However, palm oil oxidation occurs due to culinary purposes. Thus, the amount of palm oil in its oxidized form must be considered because it poses a risk to the physiological and biochemical functions of the body (16).

Palm oil is unique from other forms of vegetable and animal oils. Its antioxidant activity is quite potent because of its high content of tocopherols, tocotrienols and beta-carotene (13). In addition, palm oil also has effectiveness in reducing the risk of arterial thrombosis, atherosclerosis, cholesterol biosynthesis, platelet aggregation and blood pressure. PO abilities in reducing oxidative stress are promising as an adjunct to antihypertensive therapy (14,16).

The unsaturated fatty acids found in palm oil exhibit their antihypertensive effect by relaxing blood vessels. Unsaturated fatty acids act by several mechanisms such as direct relaxant actions on the blood vessel wall, inhibition of intracellular calcium release or interference with contractile proteins. Unsaturated fatty acids also

cause the increased production of vasodilatory prostaglandins, PGF1 and PGI2. It has been determined that palm oil is attributed to the protective effect on the endothelium of the blood vessels (16).

However, most lipophilic active compounds are susceptible to chemical degradation due to gastrointestinal conditions and environmental effect during storage. The production process also allows palm oil to undergo oxidation and lose its vitamin and provitamin content. Oxidation also reduces the half-life of the product. Encapsulation is one of the systems prepared to protect the compounds from environmental effects and is generally used to develop lipids delivery systems. This nanoencapsulation can also be done by adding the wall material by spray drying the nanoemulsion products (17,18).

2.5. Bioavailability enhancement

Synthetic and natural active compounds are categorized in Biopharmaceutical Classification System (BCS) class I which have high solubility in water and well absorbed in GI tract. Moreover, APIs which have low solubility but high permeability are classified in BCS II and which have poor permeability and high solubility are classified as BCS III. The worst is the substance with low solubility and permeability is BCS class IV drug.
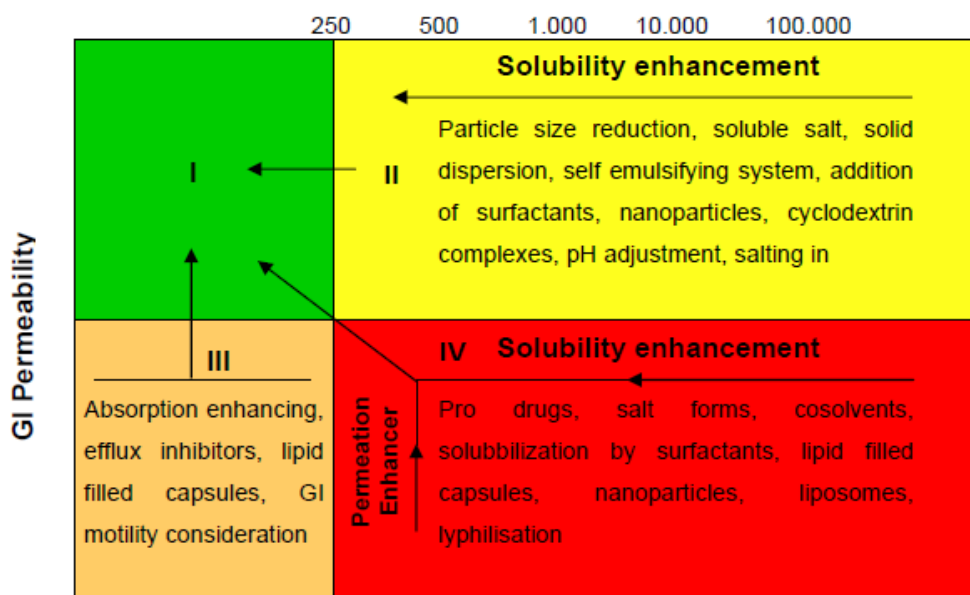
Figure 7 Solubility and permeability enhancement in BCS diagram (34)

Bioavailability is the key factor to obtain pharmacological effects of an oral drug. The bioavailability of a solid compound which is categorized as class II in the Biopharmaceutical Classification System depends on its low solubility and dissolution rate (35). Based on the Figure 7, solubility enhancement could be done with several modifications such as particle size reduction, soluble salt formation, solid dispersion, cyclodextrin complexes and nanoparticles formation. Currently, several studies have shown that encapsulation through nanoemulsion formulation successfully increased the bioavailability of active compounds. Nanoemulsion (oil-in-water) as a dosage form, is capable to incorporate hydrophobic and amphipathic drugs into its systems (36).

2.6. Nanoemulsion

Emulsion-based system is a form of encapsulation suitable for lipophilic compounds (17). Emulsion is a colloidal system where the oil phase is dispersed in

the aqueous liquid. However, an emulsifier also needs to be added to the system to get the oil phase emulsified. The emulsifier can reduce the interfacial tension between the oil and aqueous phase and prevents the possibility of the aggregation (20). Selection of the best combination of emulsifier concentration is very important to get emulsions that are thermodynamically stable (19,37). Particle size reduction in nanoemulsion also increases Brownian motion of the substance which prevents creaming and sedimentation (38).

The nanoemulsion system has several advantages to be used as an active compound delivery system, including:

1) Thermodynamically and kinetically stable

2) Increase the physical stability of conventional dosage forms

3) Non-toxic and non-irritant

4) Can be used on various administrative routes

5) Can be used to dissolve hydrophilic and lipophilic drugs

6) Encapsulates oil based active compound and protects against hydrolysis and oxidation

7) Increase the surface area of nanodroplets that contact with media, so that it can increase absorption and bioavailability

8) Encapsulate for taste and odor masking, and increase patient compliance.

9) Increase drug efficacy, reduce dose requirements and the risk of side effects (39).

In addition, nanoemulsion can also be a solution in the preparation of essential oils as active compounds. The weakness of this compound which generally has poor water solubility, low stability and high volatility can be improved with nanoemulsion

formulation, so that the solubility can be increased by the formation of oil droplets in the surfactant-water phase (40).

Nanoemulsion production initiates the formation of the nanoencapsulation system, in which the oil phase is emulsified through the use of an emulsifier. Furthermore, the nanoemulsion is formed into small drop sizes with high surface areas. Nanoemulsion system offers several potential advantages over conventional emulsions, such as a good physical stability, higher solubility, increase bioavailability, targeted delivery of encapsulated substances, and able to incorporate high nutritional value oils (19).

2.7. Techniques of nanoemulsion formulation

The nanoemulsion is formed from a colloidal nanosystem, where there is a dispersed phase which is stabilized by the addition of a surfactant. Two continuous phases of nanoemulsion consists of oil and water phases. These two phases are immiscible each other. Surfactants help as interfacial surface agents. In addition, external mechanical and chemical energy is also required in the preparation of nanoemulsion systems. The preparation methods used to form nanoemulsions can be classified into two types, namely high-energy emulsification methods and low-energy emulsification methods (39).
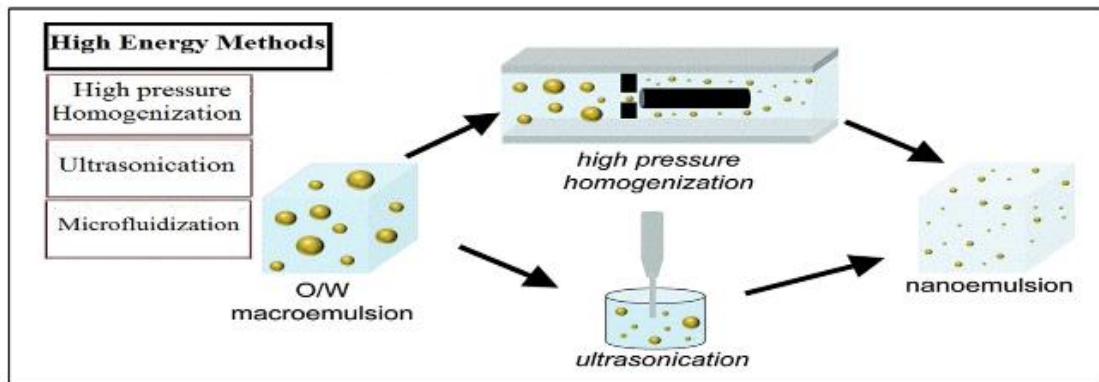
Figure 8 Illustration of high energy method of nanoemulsion preparation (39)
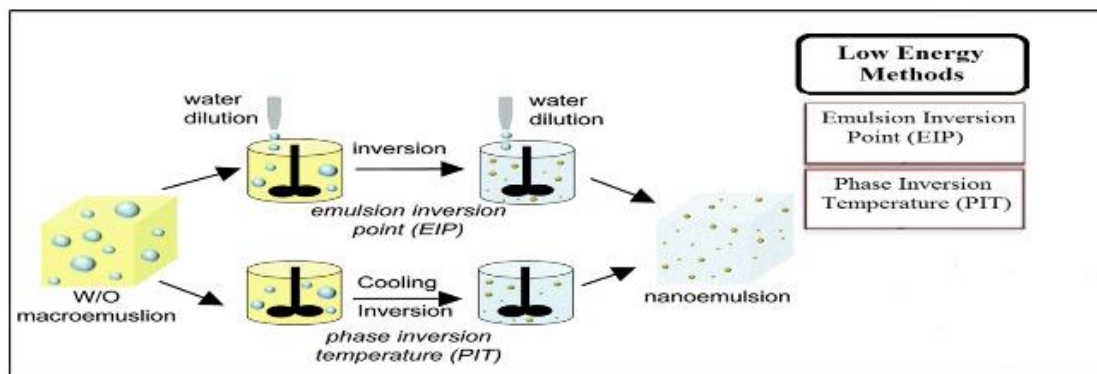
Figure 9 Illustration of low energy method of nanoemulsion preparation (39)

High-energy emulsification methods (Figure 8) are method that involve mechanical energy. Meanwhile, low-energy emulsification methods, as shown in Figure 9 utilize chemical energy to form an emulsion system. Some examples of techniques that are classified as high-energy emulsification methods are high-shear blending, high-pressure homogenization, and ultra-sonication. Meanwhile, phase inversion temperature, emulsion inversion point and solvent displacement are some of the techniques included in the low energy emulsification method (39,41).

The high-energy emulsification method is used because of its ability to reduce the droplet size which is very effective in a short process time and the physical properties of the nanoemulsion are also well controlled (36). One of the high-energy

emulsification methods is high pressure homogenization or microfluidization. Oil-based substances such as olive oil and seed oil (42,43), protein (44,45), extract (46) and isolates from herbal such as capsaicin and β-carotene (47,48) are some of the substances that had been successfully prepared into nanoemulsion with high-pressure homogenization. This technique utilizes a high-pressure homogenizer, which forces the emulsion to pass through a small orifice of a certain specification at very high pressures. The suspension or emulsion is formed from the combined effect of cavitation, shear, and impact. This process combination is effective for destroying the oil and water phase into very small size droplet in a low concentration of surfactant compared with low-energy (19,39,49,50).

Ultrasonication is also a high-energy emulsification method. The process involves droplets breakdown by high-frequency of ultrasound waves. The probe delivers very high energy, passed through the liquid medium, produces mechanical vibration and cavitation which forms a nanoemulsion (51,52). Parameters that need to be considered in sample preparation with the ultrasonicator instrument include the energy given, the probe diameter, amplitude, process time and frequency (53). High-pressure homogenizer is preferred in nanoemulsion preparation because of their relatively fast process, but this technique requires very high energy and the products particle size are less controlled. Meanwhile, ultrasonication can be more efficient in controlling the physical characteristics of the emulsion produced (54). Currently, ultrasonication has succeeded in forming nanoemulsion of various materials, such as curcumin (53), vitamin D (55), β-carotene (56), eugenol (57), valproic acid (58), D-limonene (59), and various types of oil-based substances such as garlic oil (60), eucalyptus oil (61) and other essential oil (62).

2.8. Spray drying

Spray drying is a material change technique from a fluid state to form dry particles by spraying the feed into a chamber with a hot drying air flow. The material to be sprayed on the instrument shown in the Figure 10 can be in the form of a solution, suspension or paste. Fluid feed undergoes several stages until it becomes dry form, namely: atomization of the feed into spray form, contact between spray form and air (mixing and flow), drying stage of the spray form (moisture evaporation) and separation of the final product (dry form) from the air (63). Associated with the part of the spray dryer, the drying process can be grouped into several zones, namely the zone where the sample firstly flow via a pneumatic transport system, the drying chamber zone and the integrated fluidized bed zone (64).

The drying performance and the physicochemical properties of substance are strongly influenced by the processing parameters (e.g., drying temperature, flow rate) and feed characteristics (e.g., composition, rheological properties and droplet density) (64,65). In addition, the type of atomizer used is also very important because it has an impact on the physical characteristics of the powder, such as particle size distribution, density, solubility and encapsulation efficiency (17).
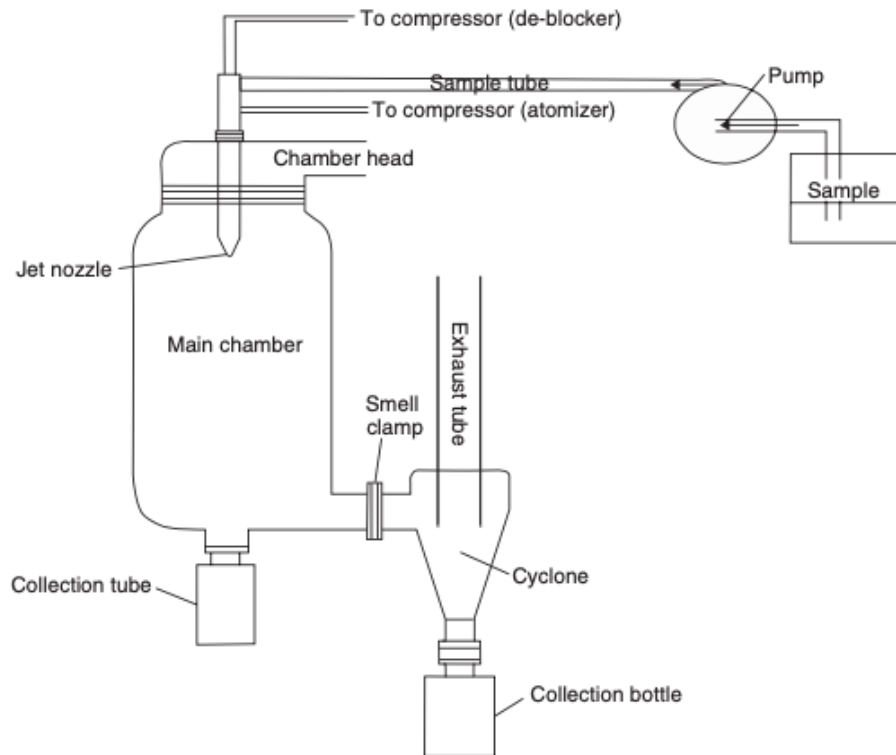
Figure 10 Spray dryer installation scheme (63)

Spray drying is used in food production to retain the substance from physical, chemical, or biological worse changes. As in powdered milk production, amphiphilic protein plays a role as a fat emulsifier and then dried with a spray dryer until it reaches the final water contents of <3% to reduce physical instability (38).

Furthermore, in improving the characteristics and sealing the compound, nanoencapsulation can be done as an option. Emulsification is carried out as an initial stage and followed by spray drying to produce the powders from oil in water (O/W) nanoemulsion (17). With this modification, the possibility of degradation caused by oxidation can also be lowered. Spray drying forms an encapsulated system to retain the active substance, although slight oxidation can still occur on the surface of the system (21). Spray drying can also maintain the stability of the nanoemulsion from possible damage caused by the Oswald ripening event (22). In several studies of nanoemulsion in enhancing the active substance, such as

vegetable oil (22), eugenol (40), citrus oil (65), α-tocopherol (66) and krill oil (21), spray dryers had succeeded in forming spherical-shape and stable nano/microencapsulate with increasement in its physicochemical characteristics.

2.9. Poloxamer 188

Poloxamer, also called lutrol, monolan, pluronic, poloxalkol, poloxamera, polyethylene–propylene glycol copolymer, supronic or synperonic is widely used as dispersing agent, emulsifying agent, and solubilizing agent (67). Poloxamer is known as triblock copolymers of poly(ethylene oxide) and poly(propylene oxide) (PEO–PPO–PEO) with the molecular structure shown in Figure 11 and has forms as shown in Table 3. The polyoxyethylene part of poloxamer is hydrophilic while the polyoxypropylene segment has hydrophobic characteristics (67,68).
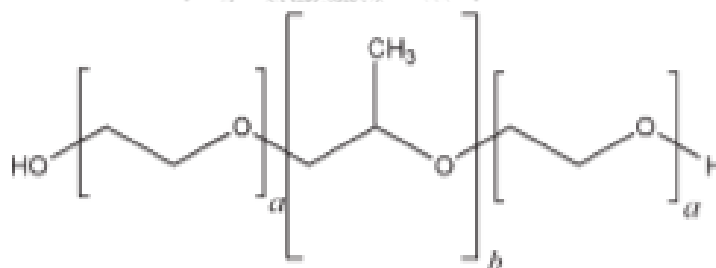
Figure 11 Molecular structure of poloxamer (67)

Table 3 Grade and molecular weight of poloxamer (67)

Poloxamer	Physical form	a	B	Average molecular weight
124	Liquid	12	20	2090-2360
188	Solid	80	27	7680-9510
237	Solid	64	37	6840-8830
338	Solid	141	44	12700-17400
407	Solid	101	56	9840-14600

Poloxamer occurs as white, waxy and free-flowing granules or cast solids. They are practically odorless and tasteless. Poloxamer 188 is freely soluble in water and organic solvent such as ethanol (67). Several kinds of active compound, such as acyclovir, rifampicin, naringenin, curcumin, soybean oil and fish oil have already formed into nanoemulsion and administered into orally (69,70), parenteral (71), ocular (72,73), until brain targeting (74) routes.

2.10. Span 80

Span 80, also known as sorbitan monooleate, is a compound that has widely used in the pharmaceutical industry. Span 80 is used in the dosage form formulation as a non-ionic surfactant, dispersing agent, emulsifying agent, solubilizing agent, suspending agent, and wetting agent (75,76). This sorbitan esters compound is used to formulate stable water-in-oil emulsions, microemulsions, nanoemulsions, liposomes and also self-emulsifying drug delivery systems for poorly soluble compounds (75,77,78).
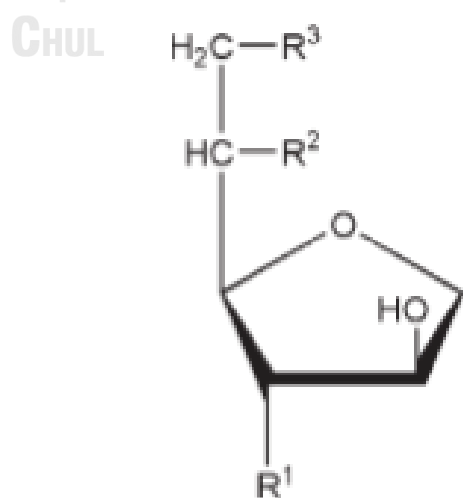
Figure 12 Molecular structure of sorbitan esters (75)

Span 80 is included in the sorbitan esters group with the formula $C_{24}H_{44}O_6$ and molecular structure as shown in the Figure 12, where R_1 and R_2 are OH groups; and R_3 is $(C_{17}H_{33})COO$ (75). The commercially Span 80 contains not only a sorbitan monoester with a molecular weight of 429, but also di-, or tri-ester. The lipid composition in the Span 80 vesicle has been reported depend on its diameter (77).

Span 80 vesicle can efficiently delivering anti-cancer drugs, resulting a significant inhibition of the tumor growth of colon carcinoma (77). In addition, span 80 is also used in the formation of nanoemulsions. It is practically insoluble in the aqueous phase, so it is possible that all amounts of Span 80 are located on the surface and into oil droplets of the nanoemulsion (79). Span 80 in nanoemulsion formulations is used for delivering several active ingredients, such as drugs, genes, and extracts (76,80), maintaining stability (79), and forming a nanofibrous membrane matrix (81).

2.11. Tween 80

Tween 80 is included in the polyoxyethylene sorbitan fatty acid esters group, also known as polysorbate 80 or polyoxyethylene 20 sorbitan monooleate. Polyoxyethylene sorbitan fatty acid esters (polysorbates) is a series of partial fatty acid esters of sorbitol and its anhydrides copolymerized with ethylene oxide. Figure 13 shows the molecular structure of polyoxyethylene sorbitan monoester, where Tween 80 has fatty acids at position R and approximately 20 moles of ethylene oxide for each mole of sorbitol and its anhydrides at w, x and z position (82).
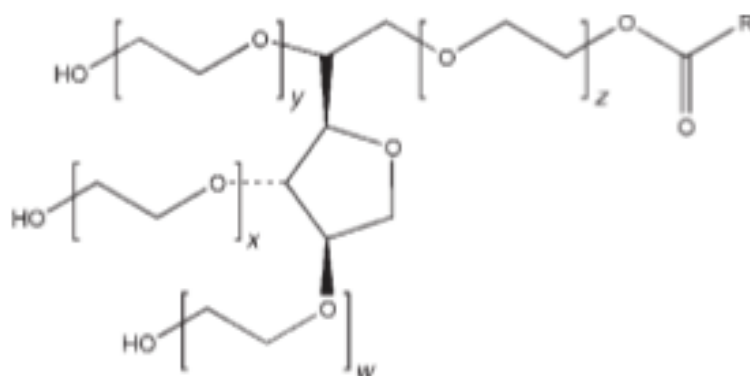
Figure 13 Molecular structure of polyoxyethylene sorbitan monoester (82)

Tween 80 is a hydrophilic non-ionic substance used as dispersing agent, emulsifying agent, solubilizing agent, suspending agent, wetting agent and surfactant based on its hydrophilic lipophilic balance. It is also known improving the oral bioavailability of drugs that are substrates for P-glycoprotein (82,83). Tween 80 has succeeded in forming nanoemulsion dosage form to improve physicochemical characteristics, solubility and stability of drugs, oil, natural extract and isolate such as indinavir (84), vitamin D (55), cinnamon oil (85), clove oil (86), and curcumin (83).

2.12. Lecithin
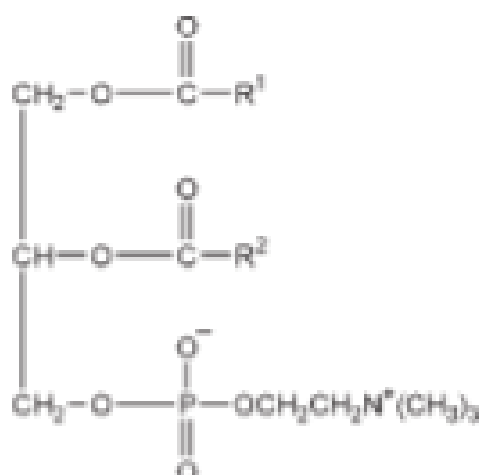
Figure 14 Molecular structure of lecithin (α-Phosphatidylcholine) (87)

The general structure of lecithin can be seen in the Figure 14. Lecithin is a complex mixture of phosphatides that consists of phosphatidylcholine, phosphatidylethanolamine, phosphatidylserine and phosphatidylinositol, combined with various amounts of other substances such as triglycerides, fatty acids, and carbohydrates as separated compound from a crude vegetable oil source. The composition of lecithin varies according to the source of the lecithin and the degree of purification. The composition variations also differentiate the physical characteristics of each type of lecithin (87).

The free fatty acid content of lecithin gives variations in the physical form of lecithin, viscous semiliquid to powder form. The brown to light yellow colour of lecithin is based on the level of purity and the bleaching process. Oxidation can occur in lecithin once exposed to water, forming a darker yellow or brown colour. Lecithin is soluble in aliphatic and aromatic hydrocarbons, halogenated hydrocarbons, mineral oil, and fatty acids. It is practically insoluble in cold vegetable and animal oils, polar solvents, and water (87). Lecithin has successfully formulated tacrolimus (88), carvacrol (89), thymol, eugenol (90), vitamin E (91), curcumin (92), and β-carotene (93) into nanoemulsion which are delivered orally and transdermal.

2.13. Maltodextrin

Maltodextrin is a white powder or granules, unsweet and odorless, nutritive saccharide mixture of polymers that consist of D-glucose units, with a dextrose equivalent (DE) less than 20. The D-glucose units are linked primarily by α- (1->4) bonds but there are branched segments linked by α- (1-> 6) bonds as shown in the Figure 15 (94).
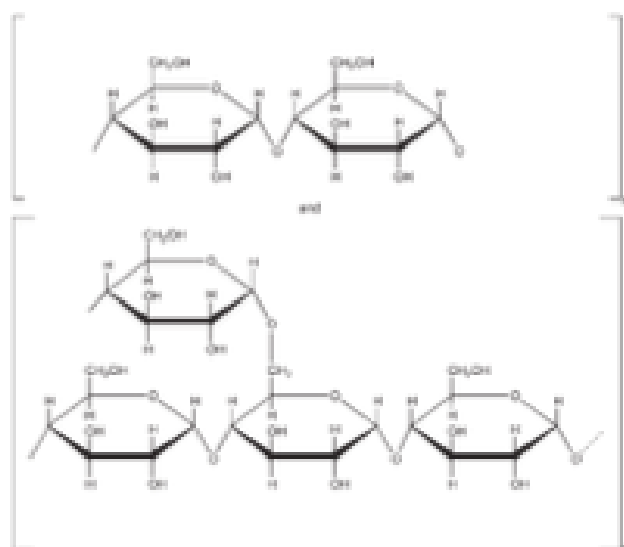
Figure 15 Molecular structure of maltodextrin (94)

The solubility, hygroscopicity, sweetness, and compressibility of maltodextrin increase as the DE increases. Maltodextrin is widely used as an aqueous coating agent, tablet and capsule diluent, tablet binder and viscosity increasing agent. It is also used as a carrier in a spray-dried redispersible oil-in-water emulsion, in order to improve the bioavailability of poorly soluble drugs (95). Many active ingredients have been successfully stabilized from nanoemulsion or nanoencapsulation form by utilizing the spray drying method and maltodextrin carrier, including carotenoids (96), *Moringa oleifera* oil (97), corn oil (98), curcumin (99), chili seed oil (100), vitamin A (101), fingered citron extract (102), and propolis (103).

2.14. Hypertension animal models

Several hypertension animal models have been developed. This was done for mimicking human hypertensive responses, understanding hypertension progress in the body, and observing antihypertensive activity of drugs. Hypertension studies have often been modeled with dogs previously, and are currently moving to rats

modeling, some other researches using mice, monkeys and pigs. Several strains of rats frequently used in hypertension animal models are Spontaneously hypertensive rat (SHR), New Zealand, Milan, Sabra, Lyon, and Dahl salt-sensitive (104).

Observations of type 1 (essential) hypertension generally focuses on the RAAS pathways. SHR (from inbreeding Wistar rats), Dahl salt-sensitive rats (that derived from normal to 8% NaCl induced Sprague-Dawley rats), and transgenic model mouse are commonly used on modeling this type of hypertension (104,105). Furthermore, hypertension can be induced by using high salt diet in outbred rats as well. Briefly, high salt diet was given to the rats ad libitum in food (4 - 8% NaCl) or drinks (1 - 2% NaCl) (105–112). High salt induction was maintained for up to 4 weeks or more. During this process, there would be an increase in blood pressure, mesangial expansion and glomerulosclerosis, which were related to sodium retention based on the duration and the route of salt administration. On long-term induction, renal damage may also occur, as indicated by fibrosis of renal interstitial and inflammation by T-cells and macrophage infiltrates. Other results seen from high salt intake were NO production improvement and impaired homeostatic responses of angiotensin (105–107,109). Other hypertension models can also be developed using DOCA-induced (with or without nephrectomy) rats for endocrine hypertension, stress-induced hypertension rats for environmental hypertension, L-Name as NOS inhibitors administered rats for pharmacological hypertension, and kidney-clip hypertension rats for renal hypertension (104,105).

CHAPTER 3

MATERIALS AND METHODS

3.1. Materials and Machines

3.1.1. Materials

1. Asiatic acid (≥ 95%) (New Natural Biotechnology Co.,Ltd, Shanghai, China)

2. Asiatic acid standard (≥99%) (LKT Laboratories, Inc, USA)

3. Palm oil (Sigma-Aldrich, St.Louis, Missouri)

4. Span 80 (S.Tong Chemicals, Nonthaburi, Thailand)

5. Poloxamer 188 (Kollliphor®, Sigma-Aldrich, St.Louis, Missouri)

6. Tween 80 (Maximax Pro Co., Ltd, Bangkok, Thailand)

7. Soy lecithin (Sigma-Aldrich, St.Louis, Missouri)

8. Maltodextrin (Sigma-Aldrich, St.Louis, Missouri)

9. Triton X-100® (Calbiochem, Merck Millipore Co., Darmstadt, Germany)

10. Magnesium stearate (S.Tong Chemicals, Nonthaburi, Thailand)

11. Absolute ethanol (Emsure, Merck Millipore, Co., Darmstadt, Germany)

12. Acetonitrile in Honeywell B&J HPLC grade (Chemical Express Co., Ltd, Samutprakarn, Thailand)

13. Methanol in Honeywell B&J HPLC grade (Chemical Express Co., Ltd, Samutprakarn, Thailand)

14. HPLC column Halo® C18 5 μm 90Å (250 x 4.6 mm) (Applied Chemical and Instrument Co., Ltd, Bangkok, Thailand)

15. ACE1 activity assay kit (colorimetric) (Sigma, St.Louis MO)

16. Sodium chloride (Supelco, Merck, Darmstadt, Germany)

17. Captopril (TCI, Shanghai, China)

18. Hydrochloric acid (Merck Milipore Co., Darmstadt, Germany)

19. Tribasic sodium phosphate (Merck Milipore Co., Darmstadt, Germany)

20. Fetal Bovine Serum (FBS) (Gibco®, Life Technologies Ltd, Paisley, UK)

21. Penicilin (10,000 units/mL)-Streptomycin (10,000 μg/mL) (Gibco®, Life Technologies Ltd, Paisley, UK)

22. L-glutamine 200mM (100X) (Gibco®, Life Technologies Ltd, Paisley, UK)

23. Dulbecco's Modified Eagle Medium (DMEM) powder (Gibco®, Life Technologies Ltd, Paisley, UK)

24. Phosphate-Buffered Saline (PBS) tablets (Gibco®, Life Technologies Ltd, Paisley, UK)

25. 0.25%Trypsin-EDTA (1x) (Gibco®, Life Technologies Co., NY, USA)

26. Sterile dimethyl sulfoxide (DMSO) (Sigma-Aldrich, St.Louis, Missouri)

27. MTT dye (Invitrogen®, Life Technologies Limited, Paisley, UK)

28. Zetasizer capillary cells (Malvern DTS 1070, UK)

3.1.2. Equipment

1. Analytical balance (Mettler Toledo, Germany)

2. Magnetic stirrer and Magnetic bar (Biosan MPS-9, Latvia)

3. Vortex mixer (Velp Scientifica ZX4, Italy)

4. Ultra turrax (IKA T25 digital, Thailand)

5. Ultrasonicator processor (Sonics Vibra-cell, USA)

6. Spray Dryer (Buchi B-290, Germany)

7. High pressure liquid chromatography (Agilent 1260 Infinity II, USA)

8. Freezer -20°C (Sharp FC-27, Thailand)

9. Climatic chamber (Binder KBF 720, Germany)

10. Morphologically-directed raman spectroscopy (MDRS) (Malvern Morphologi 4-ID, UK)

11. Zetasizer (Malvern Instruments Nano ZS, UK)

12. Dry-powder disperser (Scirocco 2000, Malvern, UK)

13. Micropipette (2-20 ml, 20-200 ml, 100-1000 ml, 1-5 ml; Gilson, USA)

14. Shaking incubator (LabTech LSI-3016R, China)

15. Powder X-ray Diffractometer (Bruker D8, UK)

16. Fourier Transform Infrared (PerkinElmer 843 System, USA)

17. Scanning electron microscope (Jeol JSM-IT500HR, Japan)

18. Transmission electron microscope (Jeol JEM-2100, Japan)

19. Thermogravimetric Analysis (TGA) Instrument (NETZCH TG 209 F3 Tarsus[®], Germany)

20. pH meter (Mettler Toledo FiveEasy, Germany)

21. Microsentrifuge (Eppendorf 5425, Germany)

22. Dissolution tester (Vankel VK 7000, USA)

23. Moisture content balance (Mettler Toledo HR83, Germany)

24. Non-invasive tail-cuff plethysmography (AD Instrument Powerlab 8/35 and NIBP controller; Dunedin, New Zealand)

25. Incubator (Thermo Scientific Steri-Cycle i160, USA)

26. Microscope with camera (Nikon Eclipse TS2, Thailand)

27. Microplate reader (CLARIOstar®, BMG LABTECH, Germany)

28. Fume hood (ProLAB DEA2014, Thailand)

29. Biological safety cabinet (Thermo Scientific 1300 Series A2, USA)

30. Utrasonic bath (Elma Transsonicdigital, USA)

3.2. Methods
3.2.1. Pre-formulation study

Pure asiatic acid and excipients powder were visually checked and tested using Fourier transform infrared spectroscopy (FTIR), thermogravimetric analysis (TGA) and x-ray diffractometer (XRD). This test was intended to ensure the purity of the material qualitatively and its similarity with the theoretical and certificate of analysis. Asiatic acid purity was quantitatively determined by validated method using High Performance Liquid Chromatography (HPLC) and ensuring the peak was not interfered

by the matrix. Preliminary studies were also done to find the value of controlled variable used in the formulation process, such as drug-surfactant ratio, speed and mixing time in ultraturrax, time and energy used in sonication, inlet temperature, flow rate and aspirator rate of spray drying process.

3.2.2. Preparation of Asiatic acid nanoemulsion
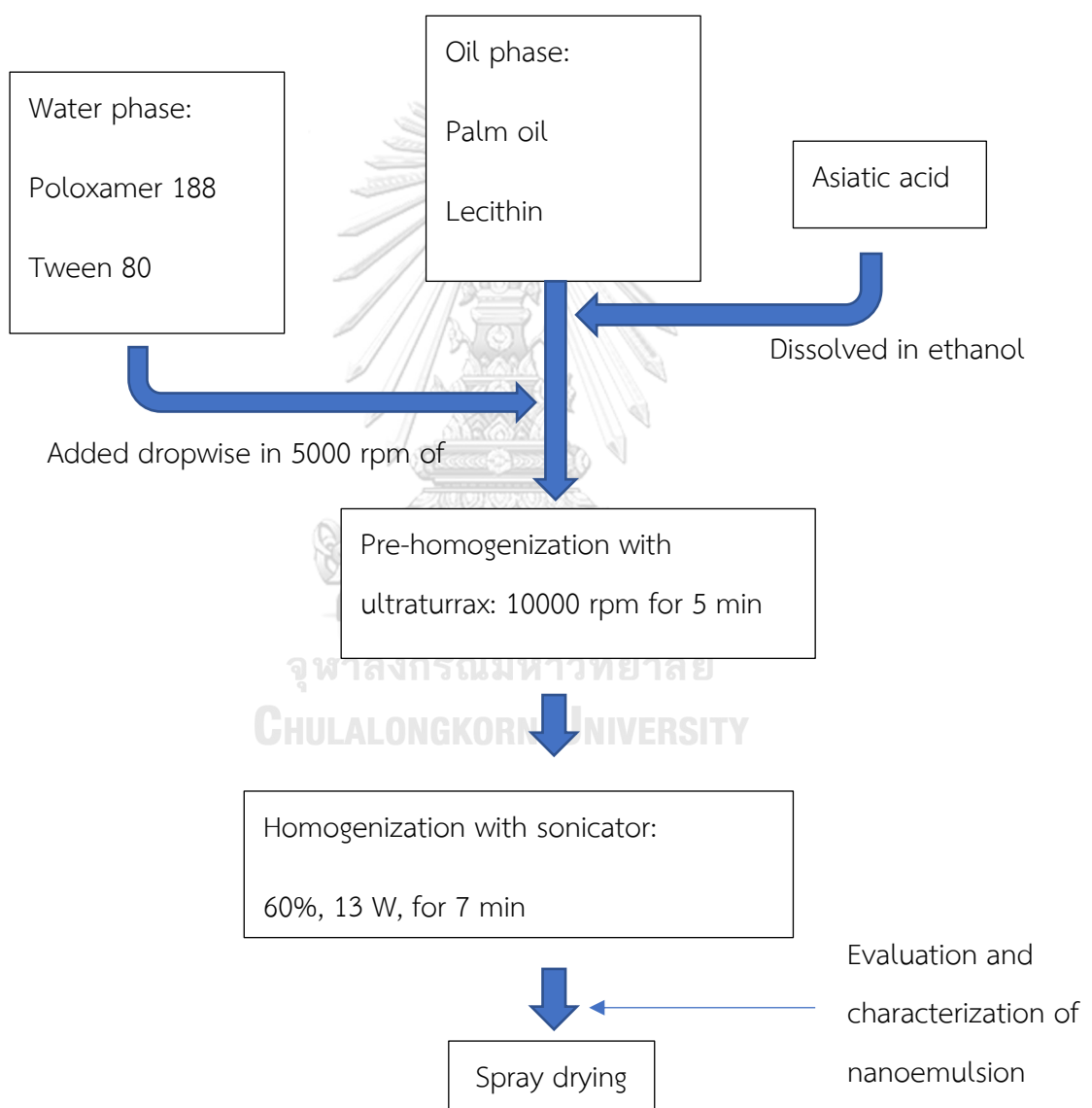
Figure 16 Schematic of asiatic acid nano/microencapsulate formulation

Table 4 Formulation of asiatic acid nano/microencapsulate

Role	Substance	LPM1	LPM2	LPM3	LTM1	LTM2	LTM3	SPM1	SPM2	SPM3
Active compound	Asiatic Acid	0.2 g	0.2 g	0.2 g	0.2 g	0.2 g	0.2 g	0.2 g	0.2 g	0.2 g
	Ethanol	9.8 mL	9.8 mL	9.8 mL	9.8 mL	9.8 mL	9.8 mL	9.8 mL	9.8 mL	9.8 mL
	Palm Oil	1 g	1 g	1 g	1 g	1 g	1 g	1 g	1 g	1 g
Oil phase	Lecithin	1 g	1 g	1 g	1 g	1 g	1 g	-	-	-
	Span 80	1 g	-	-	1 g	1 g	1 g	1 g	1 g	1 g
	Poloxamer 188	0.3 g	0.3 g	0.3 g	-	-	-	0.3 g	0.3 g	0.3 g
Water phase	Tween 80	-	-	-	0.3 g	0.3 g	0.3 g	-	-	-
	Water	25.7 mL	24.7 mL	23.7 mL	25.7 mL	24.7 mL	23.7 mL	25.7 mL	24.7 mL	23.7 mL
Spray dry carrier	Maltodextrin	1.945 g	2.945 g	3.945 g	1.945 g	2.945 g	3.945 g	1.945 g	2.945 g	3.945 g
	Magnesium stearate	0.055 g	0.055 g	0.055 g	0.055 g	0.055 g	0.055 g	0.055 g	0.055 g	0.055 g

The asiatic acid nanoemulsion formulation was carried out in both phases as shown in the Figure 16. The process was started with melting palm oil from the storage and adding oil phase surfactant. On the other hand, asiatic acid was dissolved in 9.8 mL of ethanol and added into the oil phase. Pre-homogenization was started with low speed (5000 rpm), and water phase (consisting of surfactant and deionized water) was then added dropwise to the oil phase in the glass beaker. Ultraturrax speed was then increased to 10000 rpm until it reached 5 minutes. The process was then continued with homogenization with a probe sonicator for 7 minutes in 13 W strength and 60% amplitude to form asiatic acid nanoemulsion. All weighing steps followed what was written on the Table 4 according to the prepared formula.

3.2.3. Spray drying of Asiatic acid-Palm oil nanoemulsion

The spray drying process was carried out after the nanoemulsion had formed and stored for about 5 days. Maltodextrin as a carrier and magnesium stearate as a lubricant were added just before drying. Previously, both ingredients were weighed as written in the Table 4 and dissolved in 7 ml hot deionized water. Maltodextrin solution and magnesium stearate were then poured gradually into the nanoemulsion with constant stirring of 5000 rpm. The mixing process was continued for 5 minutes and dried under the conditions written in the Table 5.

Table 5 Parameters in Spray Drying Process

Parameter	Value
Spray gas flow	40 mm (473 Liters/hour)
Inlet temperature	70°C
Aspirator rate	90% (35 m^3/hour)
Pump	15% (5.5 ml/min)
Nozzle clean	1

3.2.4. Characterization of spray dried Asiatic acid-Palm oil nanoemulsion

3.2.4.1. Particle size and zeta potential

Particle size analysis was carried out by wet and dry method. Nanoemulsion and redispersed product of nano-asiatic acid droplet size and zeta potential were determined using Zetasizer Nano ZS. The principle of this instrument involves dynamic light scattering and electrophoresis in the analysis. Prior to the measurement, all of the samples were diluted to the ratio of 1: 100 in deionized water to prevent multiple scattering effects during size analysis. Triplicate samples along with three measurements were considered for ensuring repeatability of the analysis (54). The results of this evaluation were described by the droplet size (intensity weighted mean diameter, Z-average diameter), droplet size distribution in polydispersity index (PDI) and zeta potential of the nanoemulsions (113).

In the meantime, dry products were evaluated by morphologically-directed raman spectroscopy (MDRS) using a Malvern Morphologi 4-ID in dry method. At 3 bar of air pressure, dry powder of pure asiatic acid and microparticles were spread on a glass plate and analyzed under calibrated conditions and the appropriate magnification. These observations yielded the mean particle size of number distribution, D90, D50, and D10 values. Span value was measured from D90, D50, and D10 to indicate particle size distribution, with a larger span value indicating a more extensive size distribution. Sharp and narrow peak showed homogeneous particle size (114). The sample span was defined by the equation below:

$$Span\ value = \frac{(D90 - D10)}{D50}$$

3.2.4.2. Particle shape and morphology by SEM and TEM

The morphology of asiatic acid nanoemulsion were observed with a Transmission Electron Miscroscope (TEM) at 80 kV. Approximately 5 µL of diluted

nanoemulsion (1/100) was dropped onto 3 mm carbon film coated copper grid, stained with 1% phosphotungstic acid solution for 30 seconds, and kept in room temperature for 3 h to dry, before being analyzed by TEM. Film imaging mode was used in the observation to obtain TEM images (48).

While, Scanning Electron Microscopy (SEM) was used to observe the shape and morphology of pure materials, physical mixture and microencapsulate at 10 kV and 10 mA. Samples were initially fixed on a double-sided adhesive carbon tape and sputter coated with gold for 3 min at 25 mA. Some pictures were then obtained at several magnification

3.2.4.3. Functional group changes with FT-IR

The pure materials, physical mixture and microencapsulate were studied by Fourier Transform Infrared (FT-IR) spectroscopy. IR determined interactions between asiatic acid and excipients used in formulation. Samples were prepared in potassium bromide (KBr) disks, pressed and analysed using an IR spectrophotometer. The scanning range was 400–4000 cm^{-1} at a resolution of 1 cm^{-1}, and IR spectra results were recorded (115).

3.2.4.4. Heat properties with TGA

The heat resistance of the microencapsulate, physical mixture and unprocessed compound were evaluated with Thermogravimetric Analysis (TGA). The temperature was increased from 0°C to 600°C at a rate of 10°C/min using TGA (NETZSCH TG 209 F3 Tarsus$^{®}$). In this evaluation, the mass changes and decomposition temperatures of the samples were determined.

3.2.4.5. Crystallinity changes with X-ray diffractometer

Raw materials, physical mixture and microencapsulate were analyzed by X-ray diffraction (XRD) at 40 kV and 30 mA to determine the degree of crystallinity before and after processing. Patterns were obtained with a beam angle varying from 5° to 40° and a step size of 0.023° (116). Changes in crystallinity degree were not only seen after formulation, but could also occur during storage.

3.2.5. Total product recovery (yield)

The total product recovery (PRec.) was calculated from spray drying process. Total product recovery was an important parameter to determine the efficiency of a formulation process (116). It was defined as the percentage ratio of the final mass that collected to the initial mass delivered to the drying vessel, as shown below (65):

$$PRec. = \frac{collected\ product - powder\ mass}{total\ mass\ of\ solid\ in\ the\ feed} \times 100\%$$

3.2.6. Asiatic acid content and recovery

Accurately weighed samples were dissolved in methanol and active substance concentration was determined using an high pressure liquid chromatography (HPLC) and calculated by proportional calibration curve of asiatic acid. The test conditions used were the mobile phase of acetonitrile : water (45: 55) which flew at a speed of 1mL/min. The injection volume of each observation was 20 μL and the asiatic acid peak was observed at a wavelength of 205 nm. Each sample was analyzed 3 times and the mean values were reported. Asiatic acid content (Cont.) was obtained by dividing the mass of asiatic acid in the analyzed sample to the total sample mass (116), as follows:

$$\text{Cont.} = \frac{\text{AA mass in sample}}{\text{Total sample mass}} \text{ x } 100\%$$

Asiatic acid recovery (AA Rec.) was calculated as shown below:

$$\text{AA Rec.} = \frac{\text{Product Rec. x Cont.}}{\text{AA content in feed}}$$

Asiatic acid content measurement used microencapsulate product and physical mixture at several sampling points to ensure product uniformity and homogeneity during mixing and precipitation process.

3.2.7. Moisture content

The microencapsulate as samples were initially weighed and the moisture content evaluation was done instrumentally. Moisture content balance was used to obtain samples moisture content by comparing the weight difference in the pan before and after drying process by infrared heat. Moisture content was automatically calculated as calculation shown below:

$$\text{Moisture content (\%)} = \frac{\text{initial weight} - \text{final weight}}{\text{final weight}} \text{x } 100$$

3.2.8. Flowing properties

Flow characteristics were determined from the compressibility index and Hausner ratio of spray dried products. The compressibilty index and hausner ratio could be determined by calculating the unsettled apparent volume (V_0) and final tapped volume (V_f) of the material as shown below:

$$\text{Compressibility Index} = 100 \times [(V_0 - V_f)/V_0]$$

$$\text{Hausner Ratio} = (V_0/V_f)$$

In addition, the compressibility index and hausner ratio could also be obtained from bulk density (P_{bulk}) and tapped density (P_{tapped}) as follows:

$$\text{Compressibility Index} = 100 \times [(P_{tapped} - P_{bulk})/P_{tapped}]$$

$$\text{Hausner Ratio} = (P_{tapped}/P_{bulk})$$

Based on these calculations, then the flow characteristics of the sample classified according to the Table 6 below (117):

Table 6 Scale of Flowability (114)

Compressibility index (%)	Flow Character	Hausner Ratio
≤ 10	Excellent	1.00-1.11
11-15	Good	1.12-1.18
16-20	Fair	1.19-1.25
21-25	Passable	1.26-1.34
26-31	Poor	1.35-1.45
32-37	Very poor	1.46-1.59
>38	Very, very poor	>1.60

3.2.9. Solubility test

The apparent solubility of the asiatic acid was analysed by adding excess sample to 10 ml of distilled water. The suspension was then sonicated at 25℃ until equilibrium or saturated solubility attained. Then the suspension was filtered with a 0.22 μm syringe filter. Asiatic acid concentration was determined by HPLC. Experiments were performed in triplicates and the mean values were calculated (116,118).

3.2.10. In-vitro release profile

Dissolution profile of asiatic acid was performed in simulated gastric and intestinal fluids. The asiatic acid release profile was determined by paddle method. The volume of the medium was 112.5 mL of 4% triton X-100$^{®}$ in 0.1 N hydrochloric acid for the first 2h, and then 37.5 mL of 4% triton X-100$^{®}$ in 0.20 M tribasic sodium phosphate solution was added to adjust the pH from 1.2 to 6.8 ± 0.05 for the remaining 1 h. The process of medium changes by adding the buffer and adjusting was within 5 minutes (119,120).

Pure asiatic acid, microencapsulate and the physical mixture (equal with 10 mg of asiatic acid) were filled in no. 1 gelatine capsule, added inside the sinker to the simulated fluids, and maintained at 37 ± 0.5℃ with 100 rpm stirring. After 5, 15, 30, 60, 120, 150, and 180 mins, 3,0 ml samples were taken, and the removed fluid was replaced by fresh simulated gastric or intestinal fluid. Samples were filtered using a pore size of 0.45 μm filter to remove undissolved particles. Afterward, samples were diluted in a mixture mobile phase to avoid the possible precipitation of solubilized asiatic acid. The concentrations of asiatic acid in the samples were measured by the HPLC assay method, and drug release data were collected (120,121).

3.2.11. Stability test

Microencapsulated asiatic acid products were stored in primary packages (glass bottle), sealed and kept in the climatic chamber. Storage conditions for accelerated conditions were at a temperature of 40 ± 2°C and a relative humidity of 75 ± 5%. Samples were kept up to six months and physical-chemical properties were evaluated at 3 and 6 months sampling time (122).

3.2.12. Molecular docking investigation

The 3D structures of the asiatic acid, captopril (as standard compound) and the target protein (ACE PDB ID 1O86) were available from PubChem (https://pubchem.ncbi.nlm.nih.gov/) and the RCSB PDB (http://www.rcsb.org/), respectively. Pymol 2.5 was used to remove water molecules and the lisinopril molecule from the 3D structure of the protein. Pyrx 0.8 was then used to perform molecular docking between asiatic acid and captopril with ACE. The conformation with the highest negative binding energy was chosen, and the docked complex was transformed to a 2D structure using BIOVIA Discovery Studio Visualizer 2021 (Biovia, San Diego, CA, USA) to analyze the interactions resulted at the binding site of 1O86 with asiatic acid and captopril (123,124).

3.2.13. Formula selection for In-vivo study

The formula that produced the product with the most optimal characteristics was selected for cell viability and in-vivo study. Physical and chemical characteristics specification of the nanoemulsion and spray dried microparticles must be met,

where the criteria or acceptance values of each specification have written in Table 7 below:

Table 7 Product specification and acceptance criteria

Specification	Acceptance value/criteria
Nanoemulsion particle size	< 500 nm
Zeta potential	> +30 mV or > -30 mV
Dry product particle size	<10 μm
Particle shape and morphology	Spherical shape and smooth surface
Product yield	> 70%
AA content recovery	> 60%

Products that met these criteria then was determined based on the increase in solubility and dissolution rate. Spray dried product with the highest solubility value and dissolution rate was observed for further safety to the cells and followed by an in-vivo study.

3.2.14. Cell viability
3.2.14.1. Cell culture

Caco-2 cells were routinely subcultured and seeded for this study. The old media was rinsed with PBS (1x, pH 7.4) and 1000 μl trypsin (0.25% Trypsin-EDTA 1x). Following that, DMEM media, heated FBS, Penicillin (10,000 units/mL)-Streptomycin (10,000 μg/mL), and L-glutamine 100mM (100X) were added and incubated at 37°C in a humidified condition of 5 percent CO_2. CaCo-2 cells with passage numbers ranging from 20 to 30 were seeded and used in viability test.

3.2.13.2. Caco-2 cell toxicity with MTT test

The seeded Caco-2 cells growth was examined microscopically for MTT assay and seeded 10 µl in 96-well plates, which were then filled with 10 µl of dissolved sample. After 24 hours, the media was replaced with MTT solution (0.5mg/ml) and incubated at 37°C for 3 hours. Light must be kept out of the incubation process. The MTT solution was then replaced with DMSO and the absorbance of each well was measured using a microplate reader (CLARIOstar®, BMG LABTECH, Germany) at 570 nm. Cell viability was calculated as a percentage of control due to the effects of asiatic acid, AA microparticle, and matrix.

3.2.15. Non-invasive antihypertensive activity

The study protocols were done in compliance with regulations for the care and use of experimental animals and were approved by the Institutional Animal Care and Use Committee of Faculty of Pharmaceutical Sciences, Chulalongkorn University (No. 21-33-009). The 12-hour dark/light HVAC (heating, ventilation, and air conditioning) system was used to house adult Sprague Dawley (SD) male rats (9 weeks old) that were purchased from Nomura Siam International, (Bangkok, Thailand), Following a week of habituation, animals were drank a high-salt (2% sodium chloride) diet for 10 weeks to develop hypertension. The treatment was then initiated after the rats blood pressure and ACE1 activity increased.
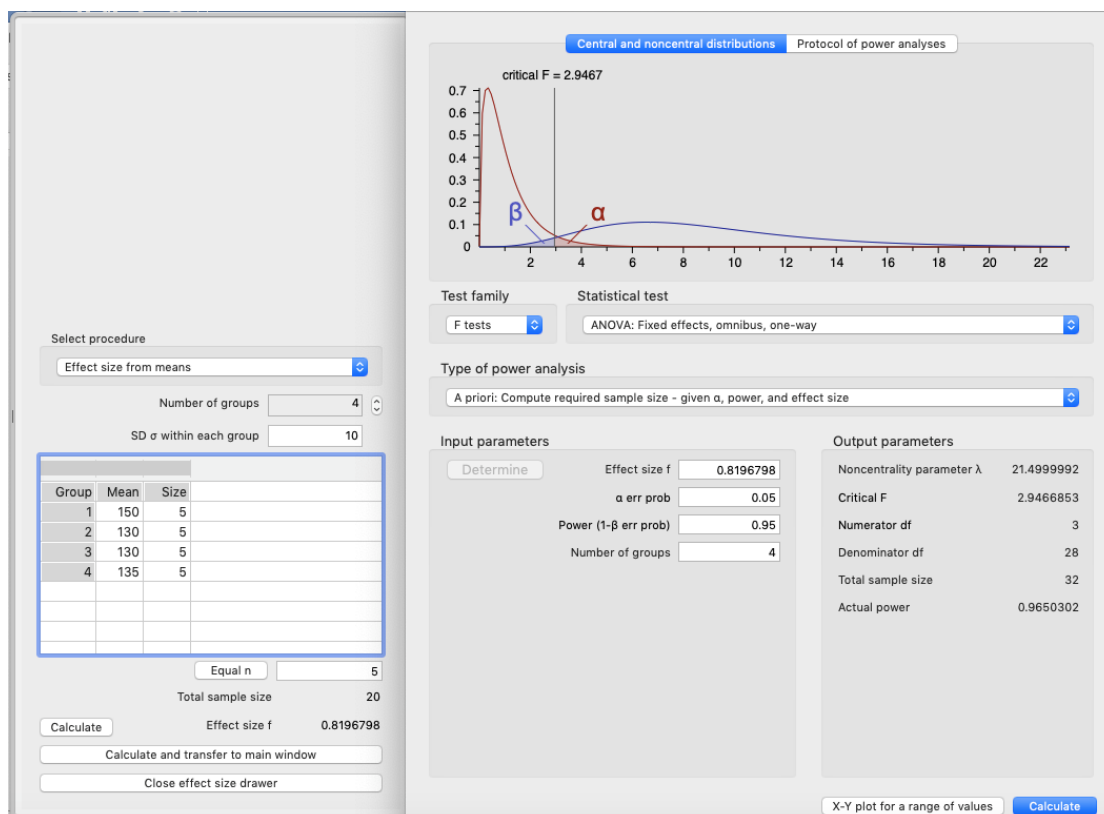
Figure 17 Minimum sample size by G* power analysis

The animals were subsequently split at random into one non-hypertensive group and four treatment groups (n = 8 per group) as calculated by G* power analysis and shown in Figure 17. The treatment was given orally asiatic acid, asiatic acid microparticle, captopril, or matrix daily. Oral dose of asiatic acid, AA microparticle (equivalent to 30 mg/kg/day of asiatic acid), matrix, or captopril (5 mg/kg/day) was provided for three consecutive weeks as shown in Figure 18 (A-B). Using non-invasive tail-cuff plethysmography, the systolic blood pressure was then recorded at 0, 2, 4, 5, 6, 7, 8, 9 and 10 weeks of salt induction and after 11, 12, and 13 weeks of treatment period. The instrument amplifier provided the pulse amplitude before recording the blood pressure as shown in Figure 18 (C-D). Each rat was measured three times, and the average values were determined. The result was then analyzed using two-way ANOVA. After euthanasia, blood samples were obtained and analyzed for ACE1 activity and the blood chemistry (6–9,32). Histological changes of aorta, heart and kidney also determined after collected in the end of the study,

embedded in paraffin, sliced in 0.3 micron of thickness, stained with hematoxylin-eosin, and observed microscopically at the appropriate magnification. The results of histology of tissue were then analyzed descriptively based on a minimal, mild, moderate or marked on scale of damage severity (124,125).
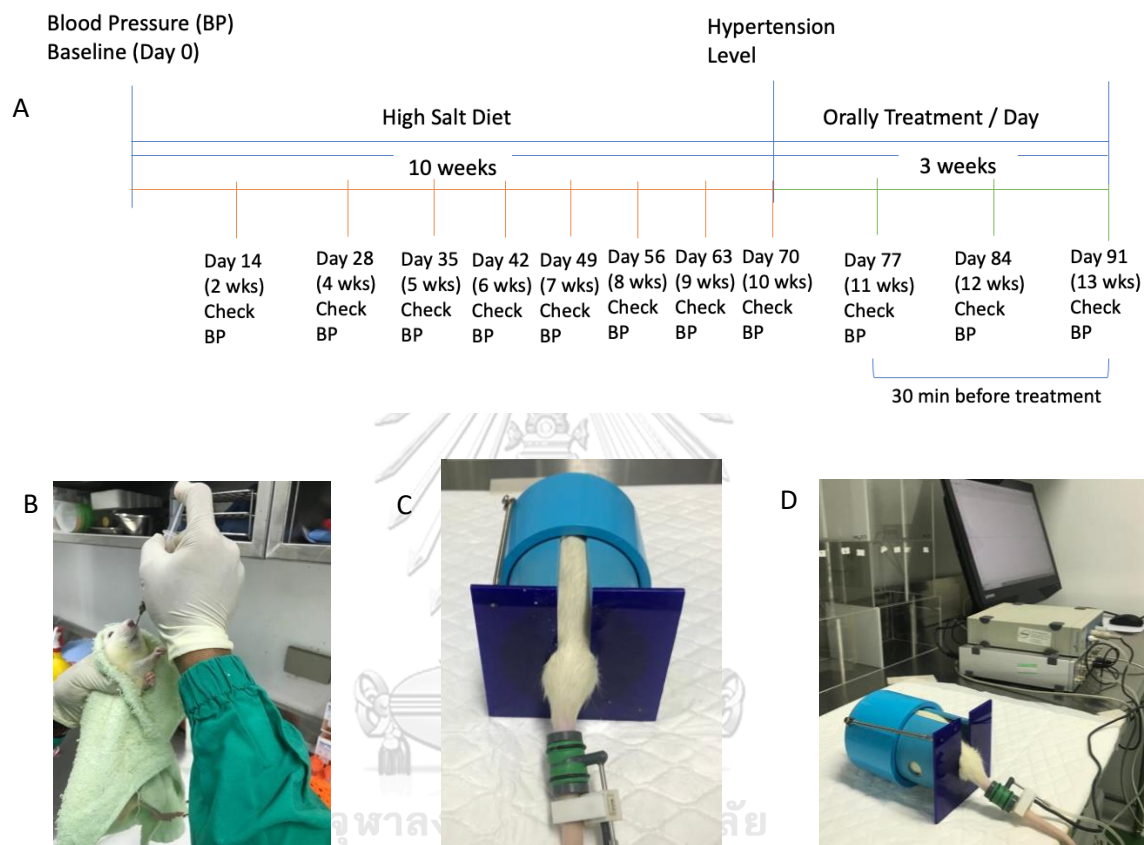
Figure 18 Antihypertensive activity study in rats: Study timeline (A), Orally treatment administration (B), Indirect blood pressure test (C), Blood pressure test instrument (D).

3.2.16. ACE1 inhibitory in serum

At week 9 of hypertension induction, serum was obtained from the tail vein, and at the end of the treatment process, serum was collected directly from the heart as shown in Figure 19. The serum of 0.5 ml collected blood was obtained then by

centrifugation. The ACE1 assay buffer, substrate, and enzyme, on the other hand, were prepared.
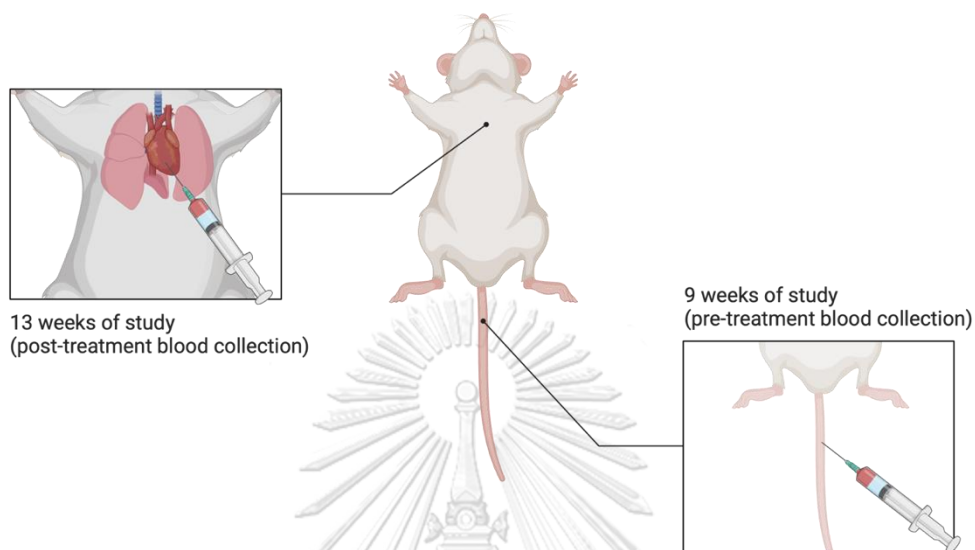
Figure 19 Rats blood collection site at pre- and post-treatment of animal study

On a 96-well clear bottom UV plate, 30 µl serum from each rat was used as a sample, with ACE1 assay buffer serving as a blank and ACE1 enzyme serving as a positive control. Each well solution was adjusted to 200 µl with ACE1 assay buffer, incubated for 10 minutes at 37℃, and then 50 µl of ACE1 substrate was added (previously diluted 5 folds with buffer). After removing the bubbles formed during mixing, the absorbance was measured using a microplate reader (CLARIOstar®, BMG LABTECH, Germany) at 345 nm for 60 minutes. The ACE1 activity of the rats in all groups was then calculated using serum absorbance and a blank by following equation:

$$\text{Sample ACE1 Activity} =$$

$$\frac{\left(\frac{|\Delta A_{345}|}{\Delta T}[Test\ Sample] - \frac{|\Delta A_{345}|}{\Delta T}[Blank]\right) \times (0.25) \times DF}{(0.34) \times V} U/ml$$

Where: $|\Delta A_{345}|$ = Absolute value of the change in absorbance

ΔT = Difference between T2 & T1 (min)

0.25 = Reaction volume (ml)

DF = Sample dilution factor

0.34 = Millimolar extinction of ACE1 Substrate

V = Enzyme/Sample volume (ml)

3.2.17. Statistical Analysis

All measurements were performed in at least triplicate. Values were given in the form of mean ± standard deviation. The statistical significance of the results was determined using one way ANOVA or two way ANOVA with GraphPad Prism Version 9.4.0, while for qualitative tests such as particle shape and morphology determined using descriptive. A p-value of less than 0.05 will be considered statistically significant. Statistical analysis ended with Tukey's post hoc determination.

CHAPTER 4

RESULTS

4.1. Physical appearances
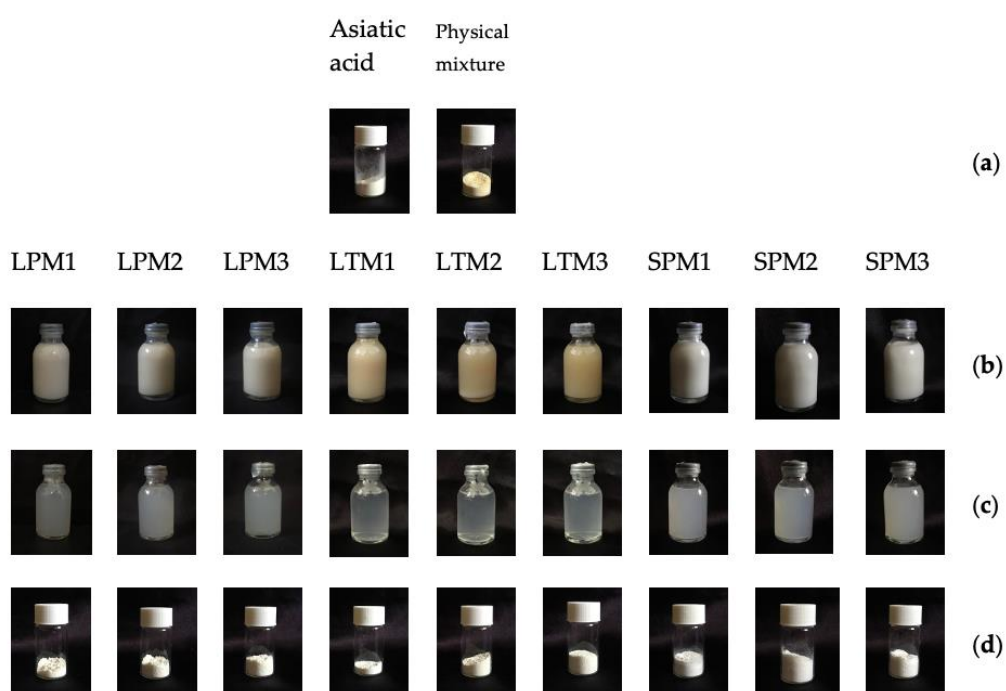
Figure 20 Physical appearances of asiatic acid, phsical mixture and all formula in several forms: (a) Powder; (b) Nanoemulsion; (c) Dispersed nanoemulsion in 1:100 ratio; and (d) Spray dried microparticle

The preparation process was successful in producing the desired output. The nanoemulsions were created and physically stable during the initial storage period, as shown in Figure 20. As the oil phase, palm oil may effectively distribute asiatic acid. As surfactants, span 80, poloxamer 188, lecithin, and tween 80 maintained the nanodroplets homogeneity in the aqueous phase.

After five days of storage, a spray drier was used to dry the nanoemulsion. As illustrated in Figure 20, maltodextrin as a carrier was successful in encapsulating the nanoemulsion and produce a microparticle matrix. The drying of the nanoemulsion resulted in the formation of microparticles that are physically good. These microparticles were continued in the evaluation that followed.

(a)   (b)   (c)
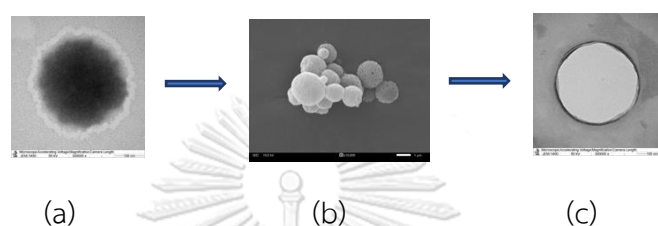
Figure   21 Droplet or particle morphology determined by SEM and TEM; (a) Nanoemulsion droplet with 300,000x magnfication by TEM; (b) Spray dried microparticle with 10,000x magnification by SEM; and (c) Redispersed nanoparticle droplet with 300,000x magnification by TEM

Figure 21 depicts the morphology of the particles and droplets that were obtained. Nanoemulsion droplets, spray-dried microparticles, and redispersed nanoparticles all had a spherical form. According to the TEM data, the inclusion of maltodextrin as a hydrophilic-nonionic carrier altered the appearance of the droplet, resulting a negative staining in a brighter core than before the spray drying procedure (Figure 21c).

4.2. Characterization of Asiatic acid nanoemulsion and microparticle
4.2.1. Particle size, distribution and zeta potential

Figure 22 illustrates the particle size, particle distribution, and zeta potential of nanoemulsion and dispersed microparticles. In the meantime, Figure 22 depicts the particle size and span value of microparticles in dry method. The droplet particle

size ranged from 181.6 to 271.1 nm, and the polydispersity index was less than 0.40, indicating the formation of a homogeneous nanoemulsion. By delaying the production of agglomerates, the nanoemulsion matrix was able to preserve its physical stability for up to five days. This was evident from the little changes in the nanoemulsion profile on the fifth day, as depicted in Figure 20. In addition, the particle size and span value of the produced microparticles were smaller than those of asiatic acid powder (6.05 µm).

The zeta potential of the produced nanoemulsions and microparticles was greater than -30 mV. It could be presumed that the stable products possessed a high resistance to particle aggregation were created. The nanoemulsion negative charge was likely due to the presence of free fatty acids of the oil phase. In the meantime, the drop in the zeta potential value of the microparticles might be a result of maltodextrin efficacy as a non-ionic carrier in the spray drying process used to encapsulate nanoemulsions, including their free fatty acid components.
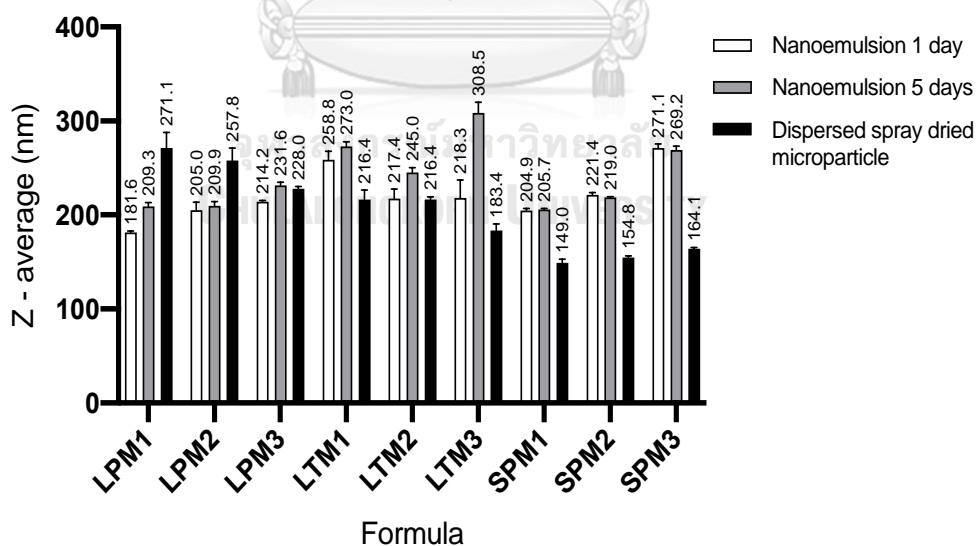
(a)
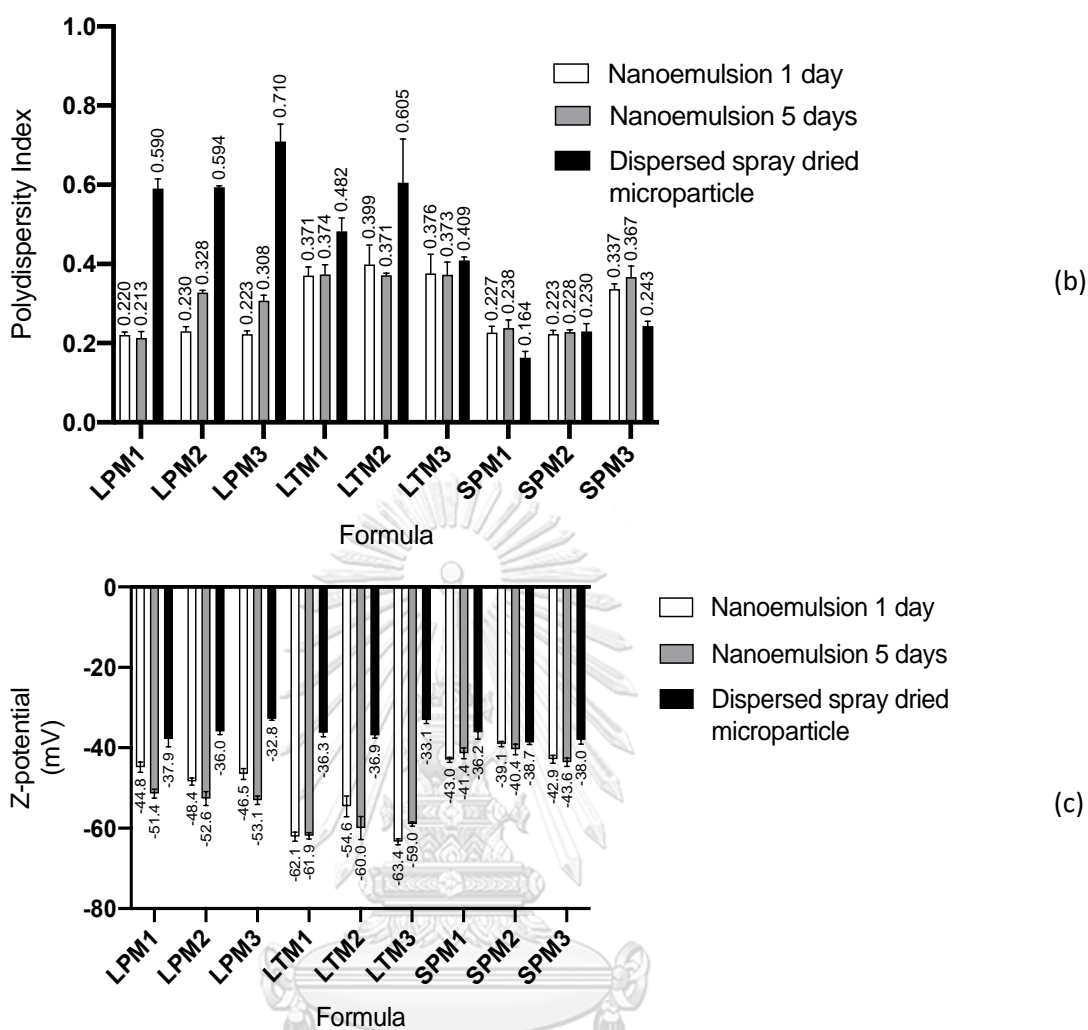
Figure 22 Zetasizer wet method result of nanoemulsion and dispersed spray dried microparticle: (a) Particle size (b) Particle distribution; and (c) Zeta potential

In Figure 23, LPM microparticles had a lower particle size, whereas LTM microparticles showed more uniform particle size. However, when dispersed in water, all microparticles could be rapidly dispersed into particle size between 149.0 and 271.1 nm. This result demonstrates that the surfactant had also been successful in creating spray-dried microparticles with a lower particle size than pure asiatic acid, which rapidly disperse in water into nanometers scale.
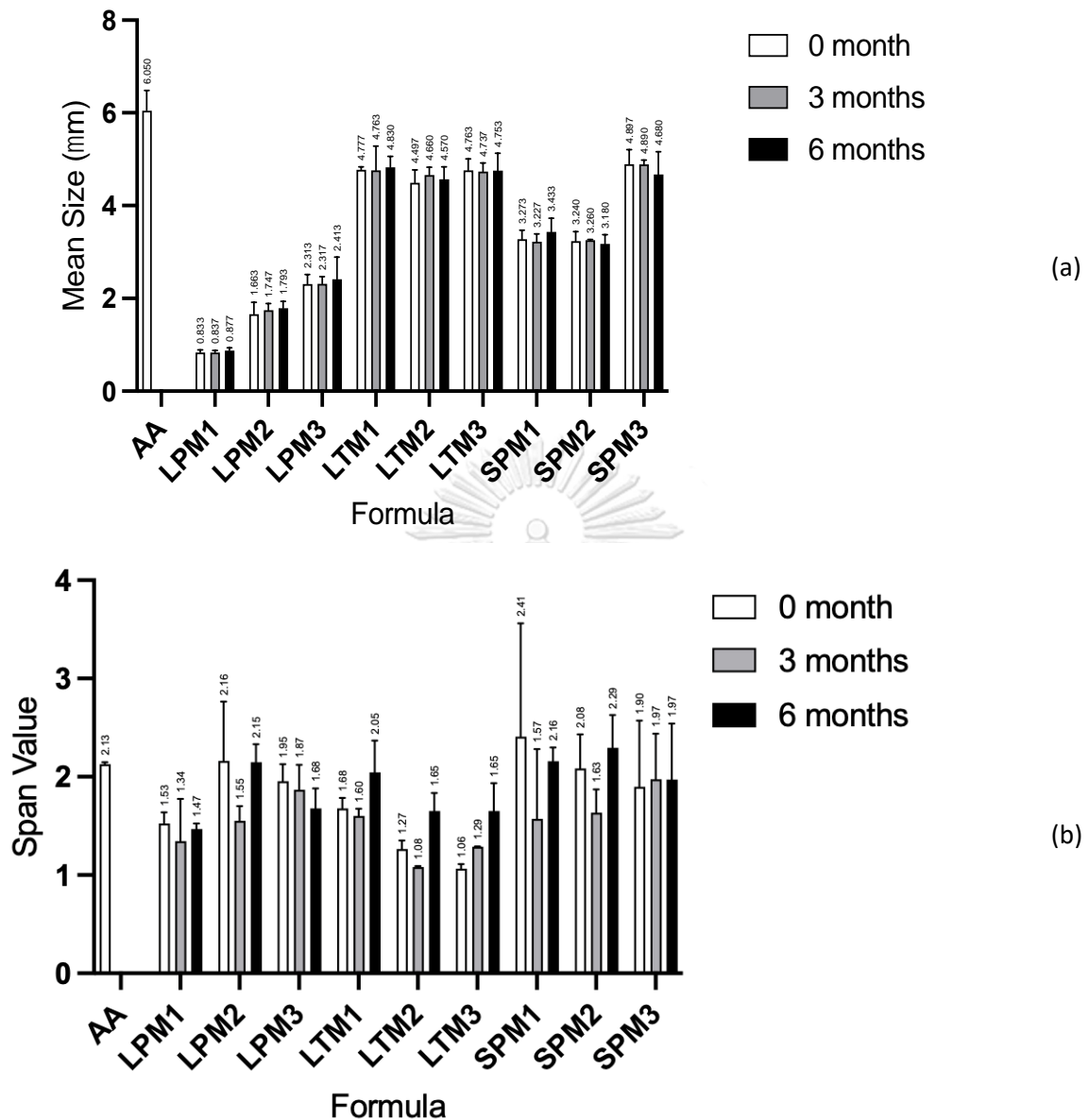
Figure 23 Dry method particle characterization of spray dried microparticle: (a) Mean particle size (b) Span value of particle distribution.

4.2.2. Particle shape and morphology

Figure 24 shows the SEM-determined particle shape and morphology of the raw material, physical mixture, and microparticle product. Figure 25 illustrates the nanoemulsion TEM results meanwhile. Asiatic acid, with its heterogeneous size and

shape produced a non-uniform shape and morphology physical mixture microparticle. However, nanoemulsions were obtained in a spherical shape, and the spray drying technique was able to produce microparticles with a spherical or nearly spherical shape and a smooth particle surface.
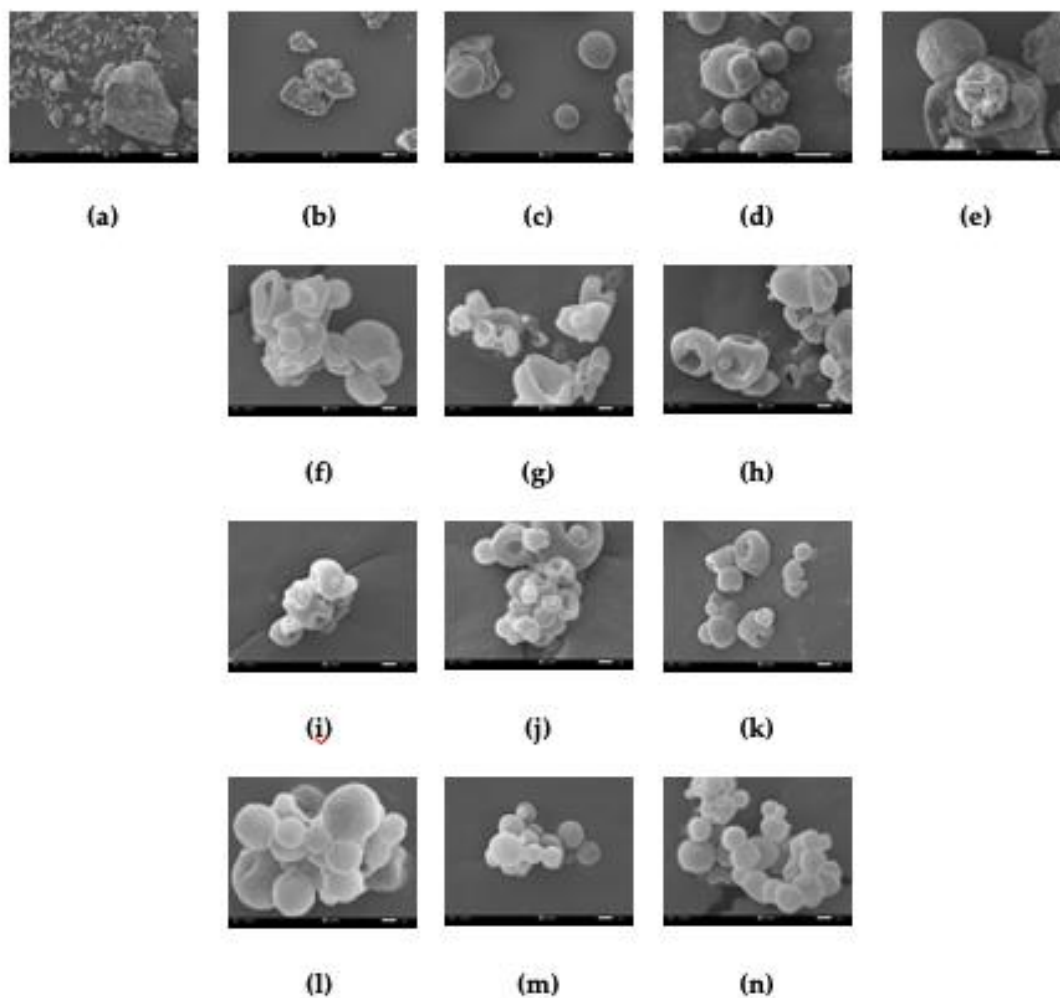
Figure 24 SEM result of raw materials, physical mixture and spray dried microparticle: (a) Asiatic acid (b) Lecithin and (c) Maltodextrin in 1000x magnification; (d) Poloxamer 188 in 50x magnification; (e) Physical mixture in 1000x magnification; (f) LPM1 (g) LPM2 (h) LPM3 (i) LTM1 (j) LTM2 (k) LTM3 (l) SPM1 (m) SPM2 and (n) SPM3 in 10,000x magnification.
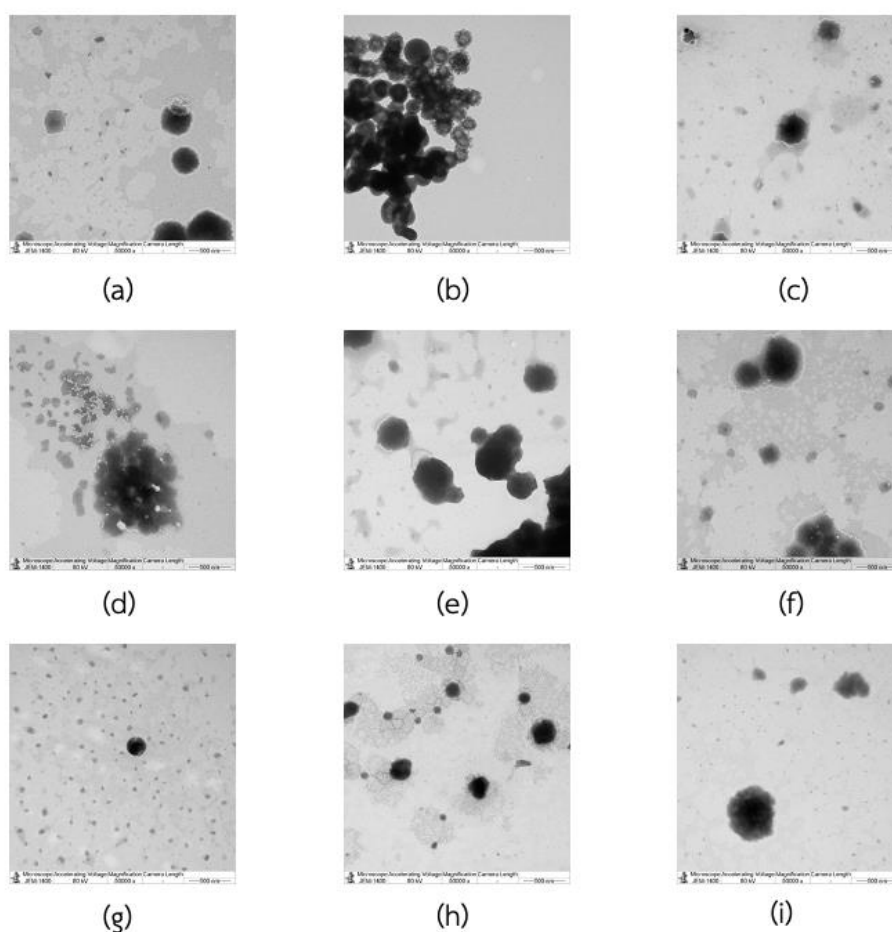
Figure 25 TEM result of nanoemulsions in 50,000x magnification: (a) LPM1 (b) LPM2 (c) LPM3 (d) LTM1 (e) LTM2 (f) LTM3 (g) SPM1 (h) SPM2 (i) and SPM3.

4.2.3. Fourier transform infrared

IR spectra of raw materials, physical mixture and products are shown in Figure 26. Asiatic acid (a) was characterized and showed principal absorption peaks at 2922.56 cm^{-1} (C-H aliphatic asymmetric), 2870.57cm^{-1} (C-H aliphatic symmetric), 1689.53cm^{-1} (C=O), 3392.90cm^{-1} (O-H), 1047.38cm^{-1} (C-O) and 680.73cm^{-1} (R-C=O). In the physical mixture (e) and products (f - n) profiles, the principal absorption peaks were not disappeared, while new peaks other than the specific peaks belonging to raw materials also did not appear. This result showed that the encapsulation by polymer and carrier was not affected by new chemical bonds that can change the molecular structure of asiatic acid significantly.
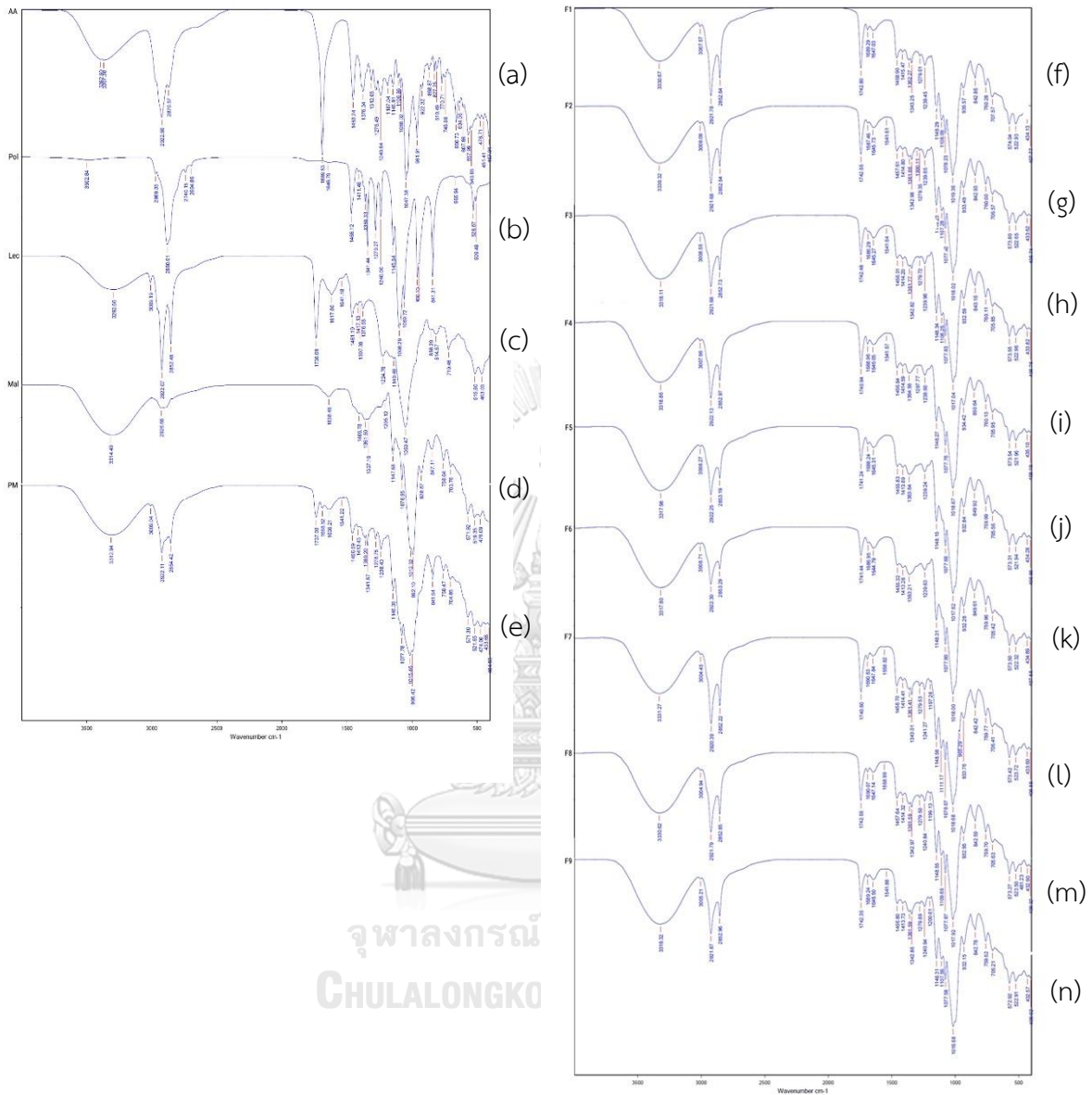
Figure 26 FT-IR spectra of raw materials, physical mixture and spray dried microparticle: (a) Asiatic acid; (b) Poloxamer 188; (c) Lecithin; (d) Maltodextrin; (e) Physical mixture; (f) LPM1; (g) LPM2; (h) LPM3; (i) LTM1; (j) LTM2; (k) LTM3; (l) SPM1; (m) SPM2; and (n) SPM3.
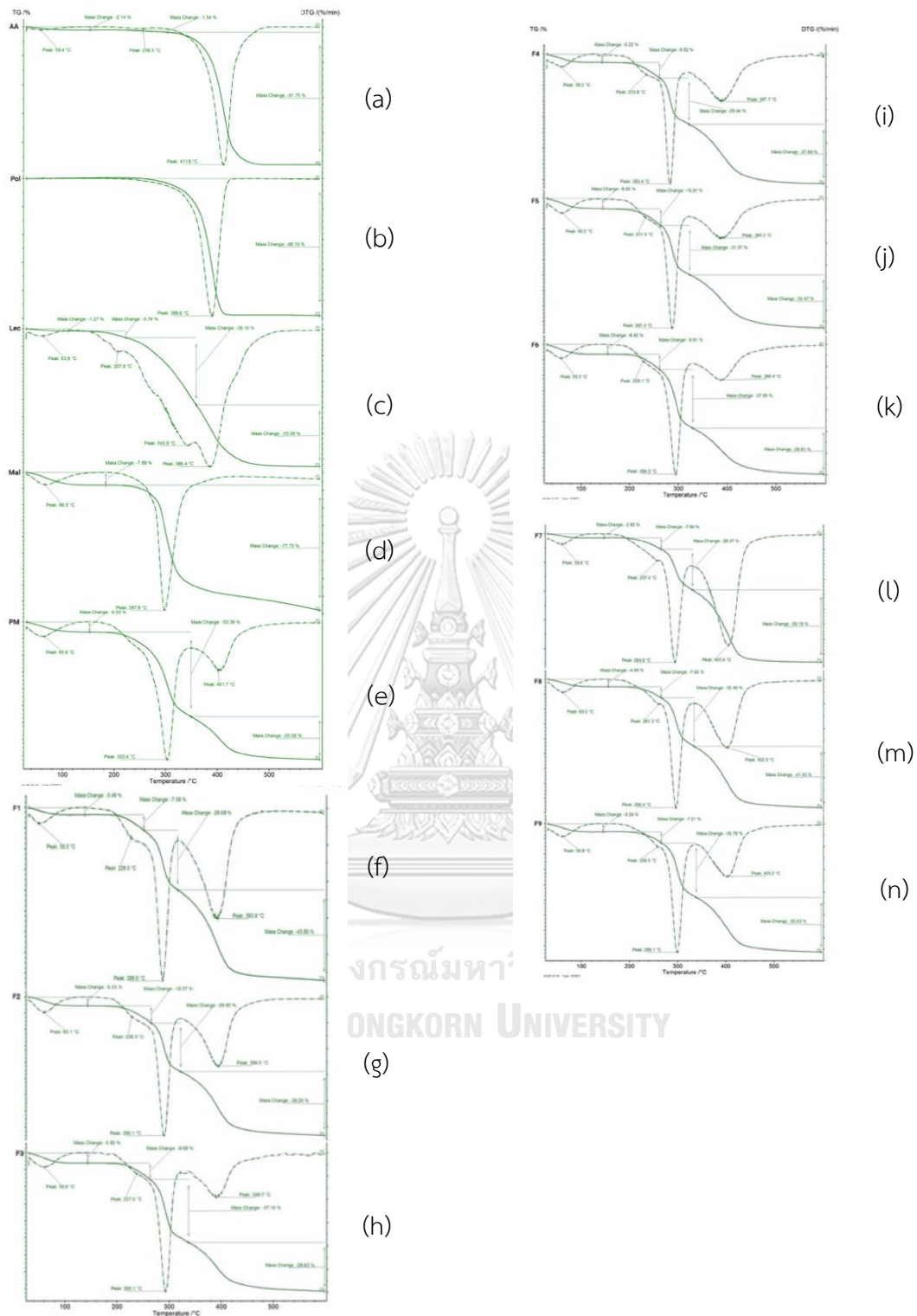
Figure 27 TGA spectra of raw materials, physical mixture and spray dried microparticle: (a) Asiatic acid; (b) Poloxamer 188; (c) Lecithin; (d) Maltodextrin; (e) Physical mixture; (f) LPM1; (g) LPM2; (h) LPM3; (i) LTM1; (j) LTM2; (k) LTM3; (l) SPM1; (m) SPM2; and (n) SPM3.

4.2.4. Heat resistance

Heat resistance characteristics of raw materials, physical mixture and products are shown in Figure 27. Products spectrum (f-n) shows a similar profile to physical mixture (e), with peaks obtained which were specific to asiatic acid and maltodextrin. This was related to the FTIR data, which illustrates that the encapsulation of asiatic acid as an active ingredient in carriers and other excipients did not form new chemical bonds.

4.2.5. X-ray diffractometer

The crystallinity of asiatic acid before and after the formulation process are shown in Figure 28. No peaks other than raw materials were observed. Peak of poloxamer 188 (b), lecithin (c) and maltodextrin (d) were shown in the physical mixture (e) and product (f - n) profiles according to the excipients of the formula, while the peak profile of asiatic acid (a) did not change. This indicated that the preparation process and stress involved did not result in a new structure or crystallinity changes.
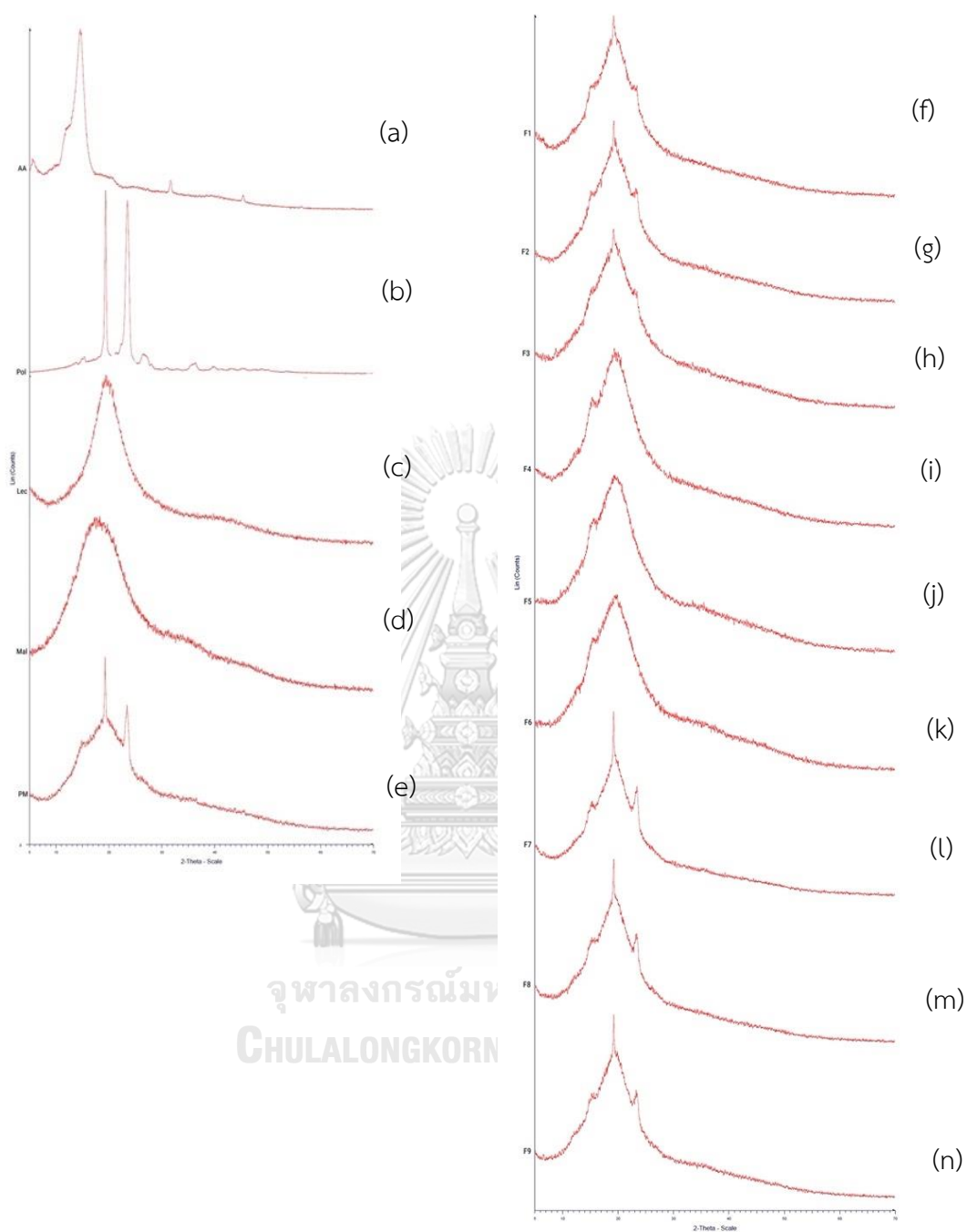
Figure 28 X-ray diffractogram of raw materials, physical mixture and spray dried microparticle: (a) Asiatic acid; (b) Poloxamer 188; (c) Lecithin; (d) Maltodextrin; (e) Physical mixture; (f) LPM1; (g) LPM2; (h) LPM3; (i) LTM1; (j) LTM2; (k) LTM3; (l) SPM1; (m) SPM2; and (n) SPM3

4.3. Total product recovery (yield)
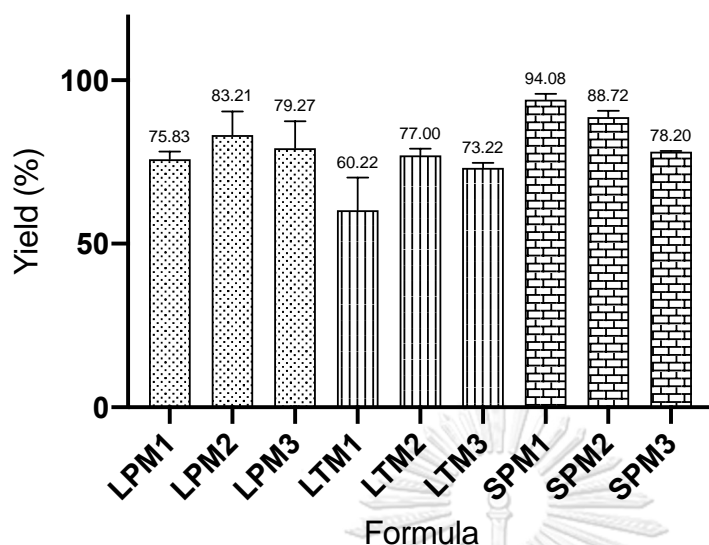
Figure 29 Yield of microparticle product after formulation

The overall manufacturing procedures included homogenization, ultrasonication, and spray drying. Figure 29 illustrates the amount of recovered product. Due to the low maltodextrin concentration in LTM 1, a portion of the mass adhered to the walls of the drying chamber and cyclone, reducing the amount of dry product that could be accommodated in the collector. In contrast, in other formulations including maltodextrin and poloxamer 188 as a surfactant, the yields were fairly high, exceeding 70 percent. These results were consistent with the target of production process efficiency.

4.4. Asiatic acid content and recovery

Figure 30 displays the results of a HPLC determination of the asiatic acid content of microparticles (a). The AA value profile for each preparation changed equally to the amount of maltodextrin utilized. The results were between 3.14 and 5.80% in all 9 formulations. As demonstrated in Figure 30 (b), the asiatic acid recoveries were range from 55.87 to 85.41 percent. This figure was determined based

on AA concentration and product yield, which reflects the proportion of asiatic acid produced relative to the beginning weight.

(a)

(b)
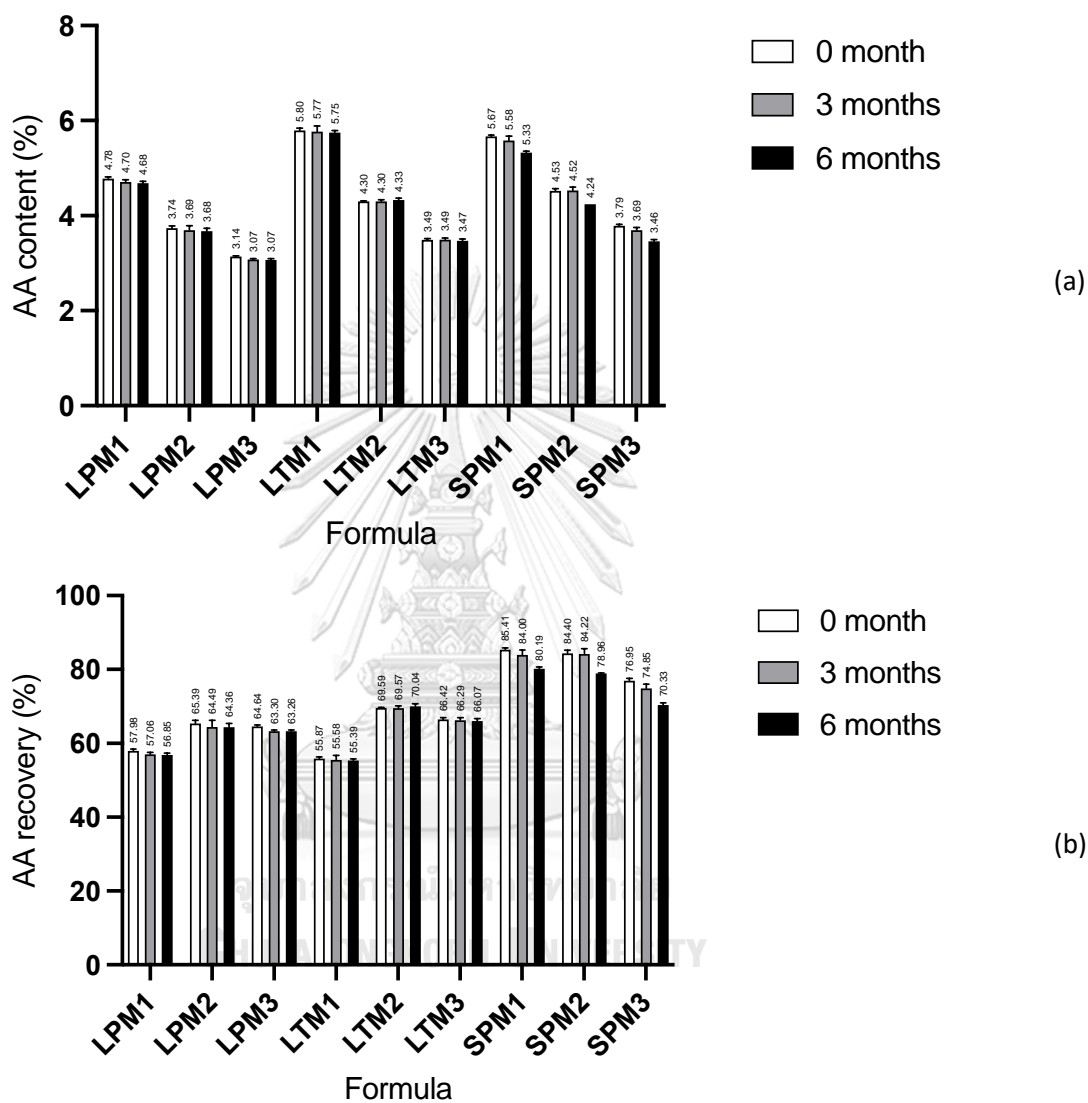
Figure 30 (a) Asiatic acid content and (b) Asiatic acid total recovery in the microparticle dry product.

Observations lasting six months were utilized to determine the chemical stability of asiatic acid under accelerated storage conditions. Both asiatic acid content and recovery did not change significantly on the 3rd and 6th month determination. The

change did not surpass 5% of the initial value, indicating that the microparticle system could retain the asiatic acid stability throughout storage under airtight conditions.

4.5. Moisture content
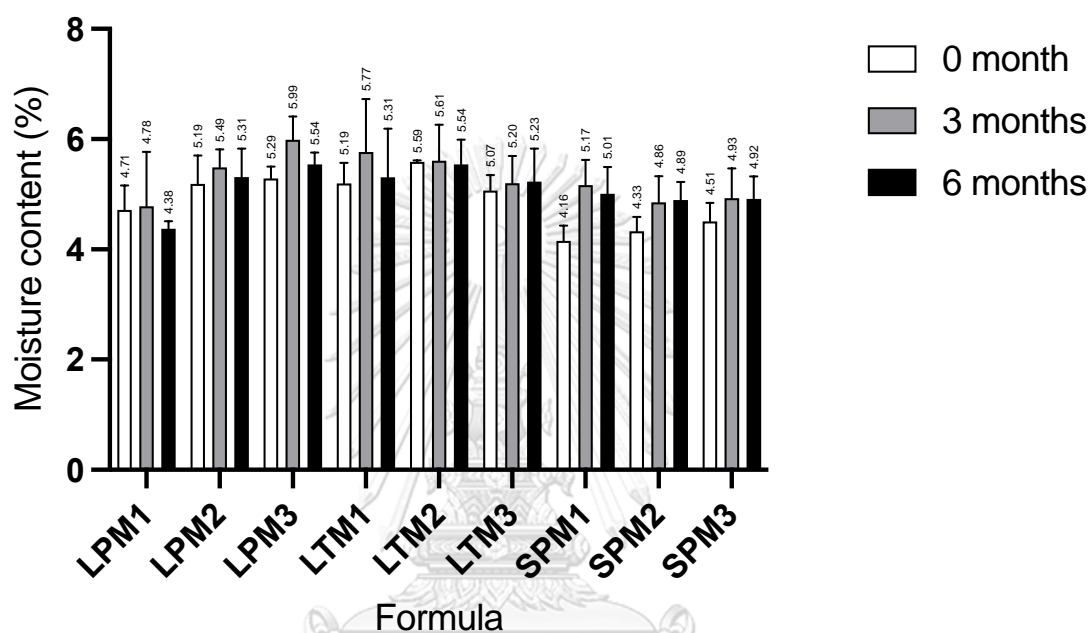
Figure 31 Moisture content of microparticle in 0, 3 and 6 months of storage

The results of observing the moisture content of all formula for six months under airtight storage are displayed in Figure 31. The obtained moisture content values are pretty satisfactory, ranging from 4.16 to 5.99%. Considering that there was no significant change in value during storage, the possibility for the formation of agglomerates with larger particle size was minimal.

4.6. Flowing Properties

Flowability of the spray dried products was obtained by calculating the Hausner ratio based on the initial volume and tapped volume. The results of 0, 3, and 6

months evaluation were written in Table 8. Based on the value of the Hausner ratio, it could be seen that the flowing properties of all formulas were not good enough and included in the Passable classification.

Table 8 **H**ausner ratio of spray dried nanoemulsion products

Formula	Hausner ratio		
	0 month	3 months	6 months
LPM1	1.31 ± 0.05	1.27 ± 0.00	1.31 ± 0.02
LPM2	1.32 ± 0.08	1.29 ± 0.04	1.28 ± 0.02
LPM3	1.33 ± 0.04	1.26 ± 0.09	1.30 ± 0.03
LTM1	1.28 ± 0.02	1.30 ± 0.02	1.31 ± 0.06
LTM2	1.24 ± 0.01	1.28 ± 0.01	1.27 ± 0.01
LTM3	1.28 ± 0.02	1.31 ± 0.01	1.30 ± 0.04
SPM1	1.33 ± 0.04	1.36 ± 0.06	1.32 ± 0.04
SPM2	1.33 ± 0.04	1.32 ± 0.03	1.32 ± 0.03
SPM3	1.33 ± 0.02	1.31 ± 0.05	1.33 ± 0.04

4.7. Solubility test

The solubility of asiatic acid in deionized water was measured after 24 hours of shaking. Figure 32 shows the visual looks of the solubility test, whereas Figure 33 depicts the solubility values. In every formulation, wettability and solubility were improved relative to asiatic acid powder. As excipients, lecithin, tween 80, and maltodextrin formed microparticles with

the maximum solubility for asiatic acid, which was 25 to 31 times higher than the powder form. The evaluation also indicated that the formula with poloxamer 188 could form microparticles with favorable physical properties, however, its presence in the vicinity of asiatic acid could limit the diffusion of water to interact and dissolve asiatic acid from the system.
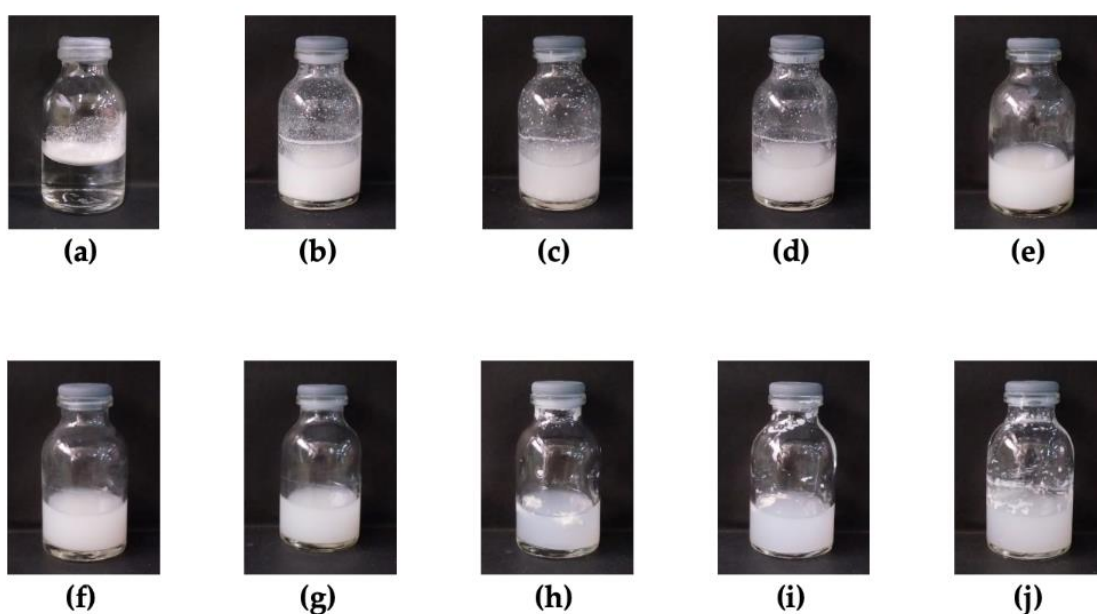
Figure 32 Visual appearance of the powder and microparticle after dispersed in deionized water: (a) Asiatic acid; (b) LPM1; (c) LPM2; (d) LPM3; (e) LTM1; (f) LTM2; (g) LTM3; (h) SPM1; (i) SPM2; (j) SPM3.
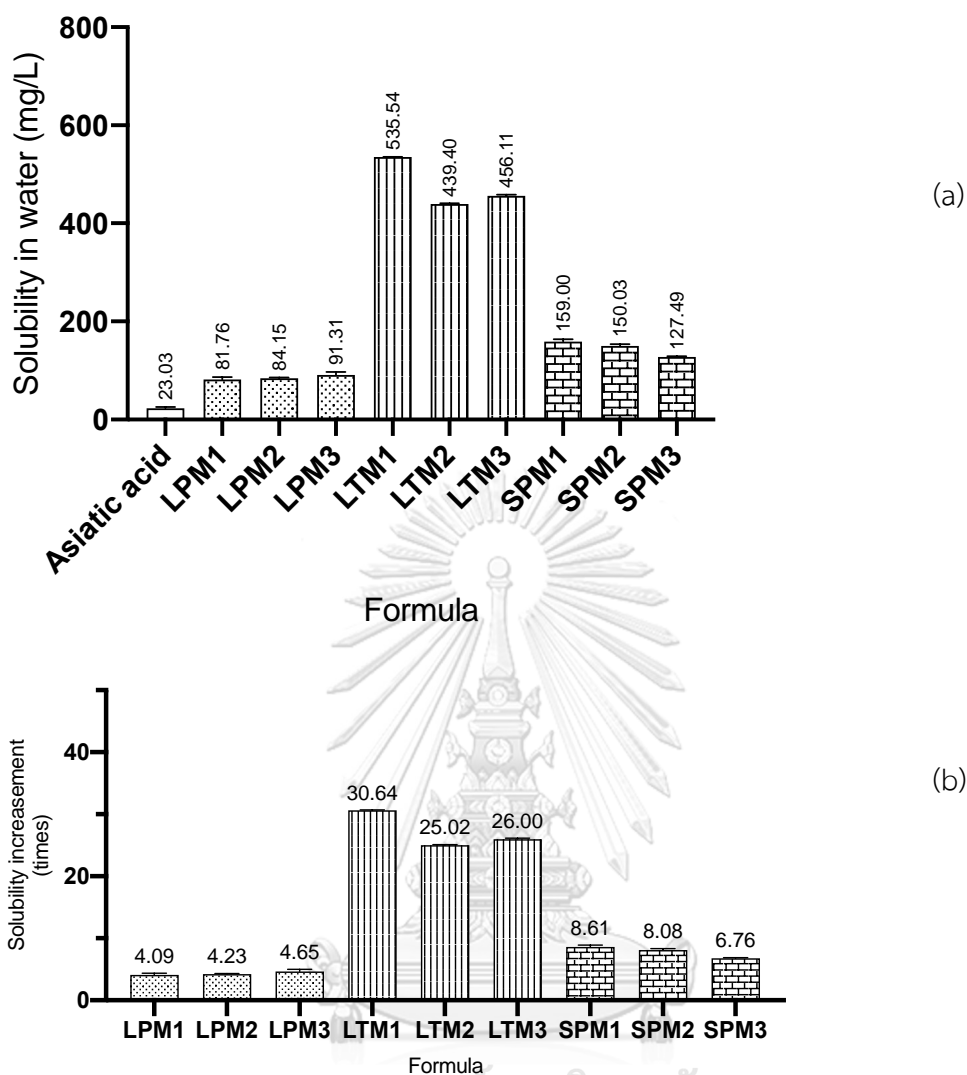
Figure 33 Solubility data of asiatic acid in deionized water: (a) Solubility of asiatic acid before and after formulation (mg/L) (b) Solubility improvement of asiatic acid in each formula compared to the pure form.

4.8. In-vitro release profile

Figure 34 displays the in-vitro dissolution profile of asiatic acid. The first two hours of AA release happened in gastric juice without pepsin, while the next 1 hour occurred in phosphate buffer pH 6.8. Both mediums were treated with 4% triton X-100 to facilitate the release of asiatic acid and make it readable on the HPLC equipment. Figure 34 (b) demonstrates that the dissolving profile of asiatic acid in the

system created with lecithin, tween 80, and maltodextrin was superior than asiatic acid powder and its physical mixture. This pertained to the asiatic acid microparticle solubility data shown in Figure 33.

Table 9 displays the area under the curve (AUC) and dissolution efficiency (DE) of asiatic acid over 180 minutes. LTM2 had greater AUC and DE values than LTM1, which were 14725.10 $\pm$ 480.60 and 81.81 $\pm$ 2.67, respectively. This result was significantly ($p < 0.05$) greater than the AUC and DE values of asiatic acid powder, which were only 11392.54 $\pm$ 649.89 and 63.29 $\pm$ 3.61, respectively. Based on these results, it was decided that LTM2 was the chosen formula for use in cell and animal studies.

(a)

(b)
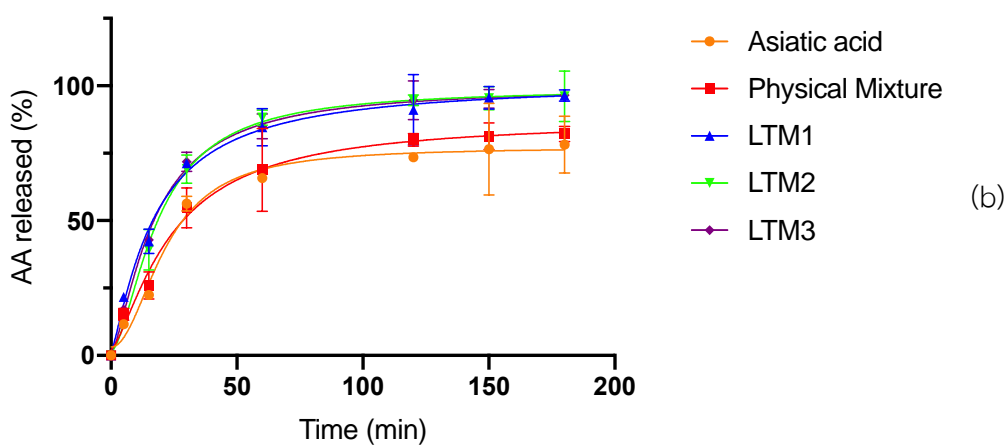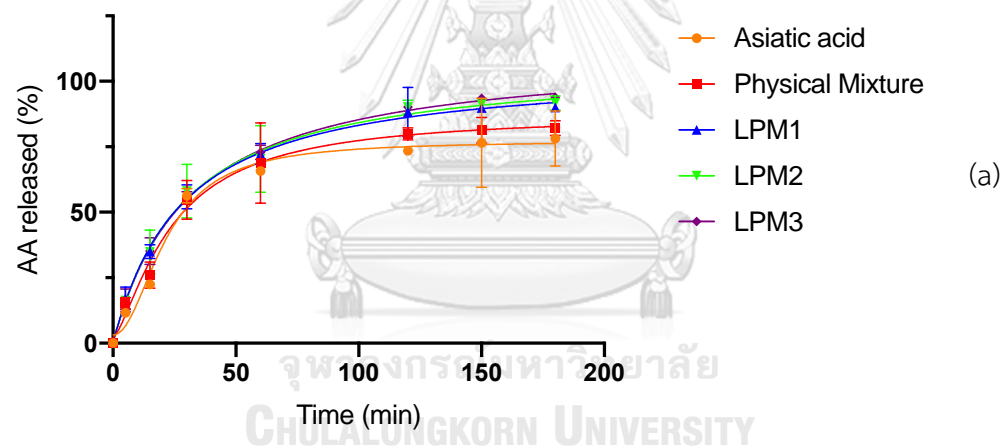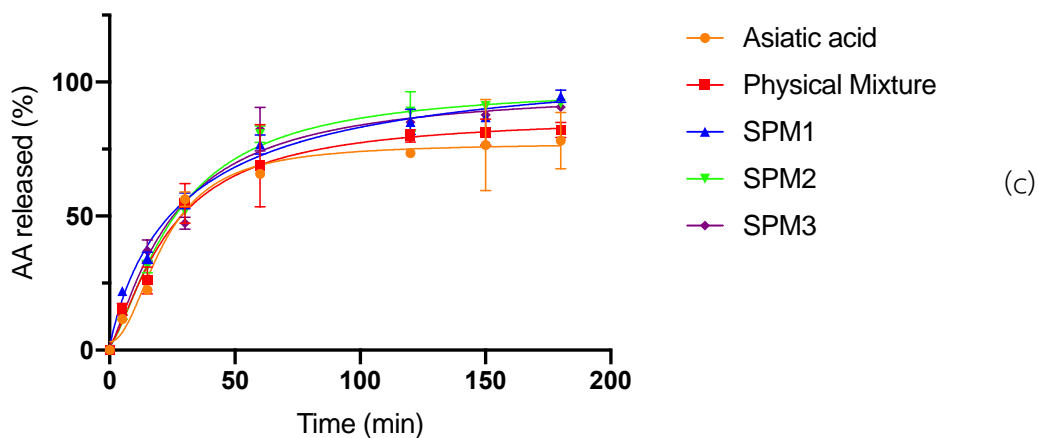
Figure 34 Asiatic acid released profile in powder, physical mixture and microparticle form: (a) AA in LPM microparticles; (b) AA in LTM microparticles; (c) AA in SPM microparticles.

Table 9 Area under curve (AUC) and dissolution efficiency (DE) of asiatic acid at 180 minutes.

Formula	AUC	DE 180 (%)
Asiatic acid	11392.54 ± 649.89	63.29 ± 3.61
Physical mixture	12066.37 ± 1388.67	67.04 ± 7.71
LPM1	13122.29 ± 244.50[*]	72.90 ± 1.36[*]
LPM2	13230.40 ± 584.22[*]	73.50 ± 3.25[*]
LPM3	13392.50 ± 123.65[*]	74.40 ± 0.69[*]
LTM1	14557.00 ± 784.13[*]	80.87 ± 4.36[*]
LTM2	14725.10 ± 480.60[*]	81.81 ± 2.67[*]
LTM3	14703.18 ± 872.81[*]	81.68 ± 4.85[*]
SPM1	13190.94 ± 350.36[*]	73.28 ± 1.95[*]
SPM2	13431.97 ± 356.72[*]	74.62 ± 1.98[*]
SPM3	13186.11 ± 452.12[*]	73.26 ± 2.51[*]

[*]Indicates statistically different than asiatic acid group with p <0.05

4.9. Molecular docking investigation

Asiatic acid and captopril bound with ACE are displayed In Figure 35 by molecular docking. Hydrogen, Van der Waals, and hydrophobic interactions, as illustrated in Table 10, were the primary stabilizing bonding for the complex. Both asiatic acid and captopril had four hydrogen bonds and two hydrophobic bonds with ACE. The free binding energies of asiactic acid and captopril with ACE were -9.7 and -5.6 kcal/mol, respectively as shown in Table 11. These findings suggested that asiatic acid may interact with ACE and hence inhibit its activity.

จุฬาลงกรณ์มหาวิทยาลัย
CHULALONGKORN UNIVERSITY
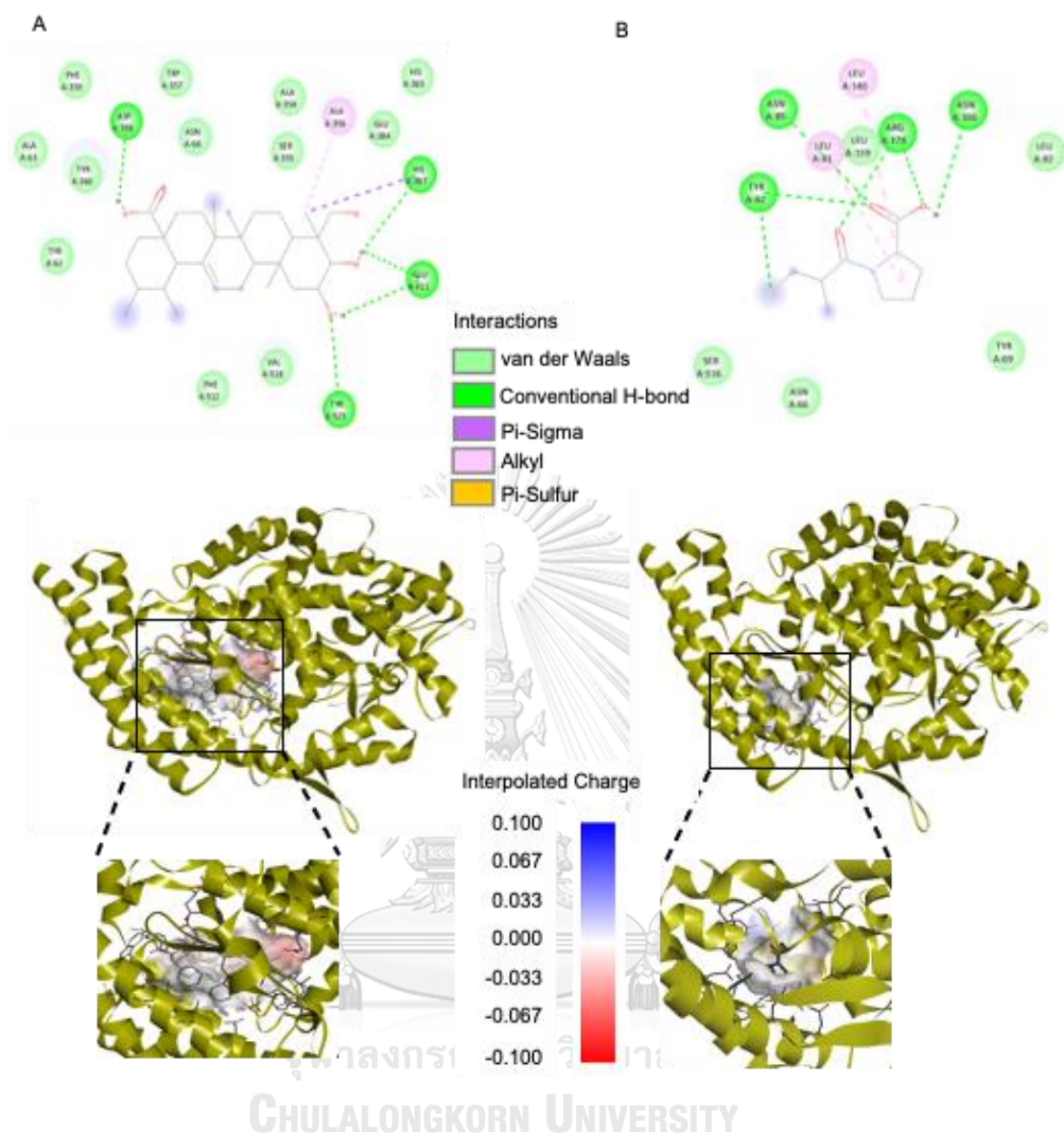
Figure 35 2D and 3D interaction between Asiatic acid (A) and Captopril (B) with ACE (PDB ID: 1O86)

Table 10 Type of interaction between Asiatic acid and captopril with ACE (PDB ID: 1O86)

Compound	Hydrogen	Van der Waals	Hydrophobic
Asiatic acid	ASP358	TYR62	ALA356
	HIS387	ALA63	HIS387
	GLU411	ASN66	
	TYR523	ALA354	
		SER355	
		TRP357	
		PHE359	
		TYR360	
		HIS383	
		GLU384	
		PHE512	
		VAL518	
Captopril	TYR62	ASN66	LEU81
	ASN85	TYR69	LEU140
	ARG124	LEU82	
	ASN136	LEU139	
		SER516	

Table 11 Binding energy between Asiatic acid and captopril with ACE (PDB ID: 1O86)

PDB	Binding energy (kcal/mol)	
1O86	Asiatic acid	Captopril
	-9.7	-5.6

4.10. Cell viability

Figure 36 shows the Caco-2 cells appearance after MTT test with matrix, AA and AA nanoparticle. While Figure 37 displays the value that indicated the viability of Caco-2 cells. Up to a concentration of 100 µM, the three groups (matrix, AA, and AA microparticle) remained non-toxic. They began to exhibit distinct toxicity levels (Figure 37A) and IC50 values (Figure 37B) at greater doses. Asiatic acid > AA microparticle > matrix was the order of toxicity value of the sample in Caco-2 cells.

จุฬาลงกรณ์มหาวิทยาลัย

CHULALONGKORN UNIVERSITY

Matrix 500 µM	AA 500 µM	AA Micro 500 µM
Matrix 250 µM	AA 250 µM	AA Micro 250 µM
Matrix 100 µM	AA 100 µM	AA Micro 100 µM
Control / Matrix 50 µM	AA 50 µM	AA Micro 50 µM
Matrix 5 µM	AA 5 µM	AA Micro 5 µM
Matrix 0.5 µM	AA 0.5 µM	AA Micro 0.5 µM
Matrix 0 µM	AA 0 µM	AA Micro 0 µM
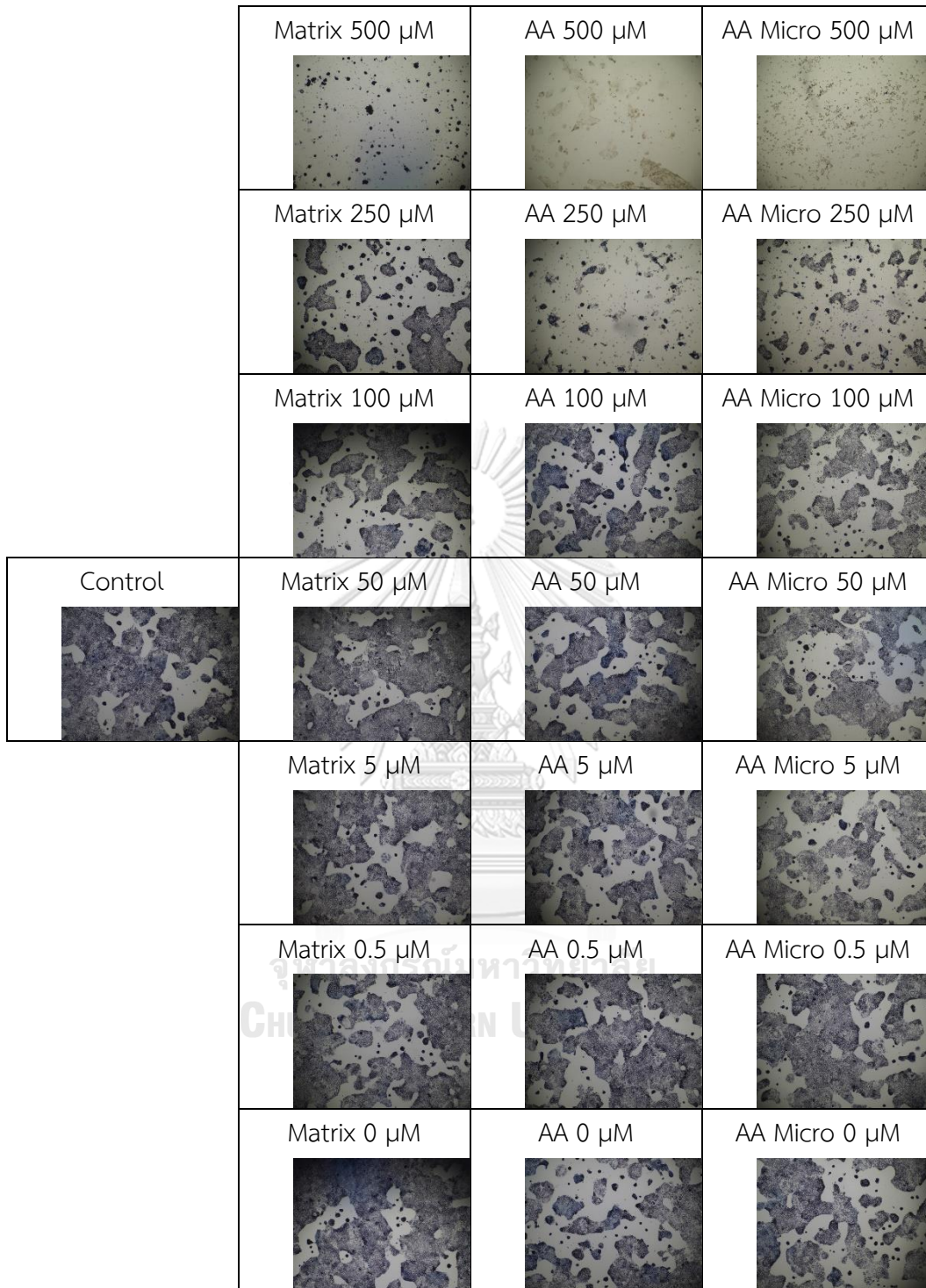
Figure 36 Visual appearance of Caco-2 cell microscopically after treatment with control, matrix, asiatic acid and AA microparticle; then continued with MTT treatment
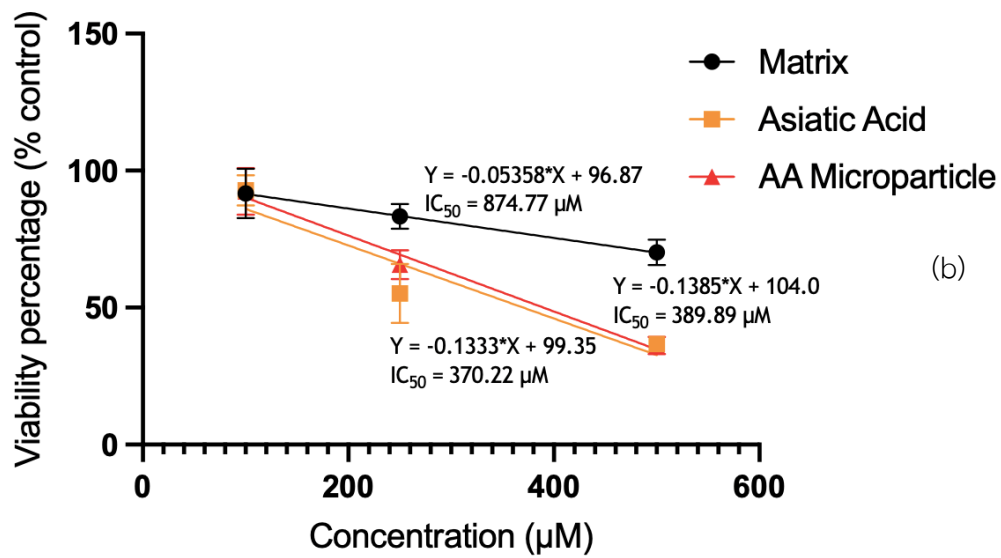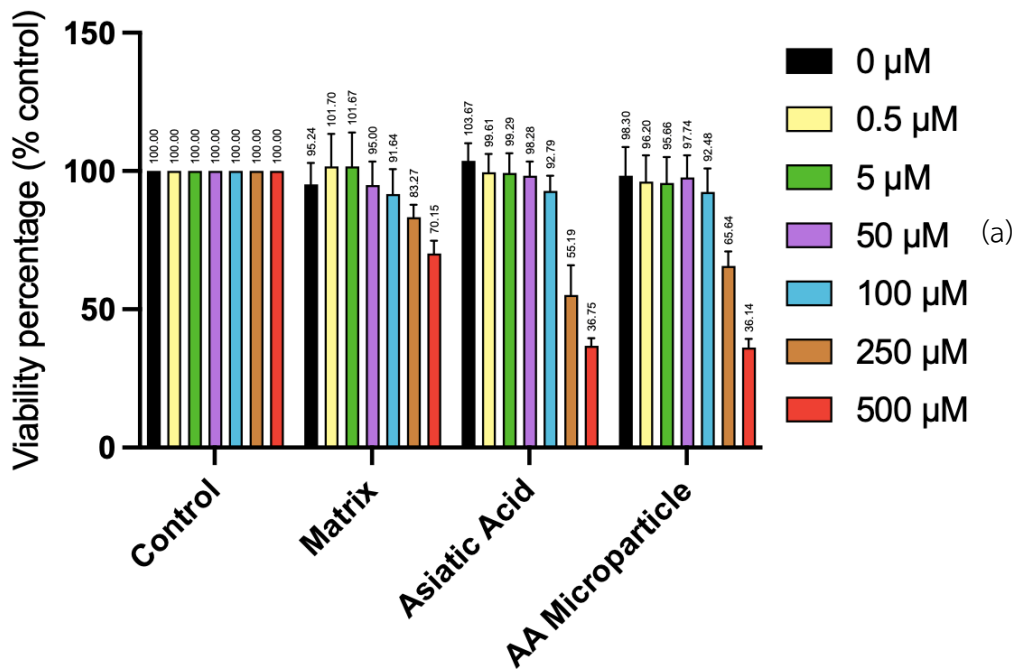
Figure 37 Viability of Caco-2 cells (a) and the IC_{50} value (b) with matrix, asiatic acid and AA microparticle.

4.11. Antihypertensive activity in SD rats

Figure 38 (a) displays the fluctuation in body weight of SD rats over a period of 13 weeks. Even after the first week of the high-salt diet induction, the non-hypertensive group body weight had increased significantly relative to the other groups and kept continues until the end of the study. In the meantime, systolic blood pressure determination was performed as displayed in Figure 38 (b), and the value of all groups were depicted in Figure 38 (c). From week 4 to week 10 of the high salt diet induction, all groups had a significant raise in blood pressure relative to the non-hypertensive group, and treatment was then initiated at this time. After treatment began, animals in the captopril and AA microparticle groups had an immediate and considerable drop in blood pressure compared to rats in the matrix group. This result was in accordance with the linear regression equation of the two groups shown in Table 12, with a high slope value of -1.318 and -1.344 for captopril and AA microparticle groups, respectively. The AA group did not experience a drop in blood pressure until the eleventh week of the experimental investigation. Meanwhile, AA microparticle decreased the systolic blood pressure in similar rate compared to the captopril.

To verify the decrease in systolic blood pressure, the ACE activity of blood serum was measured and shown in Figure 39. Before starting the treatment (9 weeks induction), ACE1 activity of matrix, captopril, asiatic acid, and AA microparticles was significantly increased ($p < 0.05$) compared to the non-hypertensive group. While at the end of the study (13 weeks), ACE activity in captopril, Asiatic acid and AA microparticle group were in the same level of non-hypertensive group, which is significantly different from the matrix group. Non-hypertensive, matrix, captopril, AA microparticles and Asiatic acid groups showed ACE activity values of 0.043 $\pm$ 0.005 U/ml, 0.062 $\pm$ 0.007 U/ml, 0.053 $\pm$ 0.004 U/ml, 0.055 $\pm$ 0.005 U/ml and 0.057 $\pm$ 0.004 U/ml, respectively.

Figure 38 In-vivo antihypertensive activity of SD rats (n = 6-8/group); Body weight result (a), Indirect blood pressure test (b) Systolic blood pressure result (c); Error bar shows SD of each point value. Symbol indicates statistically different (p <0.05), *between non-hypertensive group with all groups, #between treatment group with matrix groups, $between matrix group with non-hypertensive groups, &between captopril and AA nanoparticle groups with AA group.

Figure 39 Effect of treatment on SD rats ACE1 activity; Bar graph shows ACE activity in each group at pre-treatment and post-treatment. Error bar indicates SD of ACE activity value. *Indicates statistically different ($p < 0.05$) between the group.

Table 12 Linear regression equation of blood pressure changes after treatment

Rats group	Linear regression equation
Non-Hypertensive	y = -0.1950 x + 119.1
Matrix	y = 0.0920 x + 119.1
Captopril	y = -1.318 x + 132.5
AA Microparticle	y = -1.344 x + 132.8
Asiatic acid	y = -0.8046 x + 128.1
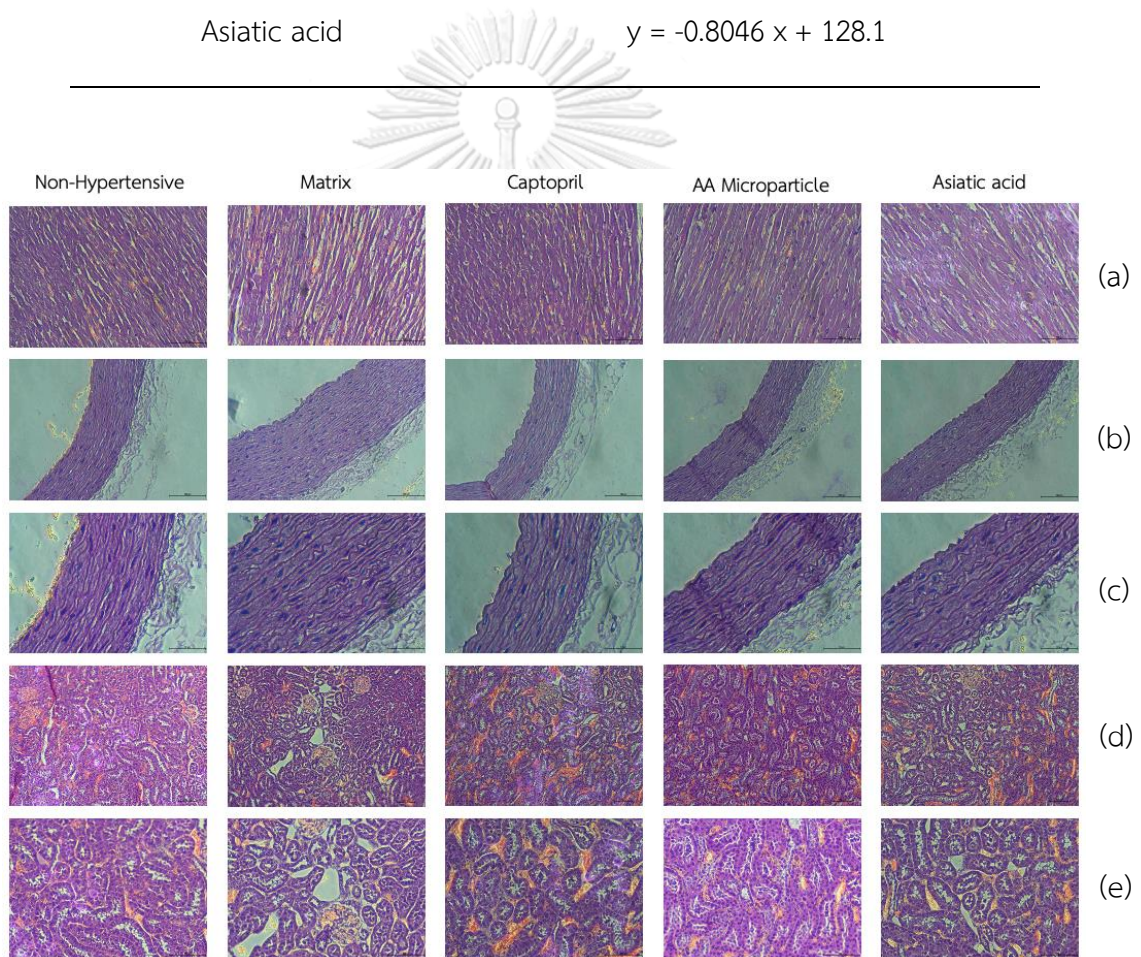
Figure 40 Rat tissue histological result of heart in 200x magnification (a), aorta in 200x magnification (b), aorta in 400x magnification (c), kidney in 100x magnification (d), and kidney in 200x magnification (e).

The results of microscopic histology observations are shown in Figure 40. Evaluations were carried out on the heart (a), aorta (b, c) and kidney (d, e). A similar picture was shown in the five rat groups, which showed that the induction of hypertension in animals did not cause severe tissue damage. However, these results also show that treatment with captopril, asiatic acid and AA microparticles was not harmful to the tissue. Blood chemistry analysis also determined that neither induction nor treatment did not affect the renal damage, as shown in Table 13. Blood urea nitrogen (BUN) value slightly increased in the matrix group, but was within the normal range. The blood sodium value was quite high in the matrix group, while in the other groups it was more controlled. These results were related to kidney histopathological reports where mild dilatation, pale staining of inner cortex, hypertrophy of glomeruli, single necrosis and mild cloudy swelling of proximal tubular epithelial cells were shown. Therefore, in general, pathological evaluation of the heart, aorta and kidney in hypertension rat model most frequently revealed non-specific changes. Furthermore, this finding suggest that spray dried AA microparticle is not the iatrogenic factor.

Table 13 Blood chemistry result post-treatment of the rat groups

Rat group	BUN (mg/dl)	Creatinine (mg/dl)	Na (mmol/L)	K (mmol/L)	Cl (mmol/L)
Non-hypertensive	19.000 ± 3.000	0.817 ± 0.081	126.433 ± 1.365	8.267 ± 0.513	97.300 ± 0.889
Matrix	21.667 ± 1.528	0.817 ± 0.085	130.867 ± 0.635[*]	7.707 ± 0.417	99.800 ± 0.889
Captopril	18.667 ± 3.215	0.817 ± 0.045	128.300 ± 0.400	7.653 ± 0.479	98.133 ± 0.503
AA nanoparticle	19.000 ± 2.000	0.800 ± 0.050	128.433 ± 2.325	8.227 ± 0.552	101.100 ± 3.214
Asiatic acid	19.667 ± 2.082	0.817 ± 0.015	128.567 ± 0.833	8.533 ± 0.470	98.133 ± 0.231
Normal value (126)	10.00 – 22.00	0.50 – 0.80	143.00 – 157.00	5.00 – 7.30	97.00 – 110.00

[*]Indicates statistically different than non-hypertensive group with p <0.05

จุฬาลงกรณ์มหาวิทยาลัย

CHULALONGKORN UNIVERSITY

CHAPTER 5

DISCUSSION AND CONCLUSION

5.1. Discussion

Spray-dried nanoemulsion formulation of asiatic acid-palm oil has been done and met certain physical and chemical parameters (18,19). The observed physical properties included the physical appearance, size, morphology, moisture content, crystallinity, product recovery, and solubility. With the ability to encapsulate molecules that were insoluble in water, palm oil served as the oil phase in the nanoemulsion system (20). As nanoemulsion surfactants, span 80, lecithin, tween 80, and poloxamer 188 were successful in producing and maintaining the asiatic acid nanodroplet stability (21–24). Maltodextrin acted very well as a carrier and stabilizer during spray drying to encapsulate and increase the stability of asiatic acid in dry microparticles as the final product (25,26). Based on the physical stability, successful preparations were obtained by the absence of visible changes or aggregation throughout 5 days of nanoemulsion storage and 6 months of microparticle observation. Despite this, the span value data displays that LTM1 produced a rising value, indicating that the resulting particle size distribution was become more heterogeneous. A small quantity of maltodextrin could not maintain the tendency of particles to aggregate. The large result variance in the measurements of moisture content, low yield, and asiatic acid recovery further appropriate to the prior statement. In other formulations, increasing the quantity of maltodextrin or combining it with poloxamer 188 and span 80 could improve the physical properties as expected.

The physical characterization results indicated the establishment of an encapsulating process that did not significantly alter the molecular structure. It was possible that the activity of asiatic acid was unaffected despite of the fact that it had been subjected to stress during the manufacture. The specific peak of microparticles in the FTIR spectra matched to the profile of asiatic acid (27), whilst the other excipient peaks remained unchanged. Peaks on absorption bands at 3314.40 cm^{-1} (O-H stretching), 2926.65 cm^{-1} (C-H stretching of the carboxylic group), 1638.48 cm^{-1} (C=O stretching), 1361.50 cm^{-1} (O-H bending), and 1147.58 cm^{-1}, 1078.96 cm^{-1}, 1012.32 cm^{-1} (C-O stretching and C-O-H bending) were identical to those published by Mahdi et al (28) for maltodextrin, as a major component. There were no missing peaks in the microparticle spectra, nor did any new peaks developed as a result of chemical interactions. In addition, the data of heat resistance indicates that microparticle was created without chemical modifications. In particular, the decomposition peaks of asiatic acid and maltodextrin occurred at 411.6°C and 297.8°C, respectively. Observations of the 9 samples and the physical mixture still revealed two peaks, but the intensity of asiatic acid was decreased. The ratio of asiatic acid peak intensity to maltodextrin was decreased as maltodextrin concentration increased. This showed that the asiatic acid microparticles in the maltodextrin matrix were created through physical encapsulation contact. Similarly, in terms of crystallinity, it was determined that the intensity of asiatic acid decreased and was partially obscured by the excipient diffractogram peak without any additional structural modifications (18,125). The formulation could also be deemed successful with a relatively high product yield, made it a good candidate for production scale-up.

Asiatic acid is a pentacyclic triterpenoid with limited solubility and bioavailability (29), and the microparticle was significant in increasing the solubility and the release of asiatic acid. In general, the dissolution rate will be influenced by the ability of dissolved and diffusion of the substance. This was a weakness of poloxamer 188 as an excipient, because the matrix formed inhibited the diffusion ability of asiatic acid,

as shown in the solubility test result. In addition, the use of triton X-100 as a surfactant and pH change of dissolution media could also increase ionization and ability to dissolve of the asiatic acid in the release study.

As a matrix, combination of lecithin, tween 80, and maltodextrin enhanced solubility up to 30.64 times. Compared to powder or physical mixture, the in-vitro release rate also became substantially more ideal. This increase was largely affected by the particle size reduction and the use of hydrophilic polymers as surfactants and carrier, which gave higher wettability (26,28). The microparticles were obtained with a size range of 0.833 - 4.897 µm, which were less than the average size of asiatic acid powder, which was 6.05 ± 0.430 µm. However, microparticle dispersion in water could rapidly produce nanoparticles in the range of 149.0 – 271.1 nm, and supporting the solubility and dissolution rate improvement. The formation of zeta potentials greater than -40 mV were believed from the introduction of palm oil hydrocarbon functional groups (30). However, encapsulation in maltodextrin as a non-ionic carrier could reduce its zeta potential in the range of -33.1 to -38.7 mV, hence maintaining its steric and electrostatic stability. Negative charge on the surface of a particle was generally less harmful to cells than positive charge. However, in the range of zeta potential obtained (lower than that of nanoemulsions), microparticles were likewise be less harmful (126,127).

The microparticle products were kept in airtight storage for 6 months and the evaluations were repeated every 3 months. Changes observed at each observation time were relatively insignificant, showing that the microparticle produced by spray drying could preserve the stability of asiatic acid. Physically defined by the absence of agglomeration or particle size improvement, and chemically defined by the stability of the asiatic acid concentration. Maltodextrin was also capable of functioning as a thermally unstable substance-loaded stabilizer and wall material. It considerably prevented the active compound lose during the drying and storage processes (26). According to the findings of this investigation, the combination of

lecithin, tween 80, and maltodextrin was a potential candidate for the formulation excipients. The success of the transformation into the spray-dried microparticle system of asiatic acid material could be continued with the development of dosage forms and in-vivo study to determine the optimal dosing regimen for clinical use.

To ensure the safety of LTM2 spray-dried nanoemulsion for in-vivo study, cell viability evaluation was carried out by MTT assay. This evaluation was carried out on control (without sample), matrix only, asiatic acid, and LTM2-AA nanoparticles. Based on the results of the MTT assay, it was seen that AA and AA nanoparticles were harmful to Caco-2 cells at a concentration of 100 µM. The nanoemulsion preparation and spray drying procedure had no effect on the toxicity of AA on Caco-2 cells, according to the toxicity values and IC_{50} of AA microparticle, which were nearly similar to AA. These findings also suggested that AA microparticle taken orally with an equal amount of AA as an antihypertensive drug would not enhance cell toxicity.

The antihypertensive activity of five groups (non-hypertensive, matrix, captopril, AA microparticle, and AA) of SD rats was then investigated. This study began with the addition of 2% NaCl to drinking water, which led to a considerable raise in blood pressure four weeks later. In comparison to the non-hypertensive group, the high-salt diet was sustained until 9 weeks. At this time, the steady blood pressure was achieved, confirmed by the result of ACE activity improvement. The oral administration of matrix, captopril, AA, and AA microparticle was started at this point. Based on research that published by Maneesai et al (9), 5 mg/kg of captopril provided a higher blood pressure reduction compared to 30 mg/kg of asiatic acid. AA microparticle dose equal to 30 mg/kg of asiatic acid was used in this study to see if post-production changes could increase antihypertensive activity higher or at least equivalent to captopril. The proposed increasement of the antihypertensive activity could be considered to reduce the dosage requirements in further clinical use.

The body weight of the non-hypertensive rat group increased very rapidly compared to the other groups. This significant difference was seen from the first

week of observation until the end of the study. On their prior work, Coelho et al. reported a similar profile of body weight fluctuations. This was not attributable to the increased food intake of the non-hypertension group; rather, the hypertensive group consumed more food. Changes in energy balance for metabolism, in which energy expenditure rose as a result of a long-term high-salt diet, and were responsible for the lower bodyweight in the high-salt groups (109).

As for blood pressure observation, significant improvement was seen in all groups compared to the non-hypertensive group since 4 weeks of high-salt induction. This high-blood pressure condition remained constant until 10 weeks of experiment and then the treatment started. Decreased blood pressure occured after treatment administered. The results of the study indicate the suitability of a prior study by Maneesai et al (9), and that asiatic acid could lower systolic blood pressure, but not as quickly as captopril. In the meanwhile, AA microparticle decreased the systolic blood pressure of hypertensive rats more quickly than the AA group, at a rate that was nearly similar to the captopril group as determined by the high slope value.

The results of ACE1 activity observation in serum also showed that asiatic acid, AA microparticle and captopril played a role in reducing the ACE activity level. This ACE1 activity data did not directly show its effect on blood pressure reduction, because the blood pressure value would be more accurate if it was calculated based on the AT2 (angiotensin II) value directly as shown by RAAS system diagram in Figure 4. However, the AT2 value could not be determined on the alive rats in the middle of the study. This indirect ACE1 activity determination caused the different deviations in the measurements at 9 and 13 weeks. In addition, different sampling methods on the tail vein or directly to the heart also affected the quality of the sample. The pressure required for vein tail sampling could cause lysis of the blood and affected the absorbance of sample observations. However, this measurement of ACE1 activity was representative enough to validate the value of decreasing blood pressure.

Based on the level of decrease in ACE1 activity value, it could be written that the ability of captopril > AA microparticle > AA, respectively. All three treatments have succeeded in lowering the serum ACE activity value of the rat close to the value of the non-hypertensive group. The results of evaluation in Sprague Dawley rats demonstrated that AA had ACE inhibitory action was comparable to captopril, which may have an effect on the RAS pathway. Moreover, the spray-dried microparticle formulation of AA gave higher effect on lowering the blood pressure and ACE inhibitory action in rats compared to the powder form (9,107).

Histological observations showed that the effectiveness of spray dried asiatic acid nanoemulsion in lowering the blood pressure was also supported by its safety on tissue. The heart, aorta and kidney did not show any damage after 3 weeks of treatment. The BUN value which generally indicated kidney damage was also controlled in a similar value to the non-hypertensive rat group. The content of ionic compounds such as sodium, potassium and chlorine which is affected by the performance of angiotensin II is also in controlled amounts based on the ACE inhibition effect of the treatment.

All of the results which have carried out in this study determine that the formation of spray-dried nanoemulsion system of asiatic acid-palm oil was promising as a choice of antihypertensive agent. Particle size reduction increased the solubility and drug dissolution rate of asiatic acid, so that its bioavailability and activity as an ACE-inhibitor could be improved superiorly.

5.2. Conclusion

By formulating asiatic acid into a nanoemulsion, its physical and chemical properties had improved. Physical appearance, particle size, zeta potential, and agglomeration retention were initial formulation success factors. In addition, effective formation of spherical microparticles was achieved by spray drying the nanoemulsion. The nanoemulsion was encapsulated into a dry form using maltodextrin as a carrier, preserving its physical and chemical stability for up to six months of storage. Product recovery was also quite high, with no change in the crystallinity or chemical structure of asiatic acid as a result of production-related stress. In the solubility test, the most important outcome was seen up to 30.64-fold increase compared to pure asiatic acid powder in water. It demonstrated the positive effect of particle size reduction and the usage of hydrophilic polymers as surfactants and carriers in the formulation. LTM2 was a formulation with optimal physical properties and asiatic acid dissolution rate in gastric juice-phosphate buffer pH 6.8 with 4% triton X-100 medium. In addition, the production process and matrix used were known safe and non-toxic for Caco-2 cells and also heart, aorta, and kidney tissues. In the activity test, AA microparticle was shown to dramatically reduce systolic blood pressure and serum ACE activity compared to AA raw powder in SD rats. These results demonstrated that the nanoparticle formulation with high-speed stirring, sonication, and spray drying reduced the particle size and enhanced the in-vitro release rate of asiatic acid, hence increasing the amount of AA absorbed and optimizing its antihypertensive effect, as previously predicted by molecular docking.

References

1. Giena VP, Thongpat S, Nitirat P. Predictors of health-promoting behaviour among older adults with hypertension in Indonesia. International Journal of Nursing Sciences 2018;Vol5:201–205. https://doi.org/10.1016/j.ijnss.2018.04.002

2. Sakboonyarat B, Rangsin R, Kantiwong A, Mungthin M. Prevalence and associated factors of uncontrolled hypertension among hypertensive patients: A nation-wide survey in Thailand. BMC Research Notes. 2019;12:380. https://doi.org/10.1186/s13104-019-4417-7

3. Mills KT, Bundy JD, Kelly TN, Reed JE, Kearney P, Reynolds K. et al. Global disparities of hypertension prevalence and control: a systematic analysis of population-based studies from 90 countries. Circulation 2016;Aug9;134(6):441–450. doi:10.1161/CIRCULATIONAHA.115.018912

4. Saseen JJ, MacLaughlin EJ. Hypertension. In: DiPiro JT, Talbert RL, Yee GC, Matzke GR, Wells BG, Posey LM, editors. Pharmacotherapy: A Pathophysiologic approach. Tenth Edition.. McGraw-Hill Education; 2017, p. 170–248.

5. Neal MJ. Drugs used in hypertension. In: Neal MJ, editor. Medical pharmacology at a glance. Eighth Edition. John Wiley & Sons, Ltd; 2016, p. 30–31.

6. Bunbupha S, Pakdeechote P, Kukongviriyapan U, Prachaney P. Asiatic acid reduces blood pressure and improves vascular function in nitric oxide deficient hypertensive rats. Srinagarind Medical Journal 2013;28:234–238.

7. Bunbupha S, Pakdeechote P, Kukongviriyapan U, Prachaney P, Kukongviriyapan V. Asiatic acid reduces blood pressure by enhancing nitric oxide bioavailability with modulation of eNOS and p47phox expression in L-NAME-induced hypertensive rats. Phytotherapy Research 2014;28(10):1506–1512. doi: 10.1002/ptr.5156

8.   Maneesai P, Bunbupha S, Kukongviriyapan U, Prachaney P, Tangsucharit P, Kukongviriyapan V, et al. Asiatic acid attenuates renin-angiotensin system activation and improves vascular function in high-carbohydrate, high-fat diet fed rats. BMC Complementary and Alternative Medicine 2016;16(123):1–11. http://dx.doi.org/10.1186/s12906-016-1100-6

9.   Maneesai P, Bunbupha S, Kukongviriyapan U, Senggunprai L, Kukongviriyapan V, Prachaney P, et al. Effect of asiatic acid on the Ang II-AT1R-NADPH oxidase-NF-**κ**B pathway in renovascular hypertensive rats. Naunyn-Schmiedeberg's Archives of Pharmacology 2017;390(10):1073–1083. doi: 10.1007/s00210-017-1408-x

10. Meeran MFN, Goyal SN, Suchal K, Sharma C, Patil CR, Ojha SK. Pharmacological properties, molecular mechanisms, and pharmaceutical development of asiatic acid: A pentacyclic triterpenoid of therapeutic promise. Frontiers in Pharmacology 2018;Vol9. doi:10.3389/fphar.2018.00892

11. Fong LY, Ng CT, Yong YK, Hakim MN, Ahmad Z. Asiatic acid stabilizes cytoskeletal proteins and prevents TNF-**α**-induced disorganization of cell-cell junctions in human aortic endothelial cells. Vascular Pharmacology 2019;117:pp 15–26. https://doi.org/10.1016/j.vph.2018.08.005

12. Osim EE, Owu DU, Etta KM. Arterial pressure and lipid profile in rats following chronic ingestion of palm oil diets. African Journal of Medicine and Medical Sciences 1996;25:335-340. Available from: https://www.researchgate.net/publication/51324711

13. Bayorh MA, Abukhalaf IK, Ganafa AA. Effect of palm oil on blood pressure, endothelial function and oxidative stress. Asia Pac J Clin Nutr 2005;Vol.14(4): pp 325-339.

14. Ganafa AA, Socci RR, Eatman D, Silvestrov N, Abukhalaf IK, Bayorh MA. Effect of palm oil on oxidative stress-induced hypertension in sprague-dawley rats.

American Journal of Hypertension 2002;Vol.15: pp 725–731. Available from: https://academic.oup.com/ajh/article-abstract/15/8/725/143992

15. Committee on Herbal Medicinal Products (HMPC). Assessment report on Centella asiatica (L.) Urb., herba. 2010. Available from: www.ema.europa.eu

16. Ebong PE, Owu DU, Isong EU. Influence of palm oil (Elaesis guineensis) on health. Plant Foods for Human Nutrition 1999;Vol.53:209-222.

17. Ricaurte L, Correa REP, de Jesus Perea-Flores M, Quintanilla-Carvajal MX. Influence of milk whey on high-oleic palm oil nanoemulsions: powder production, physical and release properties. Food Biophysics 2017;Vol12(4):439–450. doi:10.1007/s11483-017-9500-9

18. Sandoval-Cuellar CE, de Jesus Perea-Flores M, Quintanilla-Carvajal MX. In-vitro digestion of whey protein- and soy lecithin-stabilized High Oleic Palm Oil emulsions. Journal of Food Engineering 2020;278. https://doi.org/10.1016/j.jfoodeng.2020.109918

19. Ricaurte, L, Perea-Flores M.D.J.; Martinez, A.; Quintanilla-Carvajal, M.X. Production of high-oleic palm oil nanoemulsions by high-shear homogenization (microfluidization). Innovative Food Science and Emerging Technologies. 2016, 35: 75–85. http://dx.doi.org/10.1016/j.ifset.2016.04.004

20. Nirmala MJ, Nagarajan R. Recent research trends in fabrication and applications of plant essential oil based nanoemulsions. Journal of Nanomedicine & Nanotechnology 2017;8:434. doi:10.4172/2157-7439.1000434

21. El-Messery TM, Altuntas U, Altin G, Özçelik B. The effect of spray-drying and freeze-drying on encapsulation efficiency, in vitro bioaccessibility and oxidative stability of krill oil nanoemulsion system. Food Hydrocolloids 2020;106:105890. https://doi.org/10.1016/j.foodhyd.2020.105890

22. Myat, H.H.; Ritthidej, G.C. Impact of formulation parameters on physical characteristics of spray dried nanoemulsions and their reconstitutions. Asian Journal of Pharmaceutical Sciences. 2016, 11(1): 197–198. http://dx.doi.org/10.1016/j.ajps.2015.11.038

23. Sonklin C, Alashi MA, Laohakunjit N, Kerdchoechuen O, Aluko RE. Identification of antihypertensive peptides from mung bean protein hydrolysate and their effects in spontaneously hypertensive rats. Journal of Functional Foods. 2020 Jan 1;64: 103635. https://doi.org/10.1016/j.jff.2019.103635

24. Puchalska P, Marina ML, García MC. Development of a reversed-phase high-performance liquid chromatography analytical methodology for the determination of antihypertensive peptides in maize crops. Journal of Chromatography A. 2012 Apr 20;1234:64–71. doi:10.1016/j.chroma.2011.12.079

25. Hu G, Zheng Y, Liu Z, Xiao Y, Deng Y, Zhao Y. Effects of high hydrostatic pressure, ultraviolet light-C, and far-infrared treatments on the digestibility, antioxidant and antihypertensive activity of α-casein. Food Chemistry. 2017 Apr 15;221:1860–1866. http://dx.doi.org/10.1016/j.foodchem.2016.10.088

26. Alcaide-Hidalgo JM, Margalef M, Bravo FI, Muguerza B, López-Huertas E. Virgin olive oil (unfiltered) extract contains peptides and possesses ACE inhibitory and antihypertensive activity. Clinical Nutrition. 2020 Apr 1;39(4):1242–1249. https://doi.org/10.1016/j.clnu.2019.05.016

27. Anand P, Thomas SG, Kunnumakkara AB, Sundaram C, Harikumar KB, Sung B, et al. Biological activities of curcumin and its analogues (Congeners) made by man and Mother Nature. Biochemical Pharmacology. 2008;76(11):1590–1611. doi:10.1016/j.bcp.2008.08.008

28. Mohammed HS, Hosny EN, Khadrawy YA, Magdy M, Attia YS, Sayed OA, et al. Protective effect of curcumin nanoparticles against cardiotoxicity induced by

doxorubicin in rat. Biochimica et Biophysica Acta - Molecular Basis of Disease. 2020;1866(5): 165665. https://doi.org/10.1016/j.bbadis.2020.165665

29. Hadi A, Pourmasoumi M, Ghaedi E, Sahebkar A. The effect of Curcumin/turmeric on blood pressure modulation: A systematic review and meta-analysis. Pharmacological Research. 2019;150:104505. https://doi.org/10.1016/j.phrs.2019.104505

30. Grande F, Parisi OI, Mordocco RA, Rocca C, Puoci F, Scrivano L, et al. Quercetin derivatives as novel antihypertensive agents: Synthesis and physiological characterization. European Journal of Pharmaceutical Sciences. 2016 Jan 20;82:161–170. http://dx.doi.org/10.1016/j.ejps.2015.11.021

31. Yuan Y, Zhang H, Sun F, Sun S, Zhu Z, Chai Y. Biopharmaceutical and pharmacokinetic characterization of asiatic acid in Centella asiatica as determined by a sensitive and robust HPLC-MS method. Journal of Ethnopharmacology. 2015 Apr 2;163:31–38. http://dx.doi.org/10.1016/j.jep.2015.01.006

32. Pakdeechote P, Bunbupha S, Kukongviriyapan U, Prachaney P, Khrisanapant W, Kukongviriyapan V. Asiatic acid alleviates hemodynamic and metabolic alterations via restoring eNOS/iNOS expression, oxidative stress, and inflammation in diet-induced metabolic syndrome rats. Nutrients 2014;6(1):355–370. doi:10.3390/nu6010355

33. Yin MC, Lin MC, Mong MC, Lin CY. Bioavailability, distribution, and antioxidative effects of selected triterpenes in mice. Journal of Agricultural and Food Chemistry. 2012 Aug 8;60(31):7697–7701. dx.doi.org/10.1021/jf302529x

34. Hanwate RM, Mhg D, Saifee M. Solid dispersion : a tool to enhance solubility of poorly water soluble drugs. Vol. 2, Pharmatutor. 2014. p. 50–60.

35.   Ribas MM, Sakata GSB, Santos AE, Dal Magro C, Aguiar GPS, Lanza M, et al. Curcumin cocrystals using supercritical fluid technology. Journal of Supercritical Fluids. 2019;152:1–7:104564. https://doi.org/10.1016/j.supflu.2019.104564

36.   Raviadaran, R.; Chandran, D.; Shin, L.H.; Manickam, S. Optimization of palm oil in water nano-emulsion with curcumin using microfluidizer and response surface methodology. LWT - Food Science and Technology. 2018; 96: 58–65. https://doi.org/10.1016/j.lwt.2018.05.022

37.   Ricaurte L, Hernández-Carrión M, Moyano-Molano M, Clavijo-Romero A, Quintanilla-Carvajal MX. Physical, thermal and thermodynamical study of high oleic palm oil nanoemulsions. Food Chemistry. 2018 Aug 1;256:62–70. https://doi.org/10.1016/j.foodchem.2018.02.102

38.   Maher PG, Roos YH, Fenelon MA. Physicochemical properties of spray dried nanoemulsions with varying final water and sugar contents. Journal of Food Engineering.   2014   Apr;126:113–119. http://dx.doi.org/10.1016/j.jfoodeng.2013.11.001

39.   Sharma S, Loach N, Gupta S, Mohan L. Phyto-nanoemulsion: An emerging nano-insecticidal formulation. Vol. 14, Environmental Nanotechnology, Monitoring and Management. 2020;14:10031. https://doi.org/10.1016/j.enmm.2020.100331

40.   Hu Q, Gerhard H, Upadhyaya I, Venkitanarayanan K, Luo Y. Antimicrobial eugenol nanoemulsion prepared by gum arabic and lecithin and evaluation of drying technologies. International Journal of Biological Macromolecules. 2016 Jun 1;87:130–140. http://dx.doi.org/10.1016/j.ijbiomac.2016.02.051

41.   Solans C, Solé I. Nano-emulsions: Formation by low-energy methods. Current Opinion in Colloid and Interface Science. 2012;17:p. 246–254. doi:10.1016/j.cocis.2012.07.003

42. Yukuyama MN, Kato ETM, de Araujo GLB, Löbenberg R, Monteiro LM, Lourenço FR, et al. Olive oil nanoemulsion preparation using high-pressure homogenization and D-phase emulsification – A design space approach. Journal of Drug Delivery Science and Technology. 2019 Feb 1;49:622–631. https://doi.org/10.1016/j.jddst.2018.12.029

43. Wang S, Wang X, Liu M, Zhang L, Ge Z, Zhao G, et al. Preparation and characterization of Eucommia ulmoides seed oil O/W nanoemulsion by dynamic high-pressure microfluidization. LWT – Food Science and Technology. 2020 Mar 1;121:108960. https://doi.org/10.1016/j.lwt.2019.108960

44. Xu J, Mukherjee D, Chang SKC. Physicochemical properties and storage stability of soybean protein nanoemulsions prepared by ultra-high pressure homogenization. Food Chemistry. 2018 Feb 1;240:1005–1013. http://dx.doi.org/10.1016/j.foodchem.2017.07.077

45. Tabilo-Munizaga G, Villalobos-Carvajal R, Herrera-Lavados C, Moreno-Osorio L, Jarpa-Parra M, Pérez-Won M. Physicochemical properties of high-pressure treated lentil protein-based nanoemulsions. LWT – Food Science and Technology. 2019 Mar 1;101:590–598. https://doi.org/10.1016/j.lwt.2018.11.070

46. Ruiz-Montañez G, Ragazzo-Sanchez JA, Picart-Palmade L, Calderón-Santoyo M, Chevalier-Lucia D. Optimization of nanoemulsions processed by high-pressure homogenization to protect a bioactive extract of jackfruit (*Artocarpus heterophyllus* Lam). Innovative Food Science and Emerging Technologies. 2017 Apr 1;40:35–41. http://dx.doi.org/10.1016/j.ifset.2016.10.020

47. Yuan Y, Gao Y, Zhao J, Mao L. Characterization and stability evaluation of β-carotene nanoemulsions prepared by high pressure homogenization under various emulsifying conditions. Food Research International. 2008;41(1):61–68. doi:10.1016/j.foodres.2007.09.006

48. Akbas E, Soyler B, Oztop MH. Formation of capsaicin loaded nanoemulsions with high pressure homogenization and ultrasonication. LWT – Food Science and Technology. 2018 Oct 1;96:266–273. https://doi.org/10.1016/j.lwt.2018.05.043

49. Ren Z, Chen Z, Zhang Y, Lin X, Li B. Characteristics and rheological behavior of pickering emulsions stabilized by tea water-insoluble protein nanoparticles via high-pressure homogenization. International Journal of Biological Macromolecules. 2020 May 15;151:247–256. https://doi.org/10.1016/j.ijbiomac.2020.02.090

50. Shen L, Tang CH. Microfluidization as a potential technique to modify surface properties of soy protein isolate. Food Research International. 2012 Aug;48(1):108–118. doi:10.1016/j.foodres.2012.03.006

51. Håkansson A, Rayner M. General principles of nanoemulsion formation by high-energy mechanical methods. In: Nanoemulsions: formulation, applications, and characterization. Elsevier Inc.; 2018. p. 103–139.

52. Abbas S, Hayat K, Karangwa E, Bashari M, Zhang X. An overview of ultrasound-assisted food-grade nanoemulsions. Food Engineering Reviews. 2013;5:p. 139–157. doi: 10.1007/s12393-013-9066-3

53. Páez-Hernández G, Mondragón-Cortez P, Espinosa-Andrews H. Developing curcumin nanoemulsions by high-intensity methods: Impact of ultrasonication and microfluidization parameters. LWT – Food Science and Technology. 2019 Aug 1;111:291–300. https://doi.org/10.1016/j.lwt.2019.05.012

54. Carpenter J, Saharan VK. Ultrasonic assisted formation and stability of mustard oil in water nanoemulsion: Effect of process parameters and their optimization. Ultrasonics Sonochemistry 2017;35:pp 422–430. http://dx.doi.org/10.1016/j.ultsonch.2016.10.021

55. Mehmood T, Ahmed A, Ahmed Z, Ahmad MS. Optimization of soya lecithin and tween 80 based novel vitamin D nanoemulsions prepared by ultrasonication using response surface methodology. Food Chemistry 2019; Aug 15;289:664–670. https://doi.org/10.1016/j.foodchem.2019.03.112.

56. Mehmood T, Ahmed A, Ahmad A, Ahmad MS, Sandhu MA. Optimization of mixed surfactants-based β-carotene nanoemulsions using response surface methodology: An ultrasonic homogenization approach. Food Chemistry. 2018 Jul 1;253:179–184. https://doi.org/10.1016/j.foodchem.2018.01.136

57. Ahmad N, Alam MA, Ahmad FJ, Sarafroz M, Ansari K, Sharma S, et al. Ultrasonication techniques used for the preparation of novel Eugenol-nanoemulsion in the treatment of wounds healings and anti-inflammatory. Journal of Drug Delivery Science and Technology. 2018 Aug 1;46:461–473. https://doi.org/10.1016/j.jddst.2018.06.003

58. Tan SF, Masoumi HRF, Karjiban RA, Stanslas J, Kirby BP, Basri M, et al. Ultrasonic emulsification of parenteral valproic acid-loaded nanoemulsion with response surface methodology and evaluation of its stability. Ultrasonics Sonochemistry. 2016 Mar 1;29:299–308. http://dx.doi.org/10.1016/j.ultsonch.2015.09.015

59. Lu WC, Chiang BH, Huang DW, Li PH. Skin permeation of d-limonene-based nanoemulsions as a transdermal carrier prepared by ultrasonic emulsification. Ultrasonics Sonochemistry. 2014;21(2):826–832. http://dx.doi.org/10.1016/j.ultsonch.2013.10.013

60. Long Y, Huang W, Wang Q, Yang G. Green synthesis of garlic oil nanoemulsion using ultrasonication technique and its mechanism of antifungal action against *Penicillium italicum*. Ultrasonics Sonochemistry. 2020 Jun 1;64:104970. https://doi.org/10.1016/j.ultsonch.2020.104970

61. Sugumar S, Ghosh V, Nirmala MJ, Mukherjee A, Chandrasekaran N. Ultrasonic emulsification of eucalyptus oil nanoemulsion: Antibacterial activity against

Staphylococcus aureus and wound healing activity in Wistar rats. Ultrasonics Sonochemistry. 2014;21(3):1044–1049. http://dx.doi.org/10.1016/j.ultsonch.2013.10.021

62. Periasamy VS, Athinarayanan J, Alshatwi AA. Anticancer activity of an ultrasonic nanoemulsion formulation of *Nigella sativa* L. essential oil on human breast cancer cells. Ultrasonics Sonochemistry. 2016 Jul 1;31:449–455. http://dx.doi.org/10.1016/j.ultsonch.2016.01.035

63. Anal AK. Controlled-release dosage forms: Pharmaceutical manufacturing handbook, production and processes. Gad SC, editor. New Jersey: John Wiley & Sons, Inc; 2008. p. 359–360

64. Fröhlich JA, Ruprecht NA, Hinrichs J, Kohlus R. Nozzle zone agglomeration in spray dryers: Effect of powder addition on particle coalescence. Powder Technology. 2020 Sep 1;374:223–232. https://doi.org/10.1016/j.powtec.2020.07.009

65. Ren W, Tian G, Zhao S, Yang Y, Gao W, Zhao C, et al. Effects of spray-drying temperature on the physicochemical properties and polymethoxyflavone loading efficiency of citrus oil microcapsules. LWT – Food Science and Technology. 2020 Nov 1;133:109954. https://doi.org/10.1016/j.lwt.2020.109954

66. Bonferoni MC, Riva F, Invernizzi A, Dellera E, Sandri G, Rossi S, et al. Alpha tocopherol loaded chitosan oleate nanoemulsions for wound healing. Evaluation on cell lines and ex vivo human biopsies, and stabilization in spray dried Trojan microparticles. European Journal of Pharmaceutics and Biopharmaceutics. 2018 Feb 1;123:31–41. https://doi.org/10.1016/j.ejpb.2017.11.008

67. Collett J. Poloxamer : Handbook of pharmaceutical excipients, Sixth edition. In: Rowe RC, Sheskey PJ, Quinn ME, editors. Handbook of Pharmaceutical

Excipients, Sixth edition. Sixth. Grayslake: Pharmaceutical Press; 2009. p. 506–509.

68. Kiran E. Supercritical fluids and polymers - The year in review - 2014. Journal of Supercritical Fluids. 2016;110:126–153. http://dx.doi.org/10.1016/j.supflu.2015.11.011

69. Jiang, T.; Liao, W.; Charcosset, C. Recent advances in encapsulation of curcumin in nanoemulsions: A review of encapsulation technologies, bioaccessibility and applications. Food Research International. 2020; 132: 109035. Available from: https://doi.org/10.1016/j.foodres.2020.109035

70. Brüsewitz C, Schendler A, Funke A, Wagner T, Lipp R. Novel poloxamer-based nanoemulsions to enhance the intestinal absorption of active compounds. International Journal of Pharmaceutics. 2007 Feb 1;329(1–2):173–181. doi:10.1016/j.ijpharm.2006.08.022

71. Mirković D, Ibrić S, Balanč B, Knez Ž, Bugarski B. Evaluation of the impact of critical quality attributes and critical process parameters on quality and stability of parenteral nutrition nanoemulsions. Journal of Drug Delivery Science and Technology. 2017 Jun 1;39:341–347. http://dx.doi.org/10.1016/j.jddst.2017.04.004

72. Mahboobian MM, Mohammadi M, Mansouri Z. Development of thermosensitive in situ gel nanoemulsions for ocular delivery of acyclovir. Journal of Drug Delivery Science and Technology. 2020 Feb 1;55:101400. https://doi.org/10.1016/j.jddst.2019.101400

73. Bazán Henostroza MA, Curo Melo KJ, Nishitani Yukuyama M, Löbenberg R, Araci Bou-Chacra N. Cationic rifampicin nanoemulsion for the treatment of ocular tuberculosis. Colloids and Surfaces A: Physicochemical and Engineering Aspects. 2020 Jul 20;597:124755. https://doi.org/10.1016/j.colsurfa.2020.124755

74. Ahmad N, Ahmad R, Ahmad FJ, Ahmad W, Alam MA, Amir M, et al. Poloxamer-chitosan-based Naringenin nanoformulation used in brain targeting for the treatment of cerebral ischemia. Saudi Journal of Biological Sciences. 2020 Jan 1;27(1):500–517. https://doi.org/10.1016/j.sjbs.2019.11.008

75. Zhang D. Sorbitan Esters (Sorbitan Fatty Acid Esters); Handbook of pharmaceutical excipients. Sixth edition. Rowe RC, Sheskey PJ, Quinn ME, editors. Grayslake: Pharmaceutical Press; 2009. p. 675–678.

76. Pensado A, Fernandez-Piñeiro I, Seijo B, Sanchez A. Anionic nanoparticles based on span 80 as low-cost, simple and efficient non-viral gene-transfection systems. International Journal of Pharmaceutics. 2014 Dec 10;476(1):23–30. http://dx.doi.org/10.1016/j.ijpharm.2014.09.032

77. Hayashi K, Tatsui T, Shimanouchi T, Umakoshi H. Membrane interaction between span 80 vesicle and phospholipid vesicle (liposome): Span 80 vesicle can perturb and hemifuse with liposomal membrane. Colloids and Surfaces B: Biointerfaces. 2013 Jun 1;106:258–264. http://dx.doi.org/10.1016/j.colsurfb.2012.12.022

78. Lin CY, Tsai SM. Comparison of engine performance between nano- and microemulsions of solketal droplets dispersed in diesel assisted by microwave irradiation. Molecules. 2019 Sep 26;24:3497. doi:10.3390/molecules24193497

79. Koroleva, M.; Nagovitsina, T.; Yurtov, E. Nanoemulsions stabilized by non-ionic surfactants: Stability and degradation mechanisms. Physical Chemistry Chemical Physics. 2018; 20: 10369–10377. doi:10.1039/c7cp07626f

80. Yang CY, Powell CA, Duan YP, Zhang MQ. Characterization and antibacterial activity of oil-in-water nano-emulsion formulation against *candidatus* liberibacter asiaticus. Plant Disease. 2016 Dec 1;100(12):2448-2454. http://dx.doi.org/10.1094/PDIS-05-16-0600-RE

81. Ding Y, Wu J, Wang J, Lin H, Wang J, Liu G, et al. Superhydrophilic and mechanical robust PVDF nanofibrous membrane through facile interfacial span 80 welding for excellent oil/water separation. Applied Surface Science. 2019 Aug 15;485:179–187. https://doi.org/10.1016/j.apsusc.2019.04.214

82. Zhang D. Polyoxyethylene sorbitan fatty ccid esters; Handbook of pharmaceutical excipients. Sixth edition. Rowe RC, Sheskey PJ, Quinn ME, editors. Grayslake: Pharmaceutical Press; 2009. p. 549–553

83. Anjana D, Nair KA, Somashekara N, Venkata M, Sripathy R, Yelucheri R, et al. Development of curcumin based ophthalmic formulation. American Journal of Infectious Diseases. 2012;8(1):41–49.

84. Prabhakar, K.; Afzal, S.M.; Surender, G.; Kishan, V. Tween 80 containing lipid nanoemulsions for delivery of indinavir to brain. Acta Pharmaceutica Sinica B. 2013; 3(5): 345–353. http://dx.doi.org/10.1016/j.apsb.2013.08.001

85. Chu Y, Cheng W, Feng X, Gao C, Wu D, Meng L, et al. Fabrication, structure and properties of pullulan-based active films incorporated with ultrasound-assisted cinnamon essential oil nanoemulsions. Food Packaging and Shelf Life. 2020 Sep 1;25:100547. https://doi.org/10.1016/j.fpsl.2020.100547

86. Wan J, Jin Z, Zhong S, Schwarz P, Chen B, Rao J. Clove oil-in-water nanoemulsion: Mitigates growth of Fusarium graminearum and trichothecene mycotoxin production during the malting of Fusarium infected barley. Food Chemistry. 2020 May 15;312:126120. https://doi.org/10.1016/j.foodchem.2019.126120

87. Sheng J. Lecithin; Handbook of pharmaceutical excipients. Sixth edition. Rowe RC, Sheskey PJ, Quinn ME, editors. Grayslake: Pharmaceutical Press; 2009, p. 385–387

88. Savić V, Ilić T, Nikolić I, Marković B, Čalija B, Cekić N, et al. Tacrolimus-loaded lecithin-based nanostructured lipid carrier and nanoemulsion with propylene glycol monocaprylate as a liquid lipid: Formulation characterization and assessment of dermal delivery compared to referent ointment. International Journal of Pharmaceutics. 2019 Oct 5;569:118624. https://doi.org/10.1016/j.ijpharm.2019.118624

89. Nash JJ, Erk KA. Stability and interfacial viscoelasticity of oil-water nanoemulsions stabilized by soy lecithin and tween 20 for the encapsulation of bioactive carvacrol. Colloids and Surfaces A: Physicochemical and Engineering Aspects. 2017 Mar 20;517:1–11. http://dx.doi.org/10.1016/j.colsurfa.2016.12.056

90. Ma Q, Davidson PM, Zhong Q. Nanoemulsions of thymol and eugenol co-emulsified by lauric arginate and lecithin. Food Chemistry. 2016 Sep 1;206:167–173. http://dx.doi.org/10.1016/j.foodchem.2016.03.065

91. Ozturk B, Argin S, Ozilgen M, McClements DJ. Formation and stabilization of nanoemulsion-based vitamin e delivery systems using natural surfactants: Quillaja saponin and lecithin. Journal of Food Engineering. 2014;142:57–63. http://dx.doi.org/10.1016/j.jfoodeng.2014.06.015

92. Vater C, Hlawaty V, Werdenits P, Cichon MA, Klang V, Elbe-Bürger A, et al. Effects of lecithin-based nanoemulsions on skin: Short-time cytotoxicity MTT and BrdU studies, skin penetration of surfactants and additives and the delivery of curcumin. International Journal of Pharmaceutics. 2020 Apr 30;580:119209. https://doi.org/10.1016/j.ijpharm.2020.119209

93. Gasa-Falcon, A.; Arranz, E.; Odriozola-Serrano, I.; Martín-Belloso, O.; Giblin, L. Delivery of β-carotene to the in vitro intestinal barrier using nanoemulsions with lecithin or sodium caseinate as emulsifiers. LWT - Food Science and Technology. 2021; 135: 110059. https://doi.org/10.1016/j.lwt.2020.110059

94. Freers S. Maltodextrin: Handbook of pharmaceutical excipients. Sixth edition. Rowe RC, Sheskey PJ, Quinn ME, editors. Grayslake: Pharmaceutical Press; 2009, p.418–420

95. Dollo, G.; le Corre, P.; Guérin, A.; Chevanne, F.; Burgot, J.L.; Leverge, R. Spray-dried redispersible oil-in-water emulsion to improve oral bioavailability of poorly soluble drugs. European Journal of Pharmaceutical Sciences. 2003; 19: 273–280. doi:10.1016 / S0928-0987(03)00134-9

96. Ribeiro MLFF, Roos YH, Ribeiro APB, Nicoletti VR. Effects of maltodextrin content in double-layer emulsion for production and storage of spray-dried carotenoid-rich microcapsules. Food and Bioproducts Processing. 2020 Nov 1;124:208–221. https://doi.org/10.1016/j.fbp.2020.09.004

97. Premi, M.; Sharma, H.K.; Effect of different combinations of maltodextrin, gum arabic and whey protein concentrate on the encapsulation behavior and oxidative stability of spray dried drumstick (Moringa oleifera) oil. International Journal of Biological Macromolecules. 2017; 105: 1232–1240. http://dx.doi.org/10.1016/j.ijbiomac.2017.07.160

98. Teo A, Lam Y, Lee SJ, Goh KKT. Spray drying of whey protein stabilized nanoemulsions containing different wall materials – maltodextrin or trehalose. LWT – Food Science and Technology. 2021 Jan;136:110344. https://doi.org/10.1016/j.lwt.2020.110344

99. Wang S, Ye F, Wei F, Zhao G. Spray-drying of curcumin-loaded octenylsuccinated corn dextrin micelles stabilized with maltodextrin. Powder Technology 2017;307:56–62. http://dx.doi.org/10.1016/j.powtec.2016.11.018

100. Wang Y, Liu B, Wen X, Li M, Wang K, Ni Y. Quality analysis and microencapsulation of chili seed oil by spray drying with starch sodium octenylsuccinate and maltodextrin. Powder Technology. 2017 May 1;312:294–298. http://dx.doi.org/10.1016/j.powtec.2017.02.060

101. Ribeiro AM, Shahgol M, Estevinho BN, Rocha F. Microencapsulation of vitamin A by spray-drying, using binary and ternary blends of gum arabic, starch and maltodextrin. Food Hydrocolloids. 2020 Nov 1;108:106029. https://doi.org/10.1016/j.foodhyd.2020.106029

102. Mahdi AA, Mohammed JK, Al-Ansi W, Ghaleb ADS, Al-Maqtari QA, Ma M, et al. Microencapsulation of fingered citron extract with gum arabic, modified starch, whey protein, and maltodextrin using spray drying. International Journal of Biological Macromolecules 2020;152:1125–1134. https://doi.org/10.1016/j.ijbiomac.2019.10.201

103. Šturm L, Osojnik Črnivec IG, Istenič K, Ota A, Megušar P, Slukan A, et al. Encapsulation of non-dewaxed propolis by freeze-drying and spray-drying using gum Arabic, maltodextrin and inulin as coating materials. Food and Bioproducts Processing. 2019 Jul 1;116:196–211. https://doi.org/10.1016/j.fbp.2019.05.008

104. Leong XF, Ng CY, Jaarin K. Animal models in cardiovascular research: Hypertension and atherosclerosis. BioMed Research International. Hindawi Publishing Corporation; 2015. http://dx.doi.org/10.1155/2015/528757

105. Mohammed-Ali Z, Carlisle RE, Nademi S, Dickhout JG. Animal models of kidney disease. 2017. P 391-395.

106. Cruz A, Rodríguez-Gmez I, Pérez-Abud R, Vargas MÁ, Wangensteen R, Quesada A, et al. Effects of clofibrate on salt loading-induced hypertension in rats. Journal of Biomedicine and Biotechnology. 2011;2011. doi:10.1155/2011/469481

107. Gu JW, Bailey AP, Tan W, Shparago M, Young E. Long-term high-salt diet causes hypertension and decreases renal expression of vascular endothelial growth factor in Sprague-Dawley rats. Journal of the American Society of Hypertension 2008; Jul2(4):275–285. doi:10.1016/j.jash.2008.03.001

108. Banday AA, Muhammad AB, Fazili FR, Lokhandwala M. Mechanisms of oxidative stress-induced increase in salt sensitivity and development of hypertension in Sprague-Dawley rats. In: Hypertension. 2007. p. 664–671. doi: 10.1161/01.hyp.0000255233.56410.20

109 Coelho MS, Passadore MD, Gasparetti AL, Bibancos T, Prada PO, Furukawa LL, et al. High- or low-salt diet from weaning to adulthood: Effect on body weight, food intake and energy balance in rats. Nutrition, Metabolism and Cardiovascular Diseases 2006;16(2):148–155. doi:10.1016/j.numecd.2005.09.001

110. Gu JW, Manning RD, Young E, Shparago M, Sartin B, Bailey AP. Vascular endothelial growth factor receptor inhibitor enhances dietary salt-induced hypertension in Sprague-Dawley rats. American Journal of Physiology-Regulatory, Integrative and Comparative Physiology. 2009;297:142–148. doi:10.1152/ajpregu.90972.2008

111. O'Donaughy TL, Brooks VL. Deoxycorticosterone acetate-salt rats: Hypertension and sympathoexcitation driven by increased NaCl levels. Hypertension. 2006 Apr;47(4):680–685. doi: 10.1161/01.hyp.0000214362.18612.6e

112. Basting T, Lazartigues E. DOCA-Salt hypertension: An update. Current Hypertension Reports. 2017:19(4):32. doi:10.1007/s11906-017-0731-4

113. Dordević S.M; Cekić, N.D.; Savić, M.M.; Isailović, T.M.; Randelović D.V.; Marković B.D.; Savic, S.R.; Stamenic, T.T.; Daniels, R.; Savic, S.D. Parenteral nanoemulsions as promising carriers for brain delivery of risperidone: Design, characterization and in vivo pharmacokinetic evaluation. International Journal of Pharmaceutics. 2015, 493(1–2): 40–54. http://dx.doi.org/10.1016/j.ijpharm.2015.07.007

114. Barick, P.; Shalini, B.V.; Srinivas, M.; Jana, D.C.; Saha, B.P. A facile route for producing spherical granules comprising water reactive aluminium nitride added composite powders. Advanced Powder Technology. 2020. https://doi.org/10.1016/j.apt.2020.03.009

115. Adeli E. A comparative evaluation between utilizing SAS supercritical fluid technique and solvent evaporation method in preparation of Azithromycin solid dispersions for dissolution rate enhancement. Journal of Supercritical Fluids. 2014;87:9–21. http://dx.doi.org/10.1016/j.supflu.2013.12.020

116. Matos, R.L.; Lu, T.; Prosapio, V.; McConville, C.; Leeke, G.; Ingram, A. Coprecipitation of curcumin/PVP with enhanced dissolution properties by the supercritical antisolvent process. Journal of CO_2 Utilization. 2019; 30: 48–62. https://doi.org/10.1016/j.jcou.2019.01.005

117. United States Pharmacopeial Convention. *USPNF 2021*: Powder Flow <1174>. Issue 1; 2020. Available from: https://online.uspnf.com/uspnf

118. Anwar M, Ahmad I, Warsi MH, Mohapatra S, Ahmad N, Akhter S, et al. Experimental investigation and oral bioavailability enhancement of nano-sized curcumin by using supercritical anti-solvent process. European Journal of Pharmaceutics and Biopharmaceutics 2015;96:p. 162–172. http://dx.doi.org/10.1016/j.ejpb.2015.07.021

119. United States Pharmacopeial Convention. *USPNF 2021*: Dissolution <711>. Issue 1; 2020. Available from: https://online.uspnf.com/uspnf

120. You C, Liang X, Sun J, Sun L, Wang Y, Fan T, Zheng Y. Blends of hydrophobic and swelling agents in the swelling layer in the preparation of delayed-release pellets of a hydrophilic drug with low MW: Physicochemical characterizations and in-vivo evaluations. Asian Journal of Pharmaceutical Sciences 2014;9:199–207. http://dx.doi.org/10.1016/j.ajps.2014.06.003

121. Fraile M, Buratto R, Gómez B, Martín Á, Cocero MJ. Enhanced delivery of quercetin by encapsulation in poloxamers by supercritical antisolvent process. Industrial and Engineering Chemistry Research. 2014;53(11):4318–4327. dx.doi.org/10.1021/ie5001136

122. European Medicines Agency. ICH Topic Q 1 A (R2) Stability Testing of new Drug Substances and Products. 2006. p. 1–20. Available from: https://www.ema.europa.eu/en/documents/scientific-guideline/ich-q-1-r2-stability-testing-new-drug-substances-products-step-5_en.pdf

123. Seeliger D, De Groot BL. Ligand docking and binding site analysis with PyMOL and Autodock/Vina. Journal of Computer-Aided Molecular Design 2010;24(5):417–22. doi: 10.1007/s10822-010-9352-6

124. Hard GC, Flake GP, Sills RC. Re-evaluation of kidney histopathology from 13-week toxicity and two-year carcinogenicity studies of melamine in the F344 rat: Morphologic evidence of retrograde nephropathy. Veterinary Pathology. 2009 Nov;46(6):1248–1257. doi: 10.1354/vp.08-VP-0317-F-FL

125 Hard GC, Khan KN. A Contemporary overview of chronic progressive nephropathy in the laboratory rat, and its significance for human risk assessment. Vol. 32, Toxicologic Pathology. 2004. p. 171–180. doi: 10.1080/01926230490422574

126 Giknis MLA, Clifford CB. Clinical laboratory parameters for Crl:CD(SD) rats. Charles River Laboratories 2006; p. 12. Available from: https://www.criver.com/sites/default/files/resources/rm_rm_r_clinical_parameters_cd_rat_06.pdf

127. Dallakyan S, Olson AJ. Small-molecule library screening by docking with PyRx. Methods in Molecular Biology. 2015;1263:243–250.

128. Rachmawati H, Safitri D, Pradana AT, Adnyana IK. TPGS-stabilized curcumin nanoparticles exhibit superior effect on carrageenan-induced inflammation in wistar rat. Pharmaceutics 2016;8(24):1–13. doi:10.3390/pharmaceutics8030024

129. Weiss M, Fan J, Claudel M, Sonntag T, Didier P, Ronzani C, et al. Density of surface charge is a more predictive factor of the toxicity of cationic carbon

nanoparticles than zeta potential. Journal of Nanobiotechnology 2021;19:5, p. 1-18. https://doi.org/10.1186/s12951-020-00747-7

130. Shao XR, Wei XQ, Song X, Hao LY, Cai XX, Zhang, ZR, et al. Independent effect of polymeric nanoparticle zeta potential/surface charge, on their cytotoxicity and affinity to cells. Cell Proliferation 2015;48,p. 465–474. doi:10.1111/cpr.12192
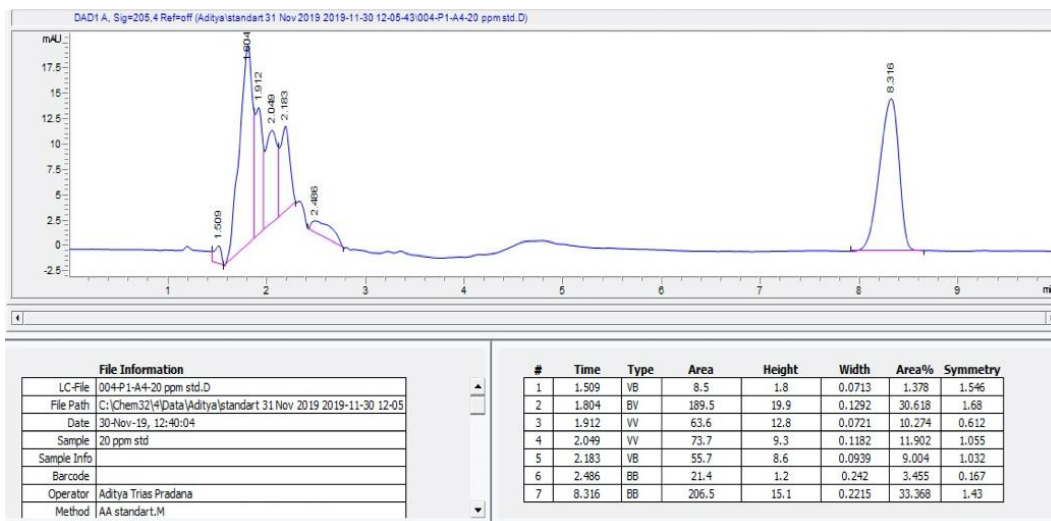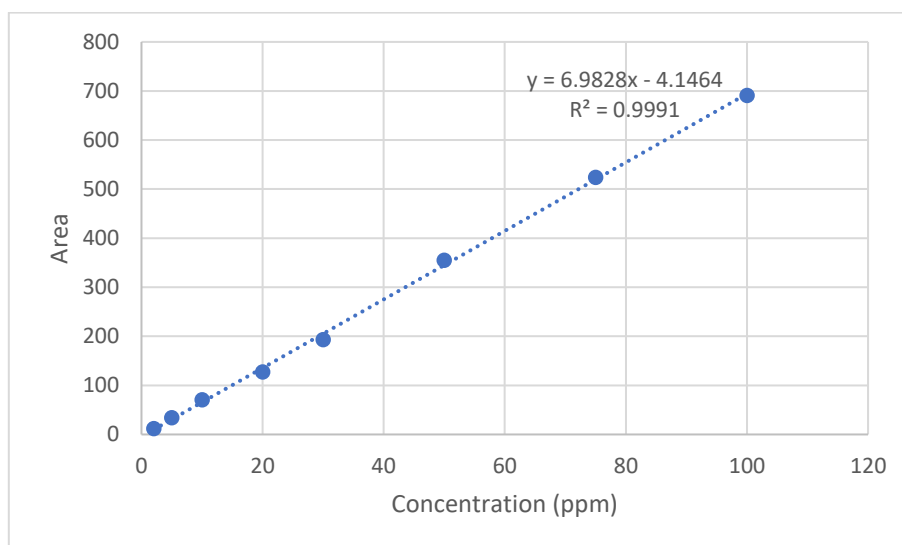
REFERENCES

Appendix 1 Example of Asiatic acid chromatogram in HPLC

DAD1 A, Sig=205,4 Ref=off (Aditya\standart 31 Nov 2019 2019-11-30 12-05-43\004-P1-A4-20 ppm std.D)

File Information	
LC-File	004-P1-A4-20 ppm std.D
File Path	C:\Chem32\4\Data\Aditya\standart 31 Nov 2019 2019-11-30 12-05
Date	30-Nov-19, 12:40:04
Sample	20 ppm std
Sample Info	
Barcode	
Operator	Aditya Trias Pradana
Method	AA standart.M

#	Time	Type	Area	Height	Width	Area%	Symmetry
1	1.509	VB	8.5	1.8	0.0713	1.378	1.546
2	1.804	BV	189.5	19.9	0.1292	30.618	1.68
3	1.912	VV	63.6	12.8	0.0721	10.274	0.612
4	2.049	VV	73.7	9.3	0.1182	11.902	1.055
5	2.183	VB	55.7	8.6	0.0939	9.004	1.032
6	2.486	BB	21.4	1.2	0.242	3.455	0.167
7	8.316	BB	206.5	15.1	0.2215	33.368	1.43

Appendix 2 Calibration curve of Asiatic acid with HPLC

Concentration (ppm)	Area	Symmetry
		Req: TF ≤ 2
2	12	0.962
5	34.1	0.993
10	70.3	1.025
20	127	1.036
30	193.1	1.116
50	354.7	1.27
75	523.8	1.404
100	690.8	1.129

Appendix 3 HPLC Assay method verification

Accuracy	• %Recovery: 100.74 %
Precision	• Relative standart deviation: 0.789 • Requirement: RSD ≤ 1%

Robustness
 	
(increasing the
temperature 0.5 point)
	• Retention time
	   • 8.378 ➔ 8.341
	• Symmetry
	   • 1.395 ➔ 1.353
	   • Requirement: Tailing Factor ≤ 2

Detection Limit / Quantitation Limit	• DL: 0.5 ppm • QL: 2 ppm

จุฬาลงกรณ์มหาวิทยาลัย

CHULALONGKORN UNIVERSITY

Appendix 4 System suitability (injection repeatability) in HPLC assay method

Concentration (ppm)	Retention time (minutes)	Area	Symmetry Requirement: TF ≤ 2	Theoretical Plate Number Requirement: N > 2000	Resolution Requirement: Rs ≥ 1.5	%CV Requirement: %CV < 2%
	8.316	206.5	1.43	8243	16.45	
	8.341	210.23	1.44	5114	16.86	
20	8.307	209.76	1.46	5608	17.08	1.790
	8.34	210.67	1.46	5115	16.13	
	8.333	210.88	1.47	5153	18.41	

Appendix 5 Animal use certificate

PharmIACUC-Form-07

**Chulalongkorn University Animal Care and Use Committee**

Certificate of Project Approval	☒ **Original** ☐ **Renew**
Animal Use Protocol No. 21-33-009	**Approval No. 21-33-009**

Protocol Title
Effect of spray dried asiatic acid-palm oil nanoemulsion on blood pressure in rat model of hypertension

Principal Investigator
Vudhipron LIMPRASUTR, D.V.M., Ph.D.

Certification of Institutional Animal Care and Use Committee (IACUC)
This project has been reviewed and approved by the IACUC in accordance with university regulations and policies governing the care and use of laboratory animals. The review has followed guidelines documented in Ethical Principles and Guidelines for the Use of Animals for Scientific Purposes edited by the National Research Council of Thailand.

Date of Approval July 1, 2021	**Date of Expiration** June 30, 2023

Applicant Faculty/Institution
Faculty of Pharmaceutical Sciences, Chulalongkorn University, Phyathai Road., Pathumwan BKK-THAILAND. 10330

Signature of Chairperson	**Signature of Authorized Official**
R. Rodsiri	
Name and Title **RATCHANEE RODSIRI, Ph.D.** **Chairman**	Name and Title **PITHI CHANVORACHOTE, Ph.D.** **Associate Dean (Research Affairs)**

The official signing above certifies that the information provided on this form is correct. The institution assumes that investigators will take responsibility, and follow university regulations and policies for the care and use of animals.   *This approval is subjected to assurance given in the animal use protocol and may be required for future investigations and reviews.*

Appendix 6 ACE1 activity pre-treatment in serum result
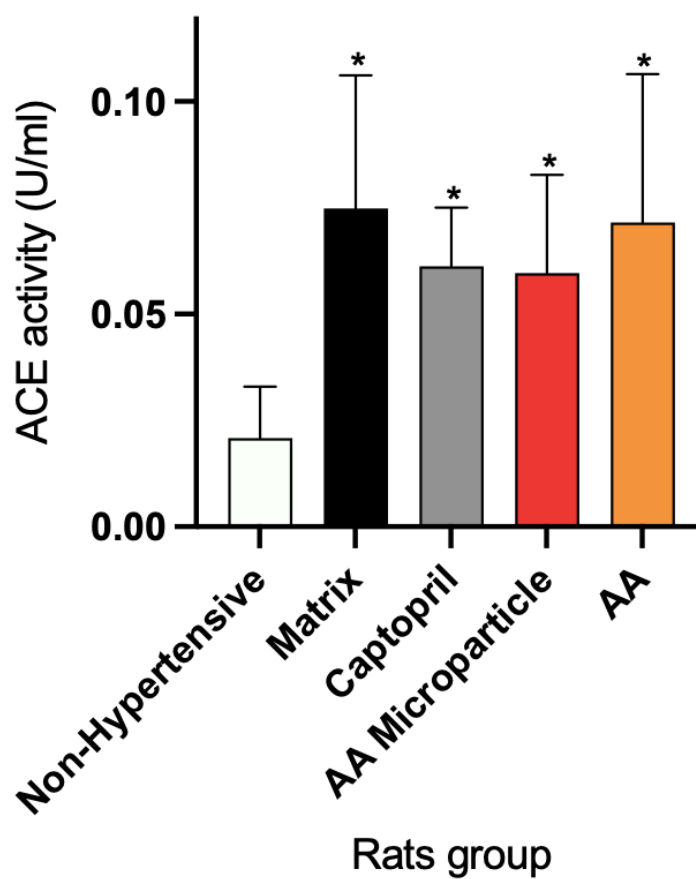
*indicates statistically different (p <0.05) between non-hypertensive group with all groups

VITA

NAME	Mr Aditya Trias Pradana
DATE OF BIRTH	3 January 1988
PLACE OF BIRTH	Malang
INSTITUTIONS ATTENDED	Bandung Institute of Technology
HOME ADDRESS	
PUBLICATION	TPGS-stabilized curcumin nanoparticles exhibit superior effect on carrageenan-induced inflammation in wistar rat. Pharmaceutics 8 (3), 24
	IMPACTS OF BINDER AND DISINTEGRANT ON DETAM II SOYBEAN (GLYCINE MAX (L.) MERR) TABLET MADE BY DRY GRANULATION. Faculty of Pharmacy, Universiti Teknologi MARA, Malaysia
	Multiple functions of D-α-tocopherol polyethylene glycol 1000 succinate (TPGS) as curcumin nanoparticle stabilizer: in vivo kinetic profile and anti-ulcerative colitis analysis. Pharmaceutics 9 (3), 24
	Formulation and physical characteristics of detam ii soybean (Glycine max (L.) merr) tablet with various concentration of silicon dioxide and magnesium stearate. Asian Journal of Pharmaceutical and Clinical Research 11 (1), 283-288
	The effect of spray-drying temperature on Centella asiatica extract-β cyclodextrin-maltodextrin nanoparticle

characteristics and stability. Pharmaciana 11 (3), 394-405

Development, Evaluation, and Molecular Docking of Oral Dissolving Film of Atenolol. Pharmaceutics 13 (10), 1727

Formulation And Stability Study Of Detam I Soybean Variety (Glycine Max (L.) Merr.) Effervescent Granules With Different Type Of Effervescent Agents. Acta Pharmaceutica Indonesia 46 (2), 38-43

AWARD RECEIVED   -